MILLIMETER WAVE MICROSTRIP LAUNCHERS AND ANTENNA ARRAYS

A THESIS SUBMITTED TO
THE GRADUATE SCHOOL OF NATURAL AND APPLIED SCIENCES
OF
MIDDLE EAST TECHNICAL UNIVERSITY

BY

ERDEM AKGÜN

IN PARTIAL FULFILLMENT OF THE REQUIREMENTS
FOR
THE DEGREE OF MASTER OF SCIENCE
IN
ELECTRICAL AND ELECTRONICS ENGINEERING

DECEMBER 2006

Approval of the Graduate School of Natural and Applied Sciences

Prof. Dr. Canan Özgen
Director

I certify that this thesis satisfies all the requirements as a thesis for the degree of Master of Science.

Prof. Dr. İsmet Erkmen
Head of Department

This is to certify that we have read this thesis and that in our opinion it is fully adequate, in scope and quality, as a thesis for the degree of Master of Science.

Prof. Dr. Altunkan Hızal
Supervisor

Examining Committee Members

Assistant Prof. Dr. Lale Alatan	(METU,EE)	_____
Prof. Dr. Altunkan Hızal	(METU,EE)	_____
Associate Prof. Dr. Şimşek Demir	(METU,EE)	_____
Associate Prof. Dr. Özlem Aydın Çivi	(METU,EE)	_____
Electronics Engineer Erhan Halavut	(ASELSAN AŞ)	_____

I hereby declare that all information in this document has been obtained and presented in accordance with academic rules and ethical conduct. I also declare that, as required by these rules and conduct, I have fully cited and referenced all material and results that are not original to this work.

Name, Last name: ERDEM AKGÜN

Signature :

ABSTRACT

MILLIMETER WAVE MICROSTRIP LAUNCHER AND ANTENNA ARRAY

Akgün, Erdem

M. S., Department of Electrical and Electronics Engineering

Supervisor : Prof. Dr. Altunkan Hızal

December 2006, 112 pages

Coaxial-to-microstrip launcher and microstrip patch array antenna are designed to work at center frequency of 36.85 GHz with a bandwidth higher than 300 MHz. The antenna array design also includes the feeding network distributing the power to each antenna element. The design parameters are defined on this report and optimized by using an Electromagnetic Simulation software program. In order to verify the theoretical results, microstrip patch array antenna is produced as a prototype. Measurements of antenna parameters, electromagnetic field and circuit properties are interpreted to show compliance with theoretical results. The values of deviation between theoretical and experimental results are discussed as a conclusion.

Keywords: Coaxial-to-Microstrip Launcher, Patch Antenna, Electromagnetic Simulation

ÖZ

MİLİMETRİK DALGA MİKROSTRİP BESLEME VE ANTEN YAPILARI

Akgün, Erdem
Yüksek Lisans, Elektrik ve Elektronik Mühendisliği Bölümü
Tez Yöneticisi : Prof. Dr. Altunkan Hızal

Aralık 2006, 112 sayfa

Bu tezde, 36.85 GHz merkez frekansında 300 MHz'den daha büyük bir bant genişliği ile çalışan koaksiyel-mikrostrip besleme ve mikrostrip yama anten dizisi tasarımları gerçekleştirilmiştir. Anten dizisi tasarımı ayrıca, enerjinin her bir anten elemanına dağıtılmasında kullanılan besleme ağı tasarımını da içermektedir. Tez raporu içerisinde tasarım parametreleri tanımlanmakta ve bu parametrelerin alabileceği en uygun değerler Elektromanyetik Simülasyon yazılım programı kullanılarak belirlenmektedir. Teorik sonuçların doğrulanabilmesi amacıyla, mikrostrip yama anten dizisi prototip olarak üretilmiştir. Anten parametreleri, elektromanyetik dalga ve devre özellikleri üzerinde yapılan ölçümler yorumlanarak teorik sonuçlar ile uyum gözlenmiştir. Teorik ve deneysel sonuçlar arasındaki sapma değerleri sonuç kısmında değerlendirilmektedir.

Anahtar Kelimeler: Koaksiyel-Mikrostrip Besleme, Yama Anten, Elektromanyetik Simülasyon

To Hale

TABLE OF CONTENTS

LIST OF TABLES

LIST OF FIGURES

CHAPTER 1

INTRODUCTION

In millimeter wave K_a region, constructing electromagnetic circuit elements is known as a very tough subject to achieve. The free-space wavelength is in the order of 7.5 mm (at 40 GHz) to 15 mm (at 26.5 GHz) and the fabrication requires very sensitive processes. Slight misalignments on parameters in the order of 0.1 millimeter change the characteristic of circuit elements and result in unexpected consequences. The formulations are getting more complex with higher error rate, characteristics of circuit elements show more deviations between theory and real environment and designing a circuit element having exactly the required parameters becomes more difficult while increasing the frequencies up to K_a region and higher. Despite all the drawbacks of working at K_a band frequencies, this does not mean that some careful and strict work will not succeed. Thus, the thesis subject is decided to deal with a circuit element at this frequency range. Consequently, constructing a microstrip patch array antenna with a coaxial-to-microstrip launcher at the center frequency of 36.85 GHz is accepted as the main topic. Microstrip antennas are common form of printed antennas which are extensively used with antenna engineers. The design of a microstrip antenna also necessitates working on coaxial–to-microstrip launcher and feeding network structures which bring matching and coupling problems with themselves. To conclude, it could be said that all these works will add significant and additional experiences for future works on the subject.

1.1. Brief History of Thesis Studies

Microstrip Antennas, Microstrip Feeding Methods, Microstrip Power Dividers, and Array Antennas are the main subjects of interest. It is mandatory to have an extensive knowledge on these subjects in order to develop a microstrip patch array

antenna which is the main goal of this thesis report. These subjects are thoroughly investigated as moving on the design steps of Microstrip Patch Array Antenna. For each design level, design alternatives are evaluated and the most suitable one is preferred to be sure that final product will work efficiently and has superior antenna parameters, electromagnetic field and circuit properties. These design steps, namely the different phases of antenna design, are listed below where the subjects of interest are given between parentheses.

1. Choosing Antenna Type (Microstrip Antennas)
2. Comparison Between Feeding Methods (Microstrip Feeding Methods)
3. Coaxial-to-Microstrip Launcher Design
4. Microstrip Power Divider Design (Microstrip Power Dividers)
5. Microstrip Patch Array Design (Array Antennas)
6. Verification of the Theoretical Design Model

The above design steps are also the main topics of the thesis report. Each design step forms a single chapter and is explained in detail on its own chapter. At this point, it will be helpful to summarize the entire thesis studies.

It may be said that the first and the basic decision of thesis is the choice of using microstrip patch antenna. This decision is given especially by considering its technological popularity and usage at higher operating frequencies belong to millimeter wave region.

At second step, it is tried to decide on feeding methods which will insert signal to the microstrip antenna and excite signals to the patch elements of an array antenna. Possible alternatives of microstrip feeding methods are researched and reported with respect to their advantages and disadvantages.

Thirdly, a coaxial-to-microstrip launcher design is needed, since the antenna must have a coaxial connector as the connection point to the system it will be operate with. Therefore, coaxial connector types are inspected working at millimeter wave region and suitable for coaxial-to-microstrip launcher. Suhner 2.92 mm panel launch connector is chosen for inserting the field into a microstrip line. An

electromagnetic software program HFSS™ v9.2 is used to model the mechanical structure of the connector mount.

The fourth step arises because of the microstrip patch array structural properties. It is known that microstrip patch array has more than one patch element and some type of feeding mechanism should be responsible for distributing the inserted field to each one of these elements. The investigations on the third design step show the possibility of using parallel feeds, therefore some works on power dividers are realized at this design step. Power divider methods are investigated and electromagnetic software simulations are realized to get the best power divider properties.

The fifth step starts from designing a single patch element. Afterwards, the antenna array structures are investigated and the relations between array antenna parameters and the arrangement of array elements are derived. The antenna parameters of a typical microstrip patch array (8 x 2 elements) are calculated by using the above relation. This array structure is also constructed on HFSS v9.2 and different feeding network alternatives are tried for this array structure by using previously designed Microstrip Power Dividers where necessary. Electromagnetic simulations are executed on the final design to evaluate the antenna parameters and plot the antenna patterns of the array.

Finally, microstrip patch array antenna with 8x2 patches, based on the calculated design parameters, is produced and observed if the experimental results comply with the theoretical results.

CHAPTER 2

MICROSTRIP ANTENNAS

Microstrip antennas are the most common form of printed antennas which is constructed like printed circuits with simple fabrication techniques (Figure 1). Microstrip antennas are conceived in the 1950s and vast amount of investigations are done since 1970s [6, 25-27]. They are widely used in recent applications by antenna engineers. This chapter explains the basic properties of microstrip antennas by giving their advantages and disadvantages. The reasons for the choice of microstrip antennas on this thesis are also presented on this chapter.

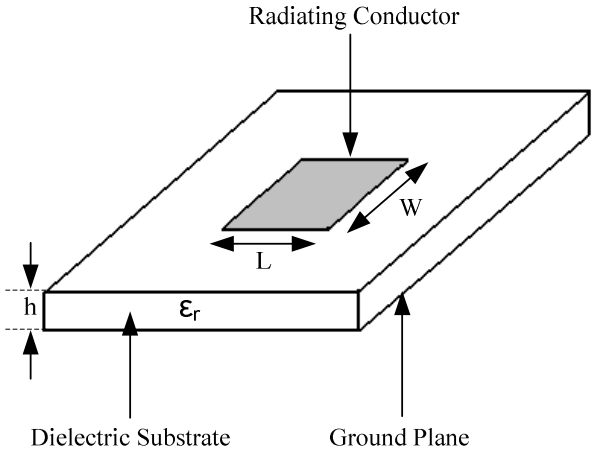

Figure 1. Microstrip Antenna

2.1. Microstrip Antenna Advantages

The advantages of microstrip antennas are listed on this section and each advantage is presented with related information on the subject.

Easier, inexpensive and reliable fabrication [1-4]:

Microstrip antennas are easier to be realized and tested. Manufacturing a microstrip prototype antenna is simpler, more inexpensive and requires much less time than other type of antennas with the help of modern printed-circuit technology. Therefore, microstrip antennas could also easily be constructed for testing purposes. In addition, when manufactured with adequate care, products will be practically identical. This means that verification of the design on a microstrip prototype antenna will also be satisfactory for other copies of the antenna.

Easier installation [1-4]:

Microstrip antennas consist of substrates having flexible structure, lower size and lower weight. These properties makes the mictrostrip antennas be mounted easily to the systems with small free space and having smoothly rounded surfaces as well as flat surfaces.

Shielded by the ground plane [2]:

The radiation patterns of many antennas are distorted when they are placed in close vicinity to each other. However, microstrip antennas are shielded by the presence of ground plane. The objects behind a microstrip antenna do not affect its radiation pattern significantly.

Compact circuit design [2-4]:

Microstrip antennas are constructed by microstrip circuits which are fabricated together with all necessary circuit devices on the same substrate. It is possible to add wide variety of active and passive circuit devices to the antenna. In some cases, holes must be drilled through the substrate to connect the ground plane. This kind of circuit type provides more compact design and combines many functions within the same circuit.

2.2. Microstrip Antenna Disadvantages

Microstrip antennas have also some disadvantages as given on this section. These disadvantages are explained with related information on the subject.

High accuracy requirement [2, 4]:

For the microstrip line used as a feed on microstrip antenna, the width determines the characteristic impedance of the line and the length determines the phase of the wave. At millimeter wave range, these dimensions become significant and a great care should be applied in fabrication processes.

Low power output [1-4]:

Microstrip antennas have comparatively low power output. The physical specifications of a microstrip antenna substrate do not let engineers for very high power applications. In addition, the efficiency values of microstrip antennas are relatively lower than other antenna types.

Narrow frequency bandwidth [1-4]:

The frequency bandwidth of microstrip antennas is usually a fraction of a percent or at most a few percent. There are some techniques for increasing the bandwidth, however these methods result in unexpected outcomes such as spurious radiation and return loss. The methods for increasing the bandwidth are described in Section 3.1.

Coaxial to microstrip transition [1, 2]:

Microstrip antennas are connected to systems by means of coaxial to microstrip transitions. These transitions require precise positioning and delicate connection operations such as bonding or soldering. This transition produces reflections, phase shifts, spurious radiation and attenuation.

Electromagnetic complexity [2]:

The microstrip antenna structure includes different types of materials such as dielectric substrate, ground plane and air requiring a variety of boundary conditions to be applied. These structural inhomogeneities are responsible for complex and time consuming electromagnetic wave propagation formulas which could be solved by software programs running on a computer with high memory space.

Difficult to adjust [2]:

Microstrip antennas are mostly not suitable for tuning purposes. At millimeter wave range, tuning elements could not be found easily. When a prototype antenna does not function properly, the production process, even the antenna design, should be repeated from the beginning.

2.3. Reasons for Microstrip Antenna Choice

The main decision of this thesis study is using microstrip antennas in order to gain experience on the field. On this section, it is tried to answer why microstrip antennas are so popular in recent antenna applications.

The main reason for extensive usage of microstrip antennas must be its easier, inexpensive and reliable fabrication. There are vast amount of inexpensive opportunities for giving the circuit shape on a substrate material and producing the related mechanical mounts. The following work will only be the soldering, mounting and testing processes that most of the time one could easily handle by itself.

Microstrip antennas have some disadvantages as explained before, but they will not be very critical when designed with some special techniques and dealt with adequate sensitivity. For example, electromagnetic complexity of the design could be overcome by using high performance software analysis programs. Moreover, increasing the bandwidth and transferring the coaxial line field to the microstrip line could be achieved by applying some special design techniques. There is also a high accuracy problem whose effect could be reduced by giving special care on fabrication.

Microstrip antennas consist of at least one copper plate on one side, ground plate on the other side and a dielectric substrate material between these plates. The copper plate different from the ground is named as patch. The main lobe of a single patch antenna extends to 180º for some cases and the 3 dB beamwidth takes values in the 60º-90º range which are really high values and not practical for most of the cases [2, 5]. The only way for achieving narrower antenna patterns is to form an array of patches. This makes the feeding network design be more

important, since each array element is fed via this network and the overall efficiency depends on the feeding network capabilities. The design of the patch array and related feeding methods will be described in corresponding sections.

CHAPTER 3

FEEDING METHODS

There are many ways of microstrip patch antenna excitation. The best feeding method could only be decided by having knowledge on some electromagnetic wave properties propagating along the microstrip structure. Excitation methods, as well as microstrip patch antenna design parameters, have particular effects on the antenna radiation and matching characteristics. There are some important topics that one should keep in mind while building a feeding design. These crucial points are summarized at the first section of this chapter. Afterwards, the main feeding methods and patch array feeding networks are discussed by considering the information given in the first section. In the conclusion part, it is described what kind of feeding methods are chosen, what the reasons for these choices are and how they will be used during thesis studies.

3.1. Significant Points to Pay Attention

Bendings, junctions, branches, transitions and terminations introduce electrical and physical discontinuities into the feed line. It is impossible to obtain perfect match because of these discontinuities. As matching decreases, more reflection losses, surface wave losses and spurious radiations [1-2, 7] start to occur. These undesired radiations travel within the substrate and they are scattered at bends and surface discontinuities. The distribution of the total energy to undesired directions raises the sidelobe and cross polarization levels. In turn, the increase on sidelobe levels results in reduction on the antenna gain. The undesired radiations also degrade the antenna polarization characteristic. Therefore, the first important factor for the feed design is to achieve matching as good as possible. In addition, the uncontrolled spurious radiation should be attenuated by using suppressing pins close to the discontinuity points.

Microstrip patch antenna should have a thicker substrate and lower permittivity [1-3], so that the patch can actually radiate. These conditions are also necessary to obtain a higher frequency bandwidth. If surface waves are not included, increasing the height of the microstrip patch antenna substrate extends the efficiency as large as 90% and bandwidth up to about 35% [22]. However, increasing height of the substrate results in excitation of surface waves which reduces the efficiency of the antenna and degrades the antenna pattern as explained above. In addition, as the permittivity decreases, the guided wavelength increases and this necessitates larger element sizes (A.6).

On the contrary with patch antenna requirements, microstrip feed line should have a thinner substrate and higher permittivity to ensure proper transmission along microstrip lines [1-2]. However, very high permittivity results in great losses because of the increasing value of dielectric loss tangent coefficient. Moreover, while the permittivity value increases, the guided wavelength value decreases; so the element sizes should be reduced (A.6). As permittivity of the feed substrate increases, more losses start to occur; feed lines become less efficient and have smaller bandwidth.

3.2. Microstrip Patch Antenna Feeding Methods

Electromagnetic wave could be coupled to a patch antenna by using one of the 5 major feeding techniques. These techniques are discussed on following sections by discussing their advantages and disadvantages.

3.2.1. Microstrip Line Feed

Microstrip Line Feed [1-3, 6-7] is easier to fabricate, since it locates the patch and the feed line on the same substrate (Figure 2). The feed line is easily matched to the patch by controlling the inset position or placing a cut on the contacting point. It is also rather simple to model. However, it is impossible to optimize the microstrip line and the patch parameters simultaneously, since they are placed on the same substrate and specific requirements are contradictory for each other. For instance, higher substrate thickness, which is made to increase bandwidth, also increases surface waves, spurious feed radiation and higher order mode generation. These

undesired radiations degrade the antenna performance as mentioned before. Moreover, in the millimeter wave region, the size of the feed line is comparable with the patch dimensions, so that this leads to an increase in spurious radiations.

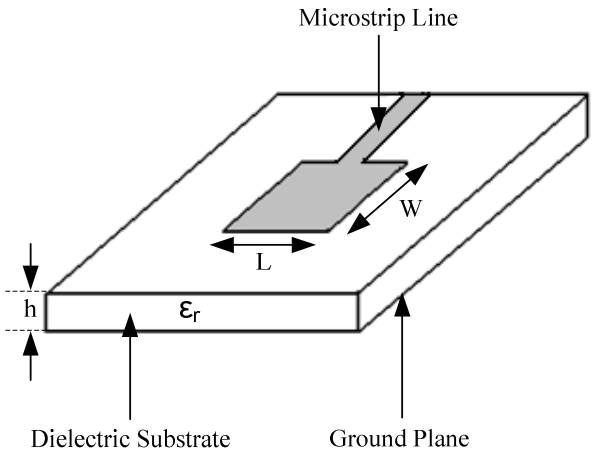

Figure 2. Microstrip Line Feed

3.2.2. Coaxial Line Feed

3.2.2.1. Buried Coaxial Line Feed

The inner conductor of the Buried Coaxial Line Feed [1-3, 6-7] extends across the dielectric substrate and is connected to the radiation patch, while the outer conductor is connected to the ground plane (Figure 3). The patch could easily be matched to the line by controlling the position of the coaxial feed. However, fabrication of this feeding method is not very practical, because drilling hole to the substrate, placing the coaxial connector inside the hole and soldering the connector to the patch and ground plane require very careful handling. The connector also stands outside the ground plane, so that it is not planar and symmetrical.

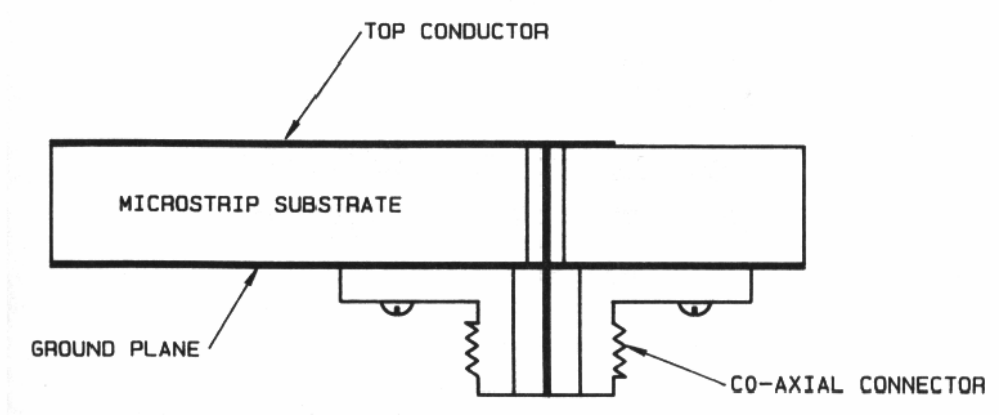

Figure 3. Buried Coaxial Line Feed [28]

Especially for millimeter wave frequencies and thick substrates ($h>0.1\lambda$), which is made to achieve broad bandwidth for the antenna, significant problems start to occur [6]. Intrinsic radiation and higher order modes occur degrading the antenna performance. The input impedance of the coaxial line feed becomes more inductive resulting in matching problems and preventing the patch from being resonant. Furthermore, the feeding method is difficult to model and the VSWR bandwidth is lower for thick substrates ($h>0.02\lambda_0$) [1].

The VSWR bandwidth of the Buried Coaxial Line Feed could be made broader by adding capacitive elements as close as possible to the induction introduced by the coaxial connector [7-8]. The capacitive elements could be included to the feed behind the patch [8], within the connector structure [9] or on the surface of the patch [10]. The capacitive element is mostly in the form of a small gap.

3.2.2.2. Panel Launch Coaxial Line Feed

The inner conductor of the Panel Launch Coaxial Line Feed [2, 7] extends over dielectric substrate and is connected to the top portion of the microstrip line while the outer conductor of the feed is connected to the ground plane of the dielectric (Figure 4). Fabrication of this feeding method is practical since it does not need to be placed inside a dielectric substrate. The common techniques such as soldering or bonding of narrow conductor strips could be used to fix the connector. However, there exist many different kinds of commercial connectors designed for coaxial-to-microstrip launch and most of these connectors could only be attached

to dielectric substrates via some special mechanical mounting structures. Fabrication of these structures and fixing the connectors may require very careful handling.

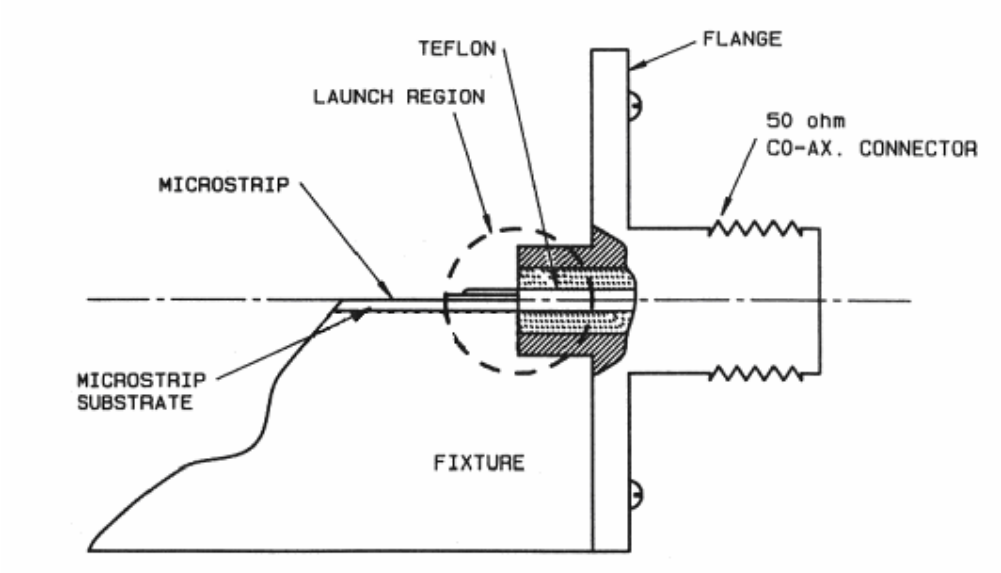

Figure 4. Panel Launch Coaxial Line Feed [28]

Because of the fringing fields over the launch region, Panel Launch Coaxial Line Feed has capacitive input impedance resulting in distortion of the matching and antenna pattern characteristics. The VSWR properties of the coaxial-to-microstrip launcher could be improved by using one of these techniques.

a. Tapering the inner and outer conductors of the connector so that the distance between conductors decreases linearly and the outer conductor ends just at the level of ground plane of the dielectric substrate (Figure 5.a) [30].

b. Inserting hole below the inner conductor of the connector by drilling the ground plane and the lower mechanical structure (Figure 5.b) [31].

c. Adding inductive notches to the microstrip line close to connection point (Figure 5.c).

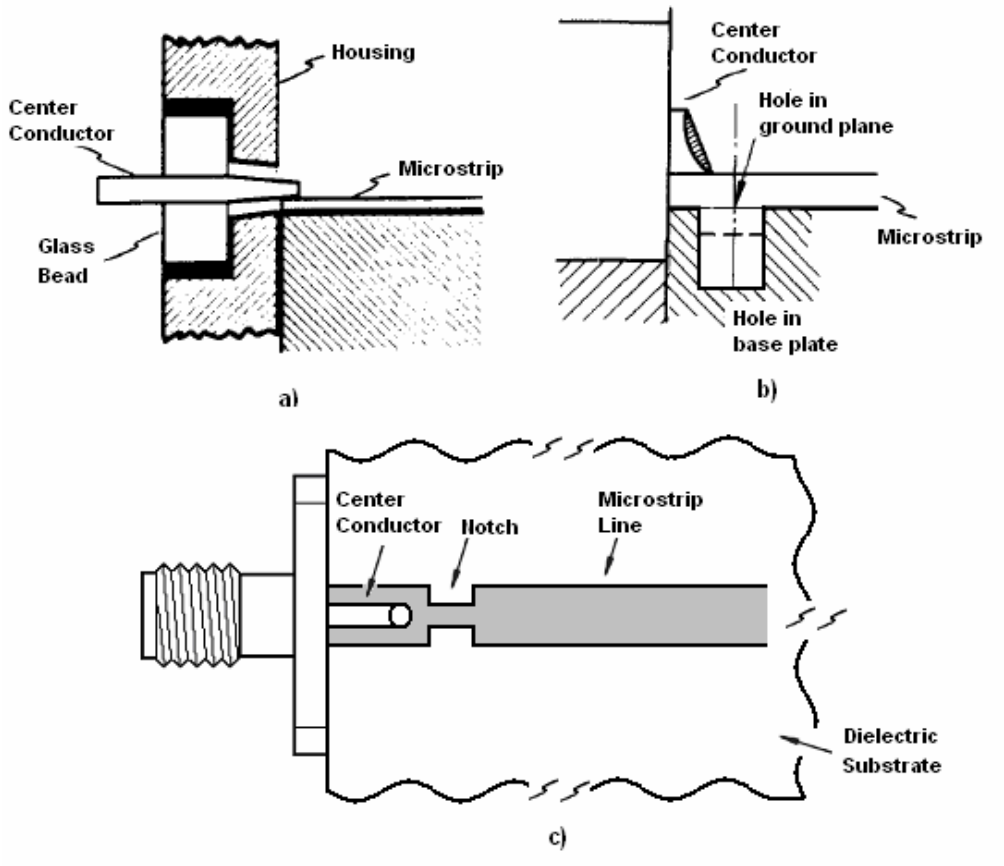

Figure 5. Techniques Used to Improve S_{11} of Panel Launch Coaxial Line Feed

The first (a) and the second (b) techniques could be achieved only by applying special processes and they are not practical to fabricate. The third technique (c) could be applied to wider microstrip lines depending on the printed circuit fabrication sensitivity. The effect of the last technique is observed on a commercial panel launch coaxial connector on Section 4.3.1 by using Electromagnetic Simulation program.

3.2.3. Coupling Feed

3.2.3.1. Microstrip Line Coupling Feed

Microstrip Line Coupling Feed [2, 7] includes the patch and the feed line which are located on the same substrate as it is done for microstrip line feed. The difference is that coupling takes place continuously along the edge of the patch instead of a narrow touch (Figure 6). This feeding method could be suitable for

linear array of patches. However, it possesses the same disadvantages of the microstrip line feed.

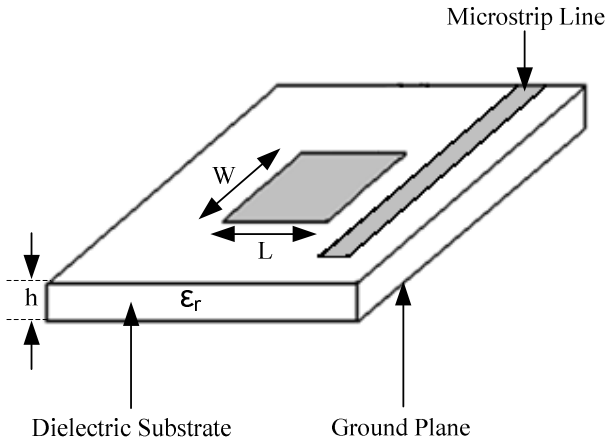

Figure 6. Microstrip Line Coupling Feed

3.2.3.2. Dielectric Waveguide Coupling Feed

As compared with Microstrip Line Coupling Feed, Dielectric Waveguide Coupling Feed [4, 24] has a substantial efficiency advantage because of the low-loss property of the dielectric waveguide (Figure 7). However, this feeding model requires an additional launching mechanism such as microstrip-to-dielectric waveguide or coaxial-to-dielectric waveguide causing additional discontinuities and reflection losses. The distances between dielectric waveguide and patches could be aligned in reducing order as going away from the source to ensure that each patch of the linear array is excited uniformly. However, the design of an antenna using this kind of feeding method is really complex to model. The coupling may also produce spurious radiation distorting the antenna pattern. In addition, the fabrication of this model is rather difficult to realize.

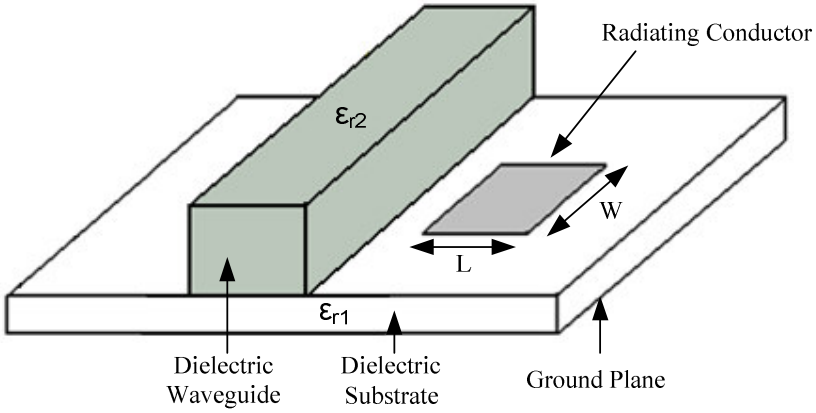

Figure 7. Dielectric Waveguide Coupling Feed

3.2.4. Proximity Coupling Feed

For Proximity Coupling Feed [1-3, 6-7, 18-21], the feed line and the patch parameters could be optimized separately, since they are located on different dielectric medium (Figure 8). Thin substrate with higher permittivity could be used on the feed line side to reduce the spurious feed radiation, while thick substrate with lower permittivity could be used on the patch side to enhance the patch radiation. By using this type of feeding method, a large bandwidth (as high as 13%) could be obtained. However, this feeding model is very difficult to analyze, since there does not exist any ground plane between the substrates and thereby simple models developed for single substrates could not be used. The length of the feeding stub and the width-to-line ratio of the patch can be used to control the match, but this requires complex calculations. In addition, its fabrication is somewhat more difficult.

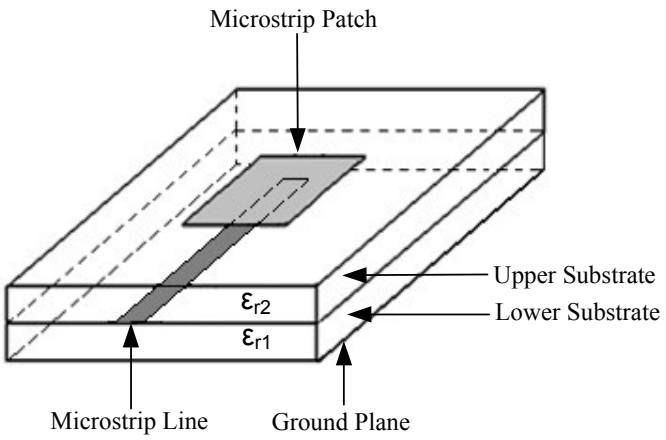

Figure 8. Proximity Coupling Feed

3.2.5. Aperture Coupling Feed

Aperture Coupling Feed [1-3, 6-7, 11-17] is shown on Figure 9 where two substrates are separated apart for illustration. The two functions of feeding and patch radiation could be separated apart and optimized simultaneously by using two different dielectric medium and placing a ground plane between them. Aperture Coupling Feed has the same advantages as Proximity Coupling Feed. Moreover, the middle ground plane makes the modeling be easier. As in the case of Proximity Coupling Feed, the substrate of the patch antenna could be thicker and has lower permittivity to promote radiation, while the substrate of the feed could be thinner and has higher permittivity to enhance binding of the fields to feed lines. The ground plane between these substrates also isolates the feed from radiating patches. This makes the feed spurious radiation do not effect much on antenna radiation pattern and polarization purity.

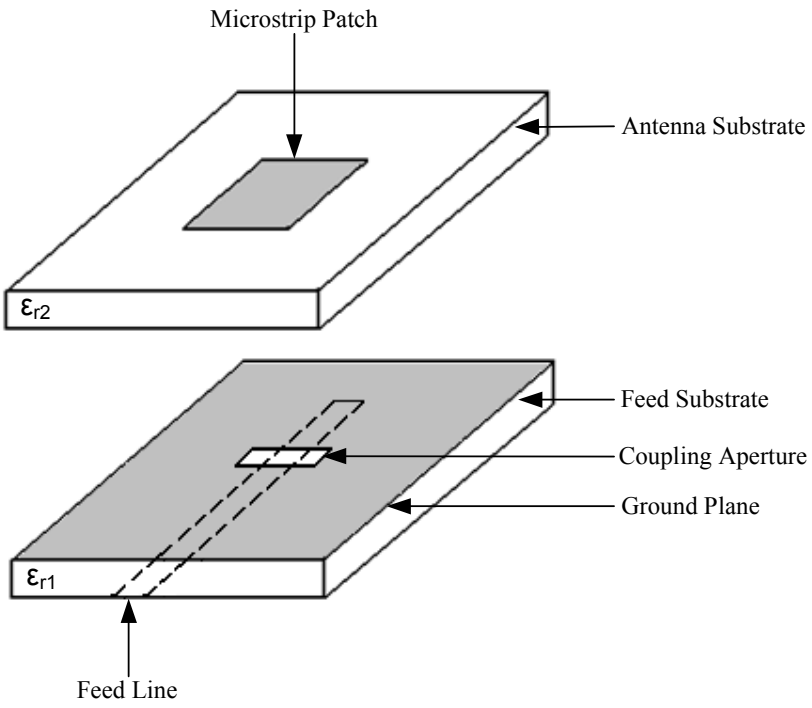

Figure 9. Aperture Coupling Feed

Aperture Coupling Feed design is made by controlling the position and the size of the aperture. The aperture should be placed at the center of patch to obtain maximum coupling and lower cross polarization due to symmetry of the configuration. By adjusting shape and size of the slot, a typical matching could be obtained [23]. Furthermore, the excess reactance of the antenna could be compensated by varying the open stub length [3].

Besides all the advantages, it could be said that this feeding method do not have many significant drawbacks. Some important disadvantages are its difficulty to fabricate and sensitivity requirement in the alignment of two layers.

3.3. Microstrip Patch Array Feeding Networks

As discussed in Section 2.3, narrower antenna patterns could be achieved by forming a microstrip patch array. In case a microstrip antenna array is excited by only one signal source, some feeding network structures should be used to distribute the inserted field to each patch element. The feeding methods of individual patches are out of the scope of this section and they were defined on

Section 3.2. This section introduces the way of transferring signal to the points where patches are excited from. The different kinds of feeding networks could be summarized as below [7].

The feeding network for a patch array could be realized with two main feed systems. These models are named as series feed and parallel feed. These two feed systems may also be used together to form parallel-series feeds.

Series feed consists of a microstrip line where small portions of energy are progressively coupled into the radiating elements (Figure 10). This method eliminates the need for a vast amount of power divider. As power flows and couples to patches, power level decreases and each time lower signal level couples to the next patch. Therefore, the excitation coefficient of each antenna element takes mostly different values. In addition, unless the distances between patches are multiples of half-guided wavelength, each patch is coupled with a different phase shift. These all result in beam shift and increase in cross-polarization level. For the cases where the beam direction should be kept between a small angle range, the usage of this feeding network requires a narrow frequency bandwidth. As the frequency moves away from the center frequency, the guided wavelength of the signal changes and the patches are excited with different phase values which is responsible for the beam shift. This array feeding method is simpler to fabricate, however a great care must be applied during design process.

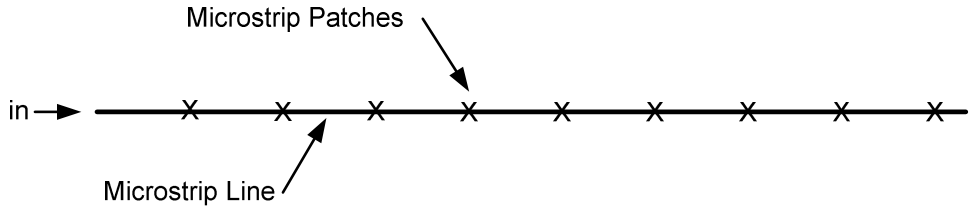

Figure 10. Series Feed

Parallel feed includes multiple microstrip lines where each feed line terminates at an individual radiating element. As an example, parallel feed for 8 patches is shown on Figure 11. Parallel feed has the advantage that one may couple easily the

same amount of energy with same phase value to each patch. This could be satisfied by aligning the distances from the input port to each patch equally and coupling the patches to the feed identically. Therefore, the antenna beam is in broadside direction and this direction is independent of frequency. This array feeding method is simpler to design, however using several power dividers make the feeding method have more transmission losses and reduced efficiency.

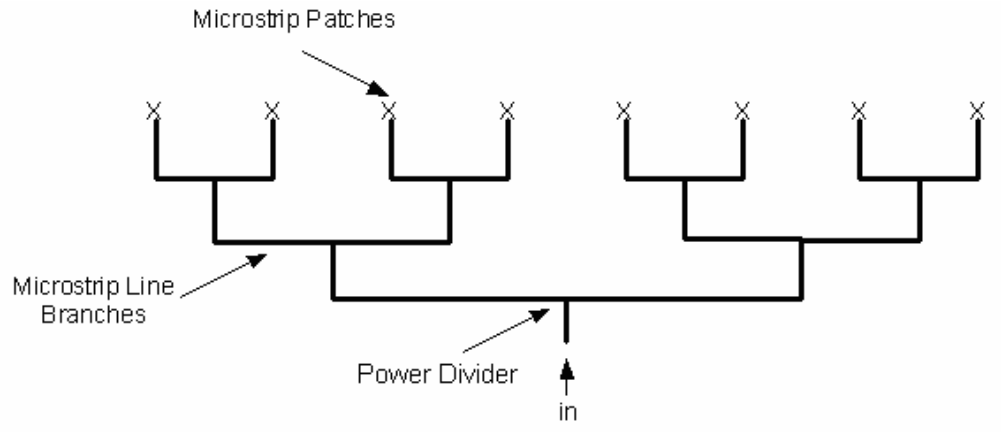

Figure 11. Parallel Feed Alternatives

If a two-dimensional feed is required in order to obtain a given antenna pattern specification and one dimension of the patch array does not necessarily need to have much elements, the parallel-series type feeding method could be used. For example on Figure 12, 2 x 8 patch array is shown and it is fed by using 2 parallel microstrip lines. Each microstrip line feeds 8 patches in series.

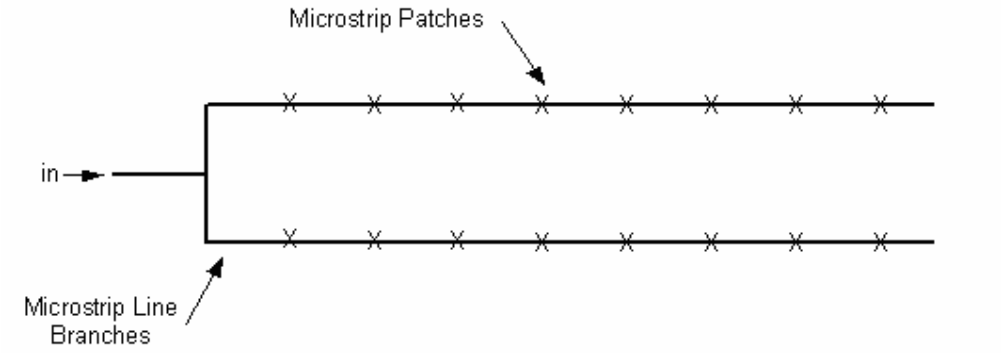

Figure 12. Parallel Series Feed

3.4. Design Decisions on Feeding Methods

The antenna design studied in this thesis is decided to include at least one coaxial connector, since it will be attached to systems via coaxial connection points. For measurement and testing purposes, it is also strongly needed that the antenna ends with a coaxial connector [7]. On section 3.2.2, two alternative coaxial line feeding methods are compared for their usefulness by taking their properties, outcomes and drawbacks into consideration. It was stated that Buried Coaxial Line Feed includes significant disadvantages especially for millimeter range frequencies and thicker substrates. On the other hand, Panel Launch Coaxial Line Feed could be realized easily by using commercial connectors designed as coaxial-to-microstrip launcher at millimeter wave frequencies. This type of coaxial feed does not produce important drawbacks if the mounting is made carefully. As a result, it is decided that Panel Launch Coaxial Line Feed will be used to excite the microstrip patch array antenna. Panel launch coaxial connector alternatives and structure of the mechanical mounting device are explained on Chapter 4 in detail.

Coaxial line feeding method is the worst method of all with respect to mismatches and spurious radiation. However, this type of feeding method has to be applied to the antenna system as explained before. Because of its higher losses, it is concluded that using more than one coaxial-to-microstrip transition could not be tolerated for the antenna design. But, the antenna design will be a patch array and there is a requirement of feeding all patch elements. This problem could be solved by inserting the field into the microstrip line by using just one coaxial-to-microstrip launcher and distributing the field to each patch by using one of the feeding network models (Section 3.3). The design of the required feeding network will be handled with microstrip patch array antenna design and it will be described on Section 6.2.

At this point, it is required to give a decision on other feeding method responsible for coupling the signal on the feeding network to each individual patch of the array. The information given on feeding methods section leads us to a decision that Aperture Coupling Feed will be used to excite each patch element. Microstrip Line Feed and Coupling Feed include the feed line and patch elements on the same

substrate resulting in significant drawbacks especially at millimeter wave region. Proximity Coupling Feed has also similar advantages with Aperture Coupling Feed; however it is not preferred because of its complexity to obtain good matching and required antenna parameters. In order to match the patch element to the microstrip line efficiently, the aperture dimension of the Aperture Coupling Feed will be adjusted on Section 6.2 by using an electromagnetic simulation program.

In conclusion, the microstrip patch array antenna will consist of two layers because of the structure introduced by Aperture Coupling Feed. On this thesis report, these layers will be named as below.

1. Feeding layer
2. Radiation layer

CHAPTER 4

COAXIAL-TO-MICROSTRIP LAUNCHER DESIGN

Designing a coaxial-to-microstrip launcher takes a crucial role on microstrip patch array antenna design. Since, it introduces the first discontinuity on the path of the signal and a mismatch at this point will be responsible for the biggest share of the total return loss. Therefore, a special care should be given to the coaxial-to-microstrip launcher.

The coaxial-to-microstrip launcher design consists of three main steps and each design step is explained on different sections. Firstly, the connector alternatives are discussed and the most suitable connector type is selected as a component of the coaxial-to-microstrip launcher. Then, the dielectric substrate of the feeding layer is selected by comparing some different types of dielectric substrates. Finally, electromagnetic simulations are executed in order to obtain some design parameters.

4.1. Coaxial-to-Microstrip Launcher Connector

As discussed on Section 3.4, the coaxial–to-microstrip launcher of the antenna will include a Panel Launch Coaxial Line Feed. Many different kinds of commercial connectors are available for this purpose on the market. This chapter inspects two different kinds of panel launcher connectors and introduces electromagnetic simulations applied for these connectors. One of these connectors is modeled and simulated to show the improvement on S_{11} characteristic of the coaxial-to-microstrip transition when notches (Figure 5.c) are added to the microstrip line (Section 4.3.1). The other one of these connectors is decided to be used on prototype fabrication. This connector is simulated to design a mechanical structure for the connector mount and obtain the best matching characteristic (Section 4.3.2).

SRI Connector Gage, SMA Female PCB Mount, 21-146-1000-01 [45, 50]:

SRI PCB Mount Connector (Figure 13) is a commercial coaxial-to-microstrip launcher and it operates normally below the frequency of 27 GHz. This connector type was highly available to get one and be used in experiments. Therefore, at the beginning of thesis studies it is decided to work with this connector type. The first electromagnetic simulations were executed by modeling the SRI PCB Mount Connector and good matching characteristics are obtained.

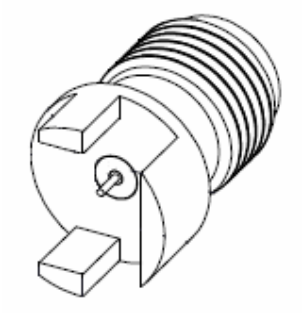

Figure 13. SRI Connector Gage, SMA Female PCB Mount, 21-146-1000-01

The simulations executed on this connector type give us very valuable information such that notches placed on the microstrip line result in improved matching characteristics. The electromagnetic simulation results will be interpreted in Section 4.3.1.

However, other investigations on commercial connectors lead the thesis study to the point that SRI PCB Mount Connector is not the correct choice for prototype fabrication of the antenna. There are two main reasons for this conclusion as given below.

1. The operating frequency of the connector is 27 GHz maximum and it is below the center frequency of the antenna design (36.85 GHz).

2. SRI PCB Mount Connector could not be mounted to the substrate tightly, since it does not contain screw holes.

Suhner, 2.92 mm Panel Launcher, 23 SK-50-0-52/ 199NE [46]:

Because of the drawbacks of previously mentioned connector type, Suhner Panel Launcher Connector (Figure 14) is decided to be used as a coaxial-to-microstrip launcher instead of SRI PCB Mount Connector. Suhner Panel Launcher Connector is a commercially available connector designed for the purpose of coaxial-to-microstrip transition. The connector has the operating frequency of maximum 40 GHz which is above the center frequency of antenna design. The connector also uses a glass bead structure which is the contact point with microstrip. The glass bead is totally replaceable. If the mounting can not be established correctly and the center pin of the glass bead is damaged, one may mount a new glass bead instead of changing the whole connector.

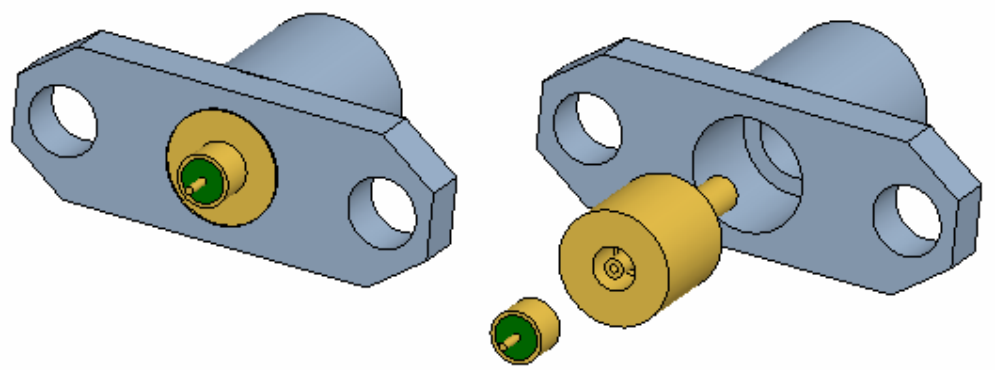

Figure 14. Suhner, 2.92 mm Panel Launcher, 23 SK-50-0-52/ 199NE

The other advantage of this type of the connector is that it could be mounted to a mechanical fixture via two screw holes. There should also be another hole for the glass bead where it is placed to achieve best matching. The cross section of the mechanical structure is shown on Figure 15 with necessary parameter values suitable to the dimensions of the glass bead. The slot where the glass bead is inserted and the place where the dielectric substrate is placed are also mentioned on the figure. The value of the air gap diameter is not mentioned deliberately since it is a design parameter and it should be optimized by using electromagnetic simulations (Section 4.3.2).

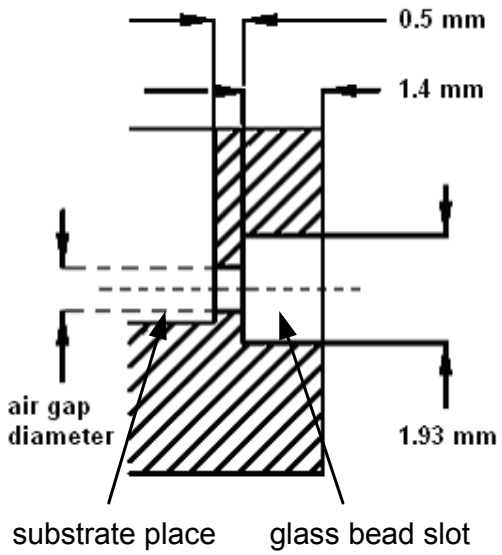

Figure 15. Cross Section of the Mechanical Structure for Suhner Panel Launcher

The cross section of the mechanical structure, the glass bead and the microstrip is shown on Figure 16 where these elements are jointed with each other appropriately. The figure is only for illustration, so the dimensions are not in correct ratios.

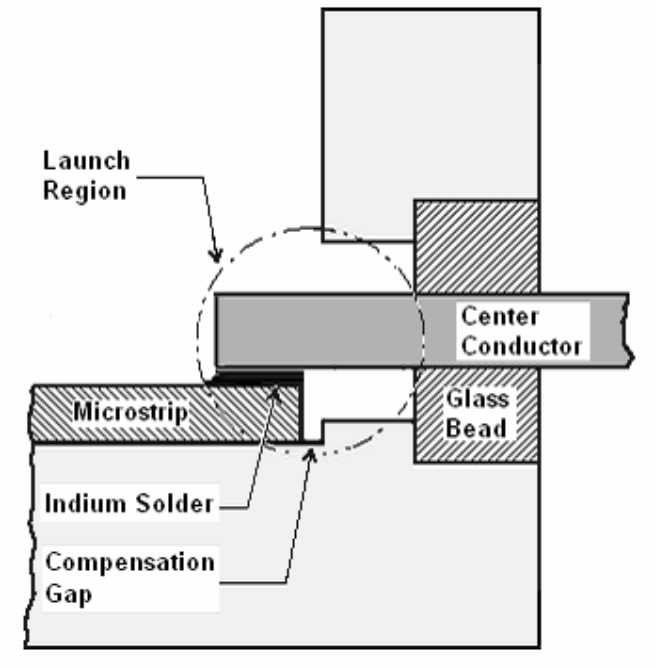

Figure 16. Cross Section of the Coaxial-to-Microstrip Transition

4.2. Dielectric Substrate of Feeding Layer

As it is described on Section 3.4, coaxial-to-microstrip launcher will insert the signal to the microstrip line and this signal will be distributed to each patch element by using Aperture Coupling Feeds. This method separates the antenna into two different dielectric substrate layers by discriminating the feeding and radiation functions. This section discusses the dielectric substrate choice for the feeding layer belonging just below the Suhner Panel Launcher Connector. The choice of the dielectric substrate for radiation layer will be discussed on Section 6.2.2.

It is known that feeding line of the antenna should have a thinner substrate and higher permittivity, so that the signal binds to dielectric substrate and do not produce higher spurious radiations (Section 3.1). In addition, for thicker substrates, the input impedance of the Panel Launch Coaxial Line Connector becomes more inductive which deteriorates the matching characteristic and produces intrinsic radiation. Therefore, the height of the dielectric substrate should be chosen as low as possible.

The other parameter important for the dielectric substrate choice is the permittivity value. Even though higher permittivity is required for proper transmission, very high permittivity will result in high amount of signal attenuation, less efficiency and narrower bandwidth.

In addition to the connector properties and inductive effects of the dielectric substrate, the other and maybe the most important factor influencing the matching of coaxial-to-microstrip launcher is the microstrip line width. The substrate thickness and permittivity values determine the microstrip line width value satisfying the required characteristic impedance, mostly the 50 Ω. As keeping the characteristic impedance value constant, the microstrip line width is narrower for lower substrate thicknesses and higher permittivity values (Table 1). The width of the microstrip line is important for fabrication process, since the sensitivity of the production devices may not give permission to obtain the required width value, especially for millimeter wave frequencies.

By using the Matlab 7.1 software program and the codes given on Appendix B, the microstrip line widths (W) are calculated for RO3000® series dielectric substrates at different permittivity and dielectric height values (Table 1). These values are adjusted to obtain the characteristic impedance of 50 Ω. The thickness of the copper cladding is used as T=0.035 mm (1 oz) and the calculations are done at center frequency of 36.85 GHz.

Table 1. Microstrip Line Widths

Material / Height	**RO3003®** ε_r**=3**	**RO3006®** ε_r**=6.15**	**RO3010®** ε_r**=10.2**
0.127 mm (0.005'')	W= 0.284 mm	W= 0.151 mm	W= 0.083 mm
0.254 mm (0.010'')	W= 0.583 mm	W= 0.313 mm	W= 0.176 mm

Among these 3 materials given in Table 2, the product of Rogers Corporation, RO3003® type dielectric substrate is decided to be used in feeding layer of the microstrip patch array antenna. The dielectric height of 0.01'' (H=0.254 mm) is also accepted to be used. Since, other dielectric materials and RO3003® with H=0.127 mm require very sensitive fabrication processes on microstrip lines. The dissipation factor of the RO3003® material is also lower than other materials (tanδ=0.0013 at 10 GHz) and it could be used at very high frequencies. The material has a permittivity value of ε_r=3. The thickness of the copper cladding is determined as T=0.035 mm (1 oz). The characteristic impedance (Z_0) and the guided wavelength (λ_g) of the microstrip line are given on Figure 17 and Figure 18 respectively. These figures are solved by using the RO3003® material and the parameter values selected to be used in this thesis study (H=0,254 mm, T=0.035 mm, ε_r=3 and W=0.583 mm).

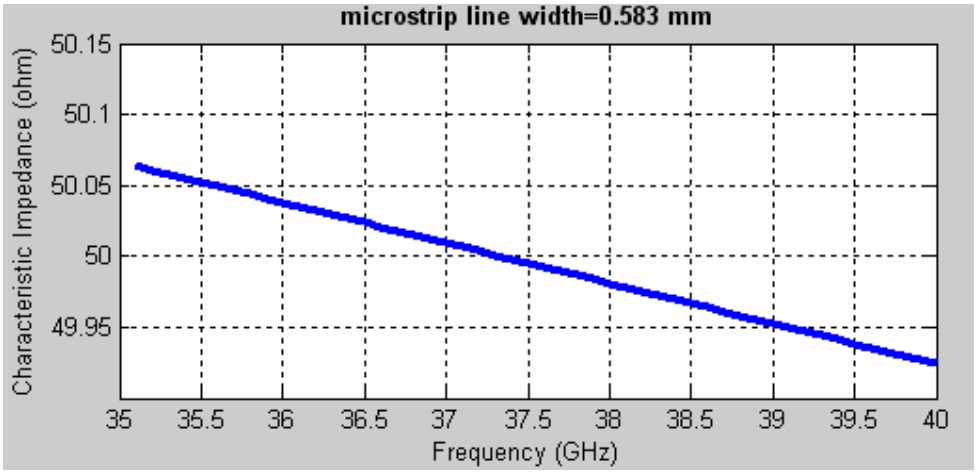

Figure 17. Characteristic Impedance vs. Frequency for Microstrip Line of Feed Layer

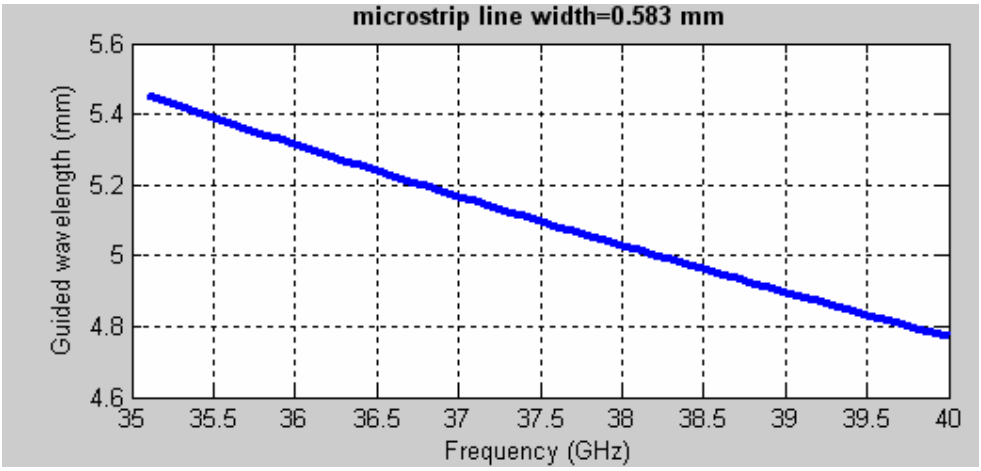

Figure 18. Guided Wavelength vs. Frequency for Microstrip Line of Feed Layer

4.3. Electromagnetic Simulations

HFSS™ v9.2 is a popular software program widely used by electronics engineers. It is mostly used for designing electromagnetic devices. The program gives highly accurate results, since even very complex projects could be entered to the program by using 3D Modeling interface and full wave electromagnetic solutions are executed on projects. In addition, commercially available materials such as RO3003® and RT/duroid® 5880 could easily be included to projects from the menu with the correct material specifications.

On this chapter, by using HFSS™ v9.2 electromagnetic software program, different design alternatives of coaxial-to-microstrip launcher are modeled and electromagnetic simulations are executed on these models. The simulation results are evaluated with respect to values of return losses and transmission losses. The simulations are helpful to see if the selected materials (connector, dielectric substrate) satisfy good matching characteristics. It is also tried to understand what the effects of changing some design parameters on matching are and what could be done to improve matching characteristic of coaxial-to-microstrip launcher.

Each simulation model includes 2 coaxial-to-microstrip launchers as shown on Figure 19, 24 and 26. This method is used to obtain matched loads at both ends of the model. So, the calculated return loss values are the sum of reflections from each launcher. Despite the additive property of the method, it is still a good way of calculating the matching characteristic of a single coaxial-to-microstrip launcher. It is expected that the total reflection loss value shows fluctuations around the reflection loss value of a single port [7]. This is due to phase differences between two reflections coming from two different discontinuity points. The phase difference changes with frequency and the magnitude of the reflected signal magnifies or diminishes depending on the value of this phase difference.

HFSS™ v9.2 software program starts the simulation by using a non-sensitive solution and increases the sensitivity level as executing the simulation. Simulation results are getting more sensitive with increasing value of last adaptive pass level. The simulations on Section 4.3.1 and 4.3.2.2 use adaptive pass level of 12. The coplanar waveguide simulation on Section 4.3.2.3 could only be realized with adaptive pass level of 10 because of the complexity of the model.

4.3.1. SRI Connector Gage SMA Female PCB Mount 21-146-1000-01

The first electromagnetic simulations were executed by using SRI SMA PCB Mount type connector and RT/duroid® 5880 type dielectric substrate. These materials were modeled as exact as possible and the coaxial-to-microstrip launcher is constructed on HFSS™ v9.2 as given on Figure 19.

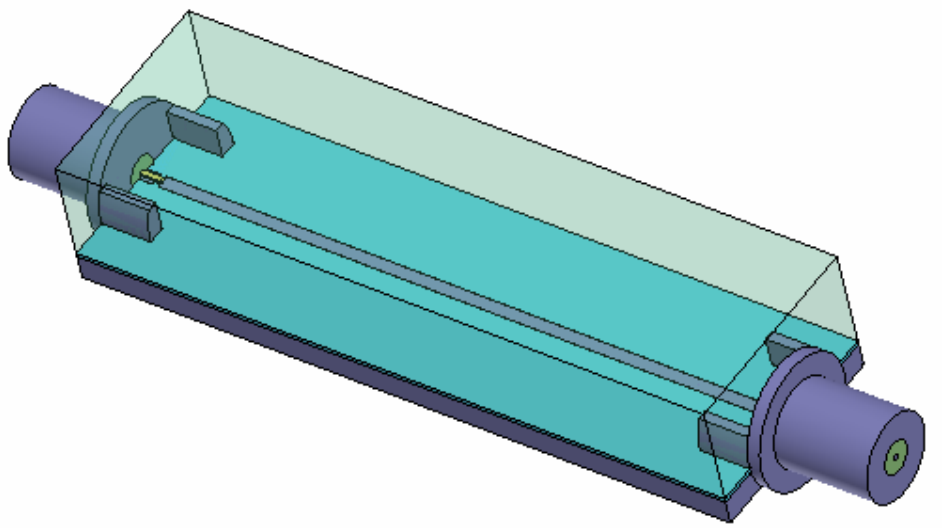

Figure 19. Coaxial-to-Microstrip Launcher Model-1 on HFSS™ v9.2

The properties of the RT/duroid® 5880 type dielectric substrate used on this simulation could be summarized as ε_r= 2.2 (dielectric constant), H=0.254 mm (dielectric height), T=0.017 mm (copper cladding thickness) and tanδ=0.0009 at 10 GHz (dissipation factor). By using these parameter values, the microstrip line width satisfying the characteristic impedance of 50 Ω is calculated as 0.75 mm (Appendix A, Appendix B). The width and the length of the substrate are also selected to be 6 mm and 40 mm respectively.

Dielectric substrate material could only be attached to the SRI SMA PCB Mount Connector by fixing the material between the three legs extending in front of the connector (Figure 20.a). The distance between the upper and lower legs is equal to 1.778 mm. However, the dielectric substrate used in this simulation has a thickness of 0.254 mm. Therefore, a copper plate with thickness of approximately 1.5 mm is placed below the dielectric substrate and they are fixed to the connector together. The mounting is shown in Figure 20.a where the materials except from the connector are made transparent for illustration.

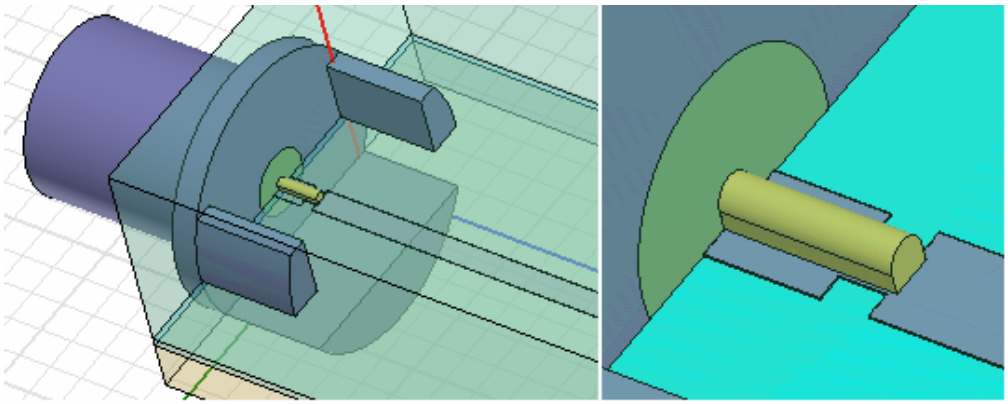

Figure 20. Coaxial-to-Microstrip Launcher Model-1 Contact Point

The matching properties of this coaxial-to-microstrip launcher design are observed for two cases. Firstly, the microstrip line is made to have a constant width and the simulation results are obtained. Matching characteristic is not satisfactory as it could be seen on Figure 22 and Figure 23 (lines of 'without notch'). Afterwards, notches are added to the microstrip line just below the contact point in order to improve the matching characteristic (Figure 20.b). Notches are known to introduce inductive effect canceling the capacitive impedance of the contact point. The capacitive impedance is caused by the fringing fields existing between the center conductor of the connector and the microstrip line. The notch dimensions that give the best matching characteristic are determined by using optimization tool of the HFSS™ v9.2. The improvement on S parameters could be seen on Figure 22 and Figure 23 (lines of 'with notch'). The notch design parameters are shown on Figure 21 and values of these parameters that are responsible for the given improvement on matching characteristic are such that Notch offset= 0.857 mm, Notch length= 0.355 mm and Notch width= 0.198 mm.

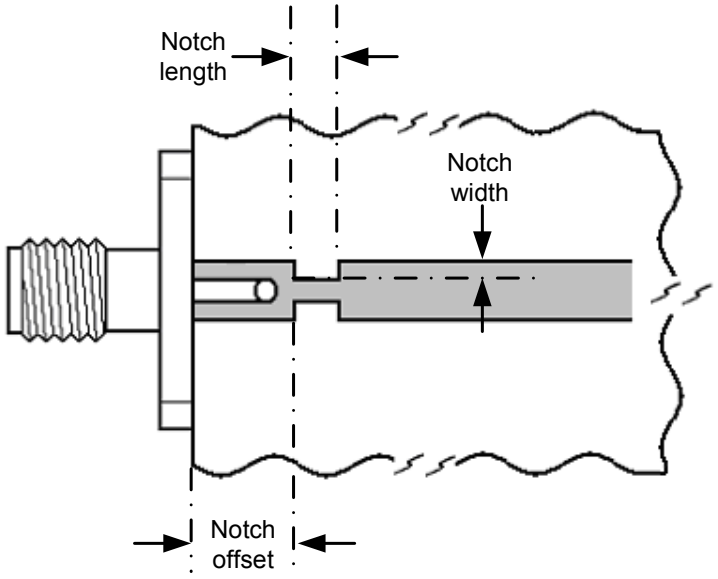

Figure 21. Coaxial-to-Microstrip Launcher Notch Design Parameters

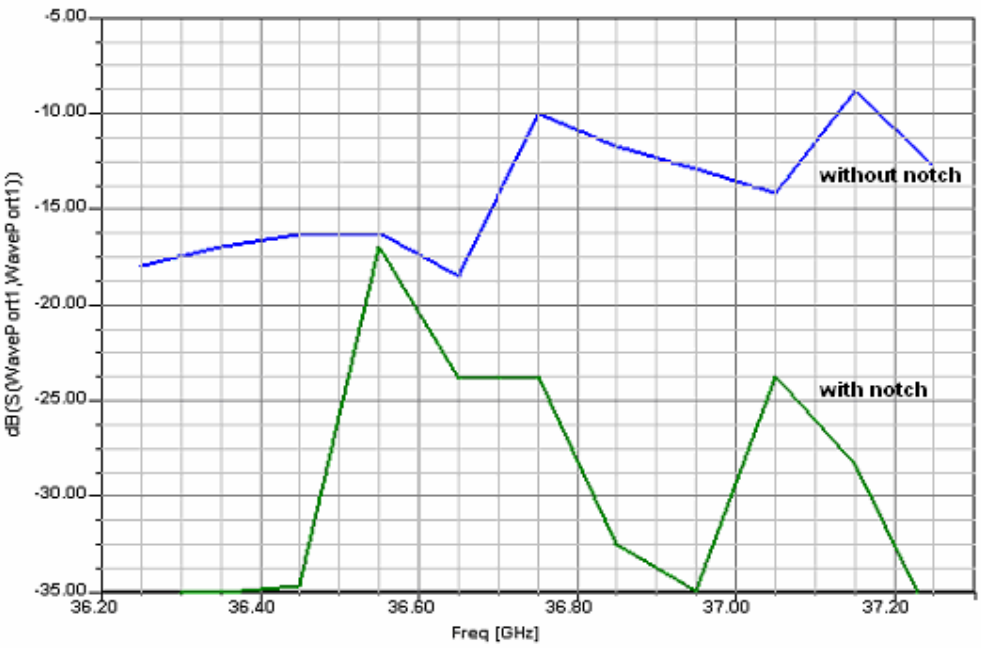

Figure 22. S_{11} vs. Frequency for Coaxial-to-Microstrip Launcher Model-1

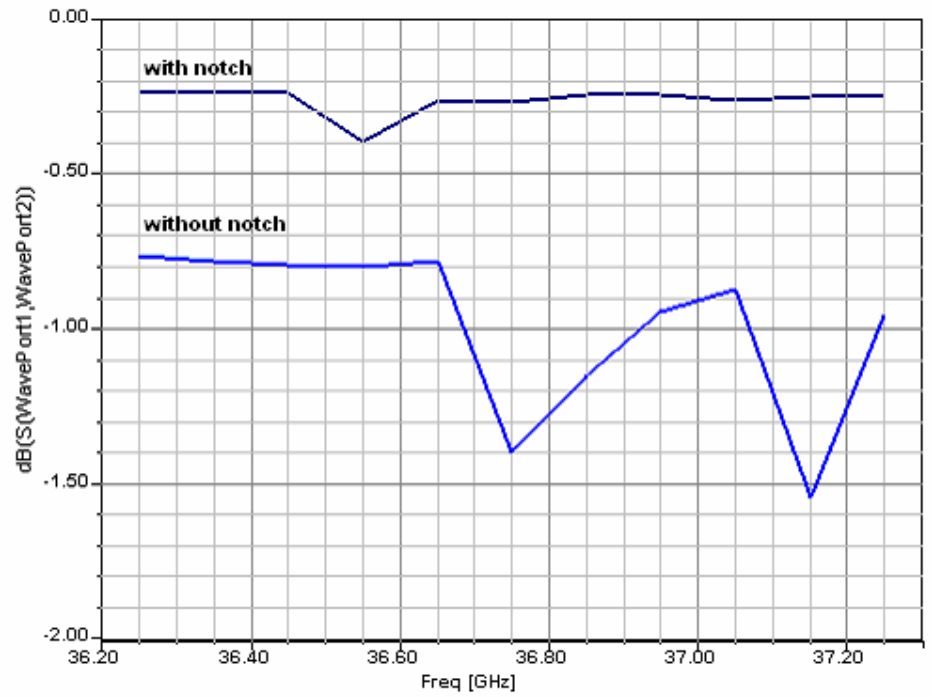

Figure 23. S_{21} vs. Frequency for Coaxial-to-Microstrip Launcher Model-1

The simulations executed on this section confirm that notches placed on the microstrip line result in improved matching characteristic. However, the fabrication of these notches is not very practical for the case studied in this section. The notches are so small that the sensitivities of available devices are not sufficient to fabricate them. Therefore, the usage of notches on microstrip line is rejected and the simulations of the following section use microstrip line models with constant width.

4.3.2. Suhner 2.92 mm Panel Launcher 23 SK-50-0-52/ 199NE

The electromagnetic simulations executed on this section include Suhner Panel Launcher type connectors and RO3003® type dielectric substrates. These materials were modeled as exact as possible and the coaxial-to-microstrip launcher is constructed on HFSS™ v9.2 as given on Figure 24. These materials are the ones that will be used in fabrication process. Therefore, these simulations need to show good matching characteristics. This will be achieved by adjusting some design parameters. The explanations of the design parameters will be given on the first part of this section. Afterwards, the results of the simulations will be introduced.

On the final part, an additional method for improving the matching characteristic will be defined and the simulations will be executed to see if it works.

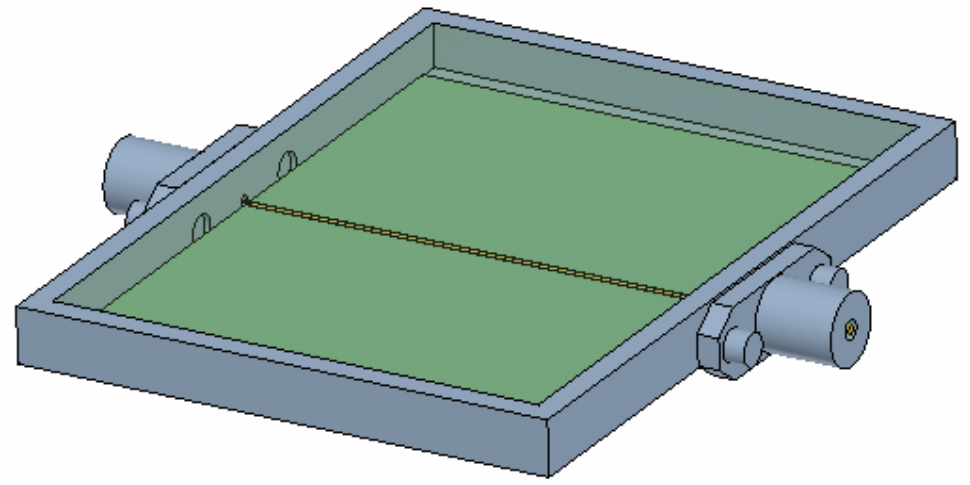

Figure 24. Coaxial-to-Microstrip Launcher Model-2 on HFSS™ v9.2

The properties of RO3003® dielectric substrate material was defined before in Section 4.2. In addition, the RO3003® dielectric substrate width are taken fixed at the value of 50 mm. The mounting of the Suhner Panel Launcher connector inside the mechanical structure and the contact point of the inner conductor with the microstrip line is shown on Figure 25.

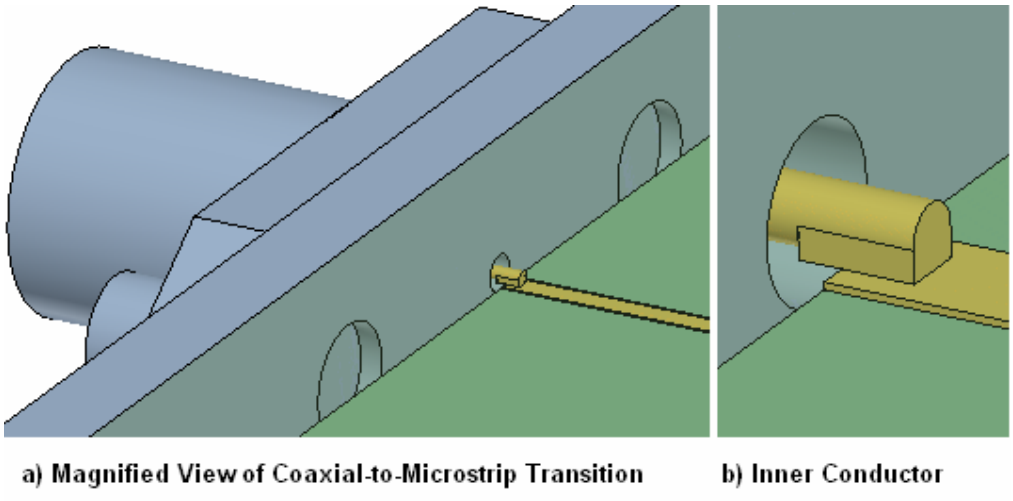

Figure 25. Coaxial-to-Microstrip Launcher Model-1 Contact Point

4.3.2.1. Design Parameters

Electromagnetic simulations are executed to optimize the design parameters of coaxial-to-microstrip launcher. These design parameters are listed below and their importance are explained on the following paragraphs.

1. Air gap radius
2. Compansation gap length

The air gap radius value is selected as the first design parameter (Figure 15). One may say that the radius of the air gap should be calculated in order to obtain characteristic impedance of 50 Ω inside the gap. The radius of the center pin extending along the air gap is 0.15 mm [46]. By applying the given value (a=0.15 mm) on the eqn. C.1, the air gap radius value satisfying characteristic impedance (Z_0) of 50 Ω is calculated as r=0.345 mm. However, the air gap radius value given on the connector catalogue is confusing and equals to r=0.445 mm. Therefore, it is understood that at the connection point the air gap radius value affects the matching characteristic and a special care should be taken on calculations. The value of the air gap radius should be calculated by building a coaxial-to-microstrip transition model as exact as possible and executing electromagnetic simulations on the model. On following section, it is inspected which one of the air gap radius value, the value given on connector catalogue or satisfying characteristic impedance of 50 Ω, gives a better matching characteristic and what the optimum air gap radius value is.

The second design parameter is the compensation gap length (Figure 16). Practical coaxial-to-microstrip launchers always leave a small compensation gap at the contact point with microstrip [51-52]. The reason for the usage of compensation gap is similar with the reason of notch usage described in Section 4.3.1 which is about canceling the effects of capacitive fringing fields at contact region. Electromagnetic simulations will be executed on the next section in order to show whether compensation gap is crucially important or not. The optimum compensation gap length value giving the best matching characteristic will also be determined.

Besides two design parameters, electromagnetic simulations are executed for different values of substrate length as keeping other parameters fixed. This is required to be sure that coaxial-to-microstrip launcher has good matching property. Since, there is always a possibility that different reflections coming from different parts of the antenna are in opposite phase and this opposite phase condition results in detection of the returned signal with reduced power. Only one simulation may orient the designer incorrectly, and the designer should be aware of this situation. The reflections on the input port include the reflections from the second coaxial connector and the dielectric substrate boundaries. These reflections are mostly counted on S_{11} calculation. If different substrate lengths are used, the phases of these returned signals will change in each simulation and any mistake on return loss calculation will be spotted. The S_{11} curve is expected to be consistent for each run in order to have a good match.

4.3.2.2. Simulation Results

Totally 13 different simulations were executed on the model shown on Figure 24. The differences between each simulation are the values of air gap radius, compensation gap length or the dielectric substrate length. These 13 simulations are grouped under 8 cases where the results of these simulations will be compared easily under meaningful conditions. The outputs of the simulations and the graphs of S parameters are collected under case numbers and presented on Appendix D. In this section, these cases are used to conclude which parameter values are to be selected in coaxial-to-microstrip launcher design.

<u>Cases to see the effect of dielectric length changes:</u>

Case 1: The substrate length is adjusted to the values of 40 mm, 45 mm, 50 mm while the design parameters are fixed at the values of compensation gap length=0 mm and air gap radius=0.4 mm.

Case 2: The substrate length is adjusted to the values of 40 mm, 45 mm, 50 mm while the design parameters are fixed at the values of compensation gap length=0.1 mm and air gap radius=0.4 mm.

Case 3: The substrate length is adjusted to the values of 40 mm, 45 mm, 50 mm while the design parameters are fixed at the values of compensation gap length=0.2 mm and air gap radius=0.4 mm.

The figures on Appendix D present that matching characteristics do not change remarkably with changes of substrate length value. This means that the graphical results obtained by the simulation program are accurate and the simulation model was not constructed with serious failures. For each substrate length, phase differences between the reflected signals change and these changes result in small shifts on matching characteristics.

Cases to see the effect of compensation gap length:

Case 4: The compensation gap length is adjusted to the values of 0 mm, 0.1 mm, 0.2 mm while other parameters are fixed at the values of substrate length=40 mm and air gap radius=0.4 mm.

Case 5: The compensation gap length is adjusted to the values of 0 mm, 0.1 mm, 0.2 mm while other parameters are fixed at the values of substrate length=45 mm and air gap radius=0.4 mm.

Case 6: The compensation gap length is adjusted to the values of 0 mm, 0.1 mm, 0.2 mm while other parameters are fixed at the values of substrate length=50 mm and air gap radius=0.4 mm.

The figures on Appendix D present that a compensation gap is strongly needed while designing a coaxial-to-microstrip launcher. The S parameters between the frequencies of 36.7 GHz and 37 GHz show the improvement on matching when a compensation gap length higher than 0 mm is used on the design. The compensation gap length value of 0.1 mm satisfies return loss values below -17 dB while the value of 0.2 mm satisfies return loss values below -24 dB which is really an expressive result. Therefore, the compensation gap value of 0.2 mm will be used in coaxial-to-microstrip launcher design. This result could also be concluded if the S_{11} lines on figures of Case 1 and Case 2 are compared to each other.

Cases to see the effect of air gap radius:

Case 7: The air gap radius is adjusted to the values of 0.35 mm, 0.4 mm, 0.45 mm while other parameters are fixed at the values of substrate length=40 mm and compensation gap length=0.1 mm.

Case 8: The air gap radius is adjusted to the values of 0.35 mm, 0.4 mm, 0.45 mm while other parameters are fixed at the values of substrate length=50 mm and compensation gap length=0.1 mm.

The figures on Appendix D present that the air gap radius value is not a crucial parameter while developing a coaxial-to-microstrip launcher. For the two cases, the changes of air gap radius value do not affect the return loss value significantly. Finally, it could be said that the air gap radius value of 0.4 mm will be used in coaxial-to-microstrip launcher design which is also reasonable with respect to fabrication capabilities.

In conclusion the design parameters of the coaxial-to-microstrip launcher is chosen as compensation gap length=0.2 mm and air gap radius=0.4 mm. The S_{11} and S_{21} parameters of this design are shown on the figures of Case 3.

4.3.2.3. Coplanar Waveguide Simulation

The figures on Appendix D do not show stable characteristics. This is mainly due to the reflections coming from many different locations of the dielectric substrate. It is known that at millimeter wave frequencies, signal flowing along the microstrip line is more likely to create higher order modes and surface wave losses. These unexpected waves are scattered all over the substrate and reflected from the boundaries towards any direction. Some amount of these waves contributes to the return loss of the input port. Hopefully, there is a method to eliminate these unexpected waves such as using a coplanar waveguide structure and adding shorting pins at some locations to short the upper and lower plates of the dielectric substrate (Figure 26 and Figure 27.a). Shorting pins creates a kind of tunnel where the signal flows more efficiently. These shorting pins absorb the unexpected waves scattered through the substrate and reduce the reflections.

The ground on the upper plate should be away from the microstrip line with a distance higher than the line width. Using below this value changes the microstrip line characteristic impedance while using above this value reduces the grounding properties of the upper ground.

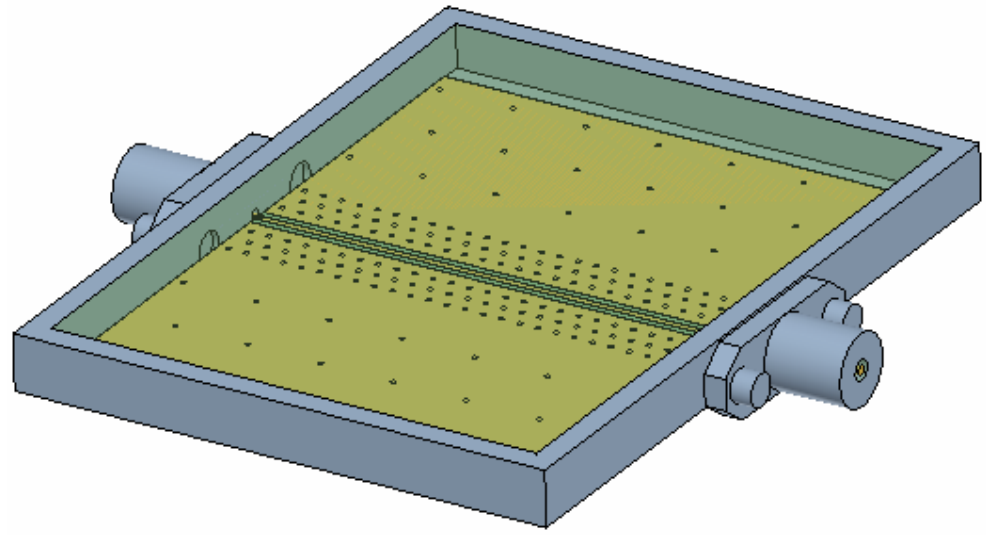

Figure 26. Coaxial-to-Microstrip Launcher Model-3 on HFSS™ v9.2

The coplanar waveguide microstrip structure is constructed by forming 2 non-copper strips on the top layer of the substrate (Figure 27.b). The widths of the non-copper lines are equal to the width of the center microstrip line (width=0.583 mm).

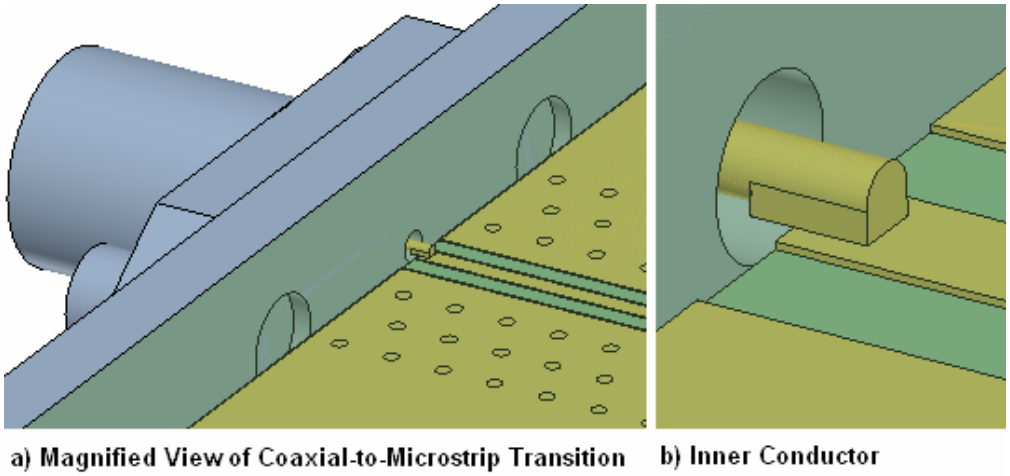

Figure 27. Coaxial-to-Microstrip Launcher Model-3 Contact Point

The shorting pins of the coplanar waveguide structure should be denser near the center line of the microstrip where surface waves are in higher amplitude. Shorting pins having the diameter value of 0.5 mm are known to be effective. There exist technologies for applying thinner shorting pins, but these are more expensive and not mandatory. In addition, the distance between the shorting pins should be higher than 0.3 mm, since fabrication faults start to occur for lower values. During this thesis studies, the distance between the shorting pins is taken as 0.5 mm for the locations having pins at high density. Actually, this distance should be lower than $\lambda_g/20$ which is equal to 0.26 mm at the center frequency of the design.

The other parameters of the simulation are taken as substrate width=50 mm, substrate length=40 mm and air gap radius=0.4 mm. The air gap radius given here is the design decision of the previous section. In this section, simulations are executed for compensation length values of 0.1 mm and 0.2 mm and the results are shown on Figure 28 and Figure 29. These figures also contain the matching characteristics of the previous section where the same design parameters are used with a normal microstrip line.

The following figures state that using coplanar waveguide reduces reflection losses, smoothes the matching characteristics and expands it to wider frequency range and improves the matching especially around the center frequency (36.5 GHz to 37 GHz).

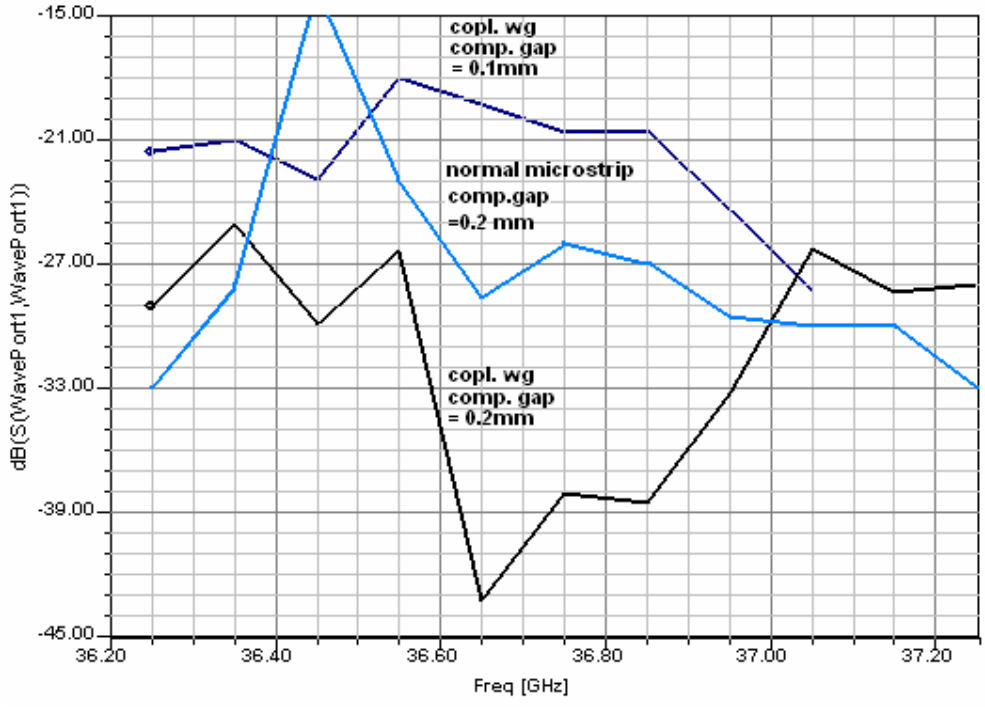

Figure 28. S_{11} vs. Frequency for Coaxial-to-Microstrip Launcher Model-3

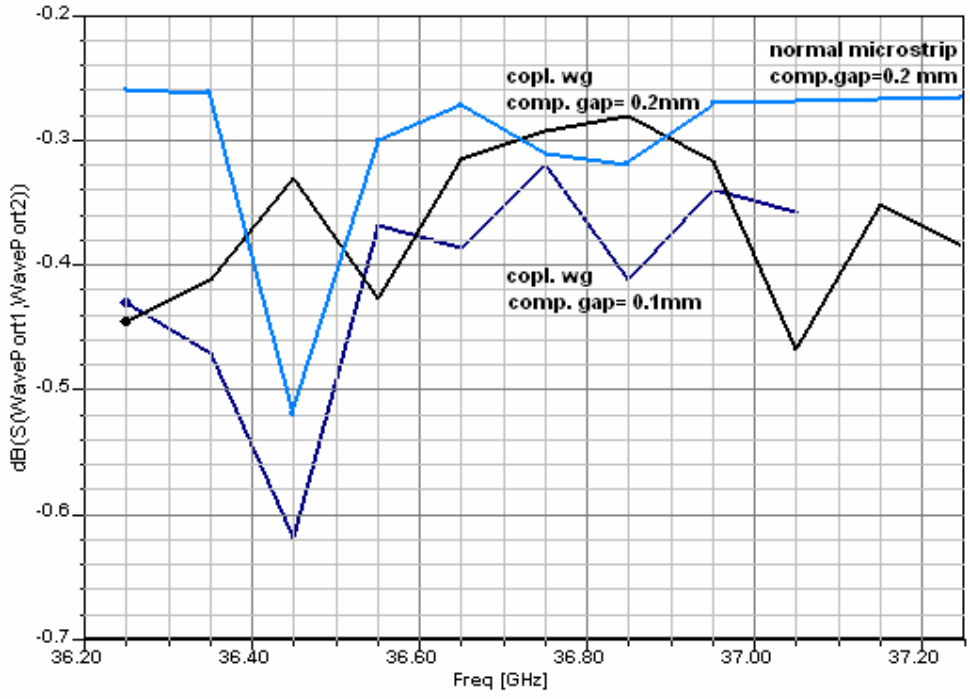

Figure 29. S_{21} vs. Frequency for Coaxial-to-Microstrip Launcher Model-3

CHAPTER 5

MICROSTRIP PRINTED POWER DIVIDER DESIGN

Antenna arrays consist of more than one antenna elements. For distributing the signal and allocating necessary amount of power to array elements, power dividers are widely used by engineers. There are vast amount of power divider design alternatives applied on microstrip systems all over the world. On this chapter, some power divider alternatives will be discussed by considering some electromagnetic simulation results.

The simulation models on Chapter 4 included all the mechanical and detailed connector structures. This was necessary to model the coaxial-to-microstrip launcher, since the design highly depends on the contact point of the connector and the mechanical structure of the launch region. But these extra elements increase the volume of simulation and slow the simulation process. From now on, it is moved to a different design step and some other components will be simulated by using electromagnetic simulation program. While designing a system, each design step should be evaluated individually to obtain the best result. The different design steps should be separated from each other to reduce work and concentrate on a small area of interest. As for the power divider design, it is independent from the coaxial-to-microstrip launcher and could be designed on its own. Therefore, the electromagnetic simulations of power divider models are executed by using simple ports inserting signal to the microstrip line.

5.1. Simple Power Divider Model

The first simulated power divider model is constructed as given on Figure 30 [7]. The model is simulated by using RO3003® type dielectric substrate properties. Microstrip line widths on different sections are calculated by using the

formulations given on Appendix A. The width of the main branches is adjusted to 0.583 mm to satisfy 50 Ω. The impedance transformer section is calculated 1.27 mm ($\lambda_g/4$) in length and 0.99 mm (35.36 Ω) in width. The electromagnetic simulation results are shown on Table 2.

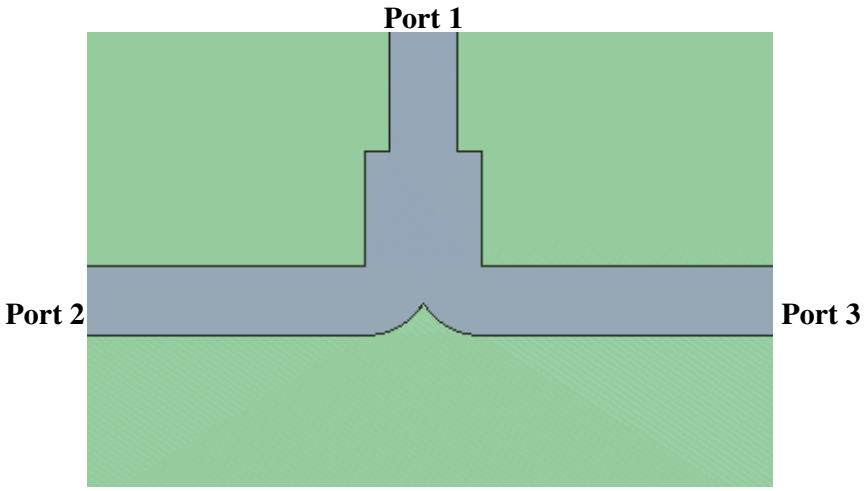

Figure 30. Simple Power Divider Model

Table 2. Simulation Results of Simple Power Divider Model (Convergence=0.048)

	F=36.7 GHz	**F=36.85 GHz**	**F=37 GHz**
S_{11} (dB,Phase)	-12.1, -146	-12.2, -171	-12.4, 164
S_{21} (dB,Phase)	-4.06, -81.4	-4.05, -103	-4.06, -125

The return loss of the model is not low enough to develop a parallel feeding network with many branches. The return loss is expected to be lower than -20 dB in order to develop efficient circuits. The reasons for the poor characteristic could be summarized as below [29].

- The transition between the 50 Ω and 35.36 Ω microstrip lines is not smooth
- There does not exist any 25 Ω microstrip line between the 50 Ω legs and the 35.36 Ω microstrip line.

- The cut region between the 50 Ω legs should not be circular; it should be triangular.

- The calculated microstrip line widths may not give the required characteristic impedances (50 Ω and 35.36 Ω) when simulated with HFSS™ v9.2.

5.2. Improved Power Divider Models

Developing superior power dividers could be managed by eliminating the problems faced with on the previous section. The models of this section are also simulated by using RO3003® type dielectric substrate properties.

Firstly, simple microstrip lines are simulated to see the relation between the line width and the characteristic impedance. It is observed that the characteristic impedance values calculated by the formulas on Appendix A and simulated by HFSS™ v9.2 show differences. To specify, the 50 Ω microstrip line width should be equal to 0.59 mm instead of 0.583 mm and the 35.36 Ω microstrip line width should be equal to 0.99 mm instead of 0.95 mm. In addition, the width of the 25 Ω microstrip line is observed to be equal to 1.44 mm.

As a second step, the bending points of the 50 Ω microstrip line are optimized by adding cuts on bends and adjusting the size of the cuts. The optimization results are shown below.

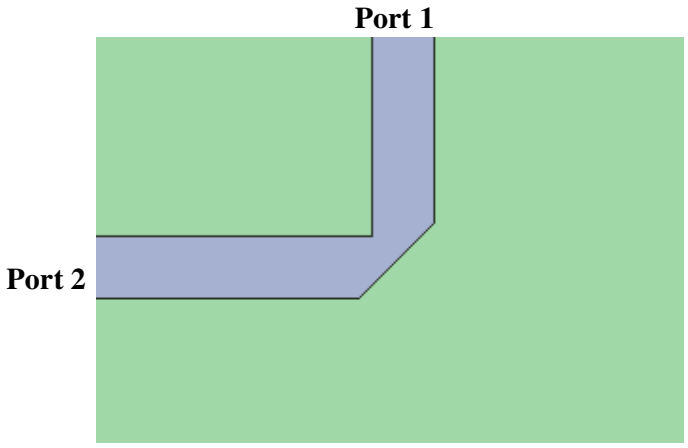

Figure 31. 90° Microstrip Line Bend

Table 3. Simulation Results of 90° Microstrip Line Bend (Convergence=0.016)

	F=36.7 GHz	**F=36.85 GHz**	**F=37 GHz**
S_{11} (dB,Phase)	-31.9, -119	-31.5, -129	-31.1, -149
S_{21} (dB,Phase)	-0.304, 77.4	-0.307, 70.2	-0.309, 63

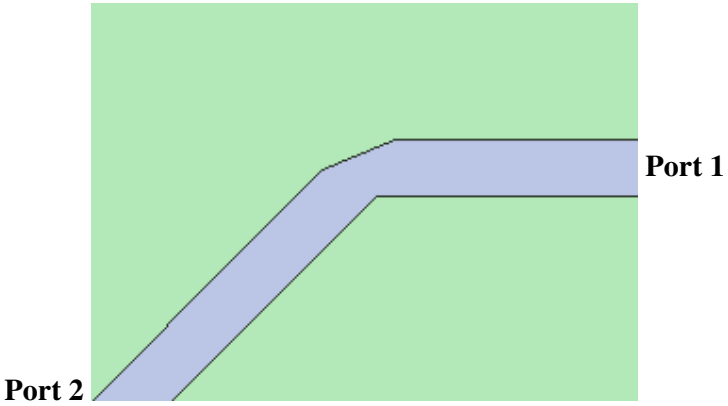

Figure 32. 45° Microstrip Line Bend

Table 4. Simulation Results of 45° Microstrip Line Bend (Convergence=0.018)

	F=36.7 GHz	**F=36.85 GHz**	**F=37 GHz**
S_{11} (dB,Phase)	-32, -111	-32, -125	-32, -139
S_{21} (dB,Phase)	-0.191, 61.9	-0.193, 54.6	-0.196, 47.3

Finally, 3 different types of power divider models are developed by using the simulated microstrip line widths, by adding a 25 Ω microstrip line between the 50 Ω legs and the 35.36 Ω microstrip line, by making the transition between the 50 Ω and 35.36 Ω microstrip lines smooth and finally by adding triangular cuts at the junction of the 50 Ω microstrip legs. The lengths of the 35.36 Ω microstrip lines are optimized for each model to obtain the best matching at the frequency range between 36.7 GHz and 37 GHz. The return and transmission losses are found to be highly satisfactory for each model. The power divider models and the simulation results are shown on following figures and tables.

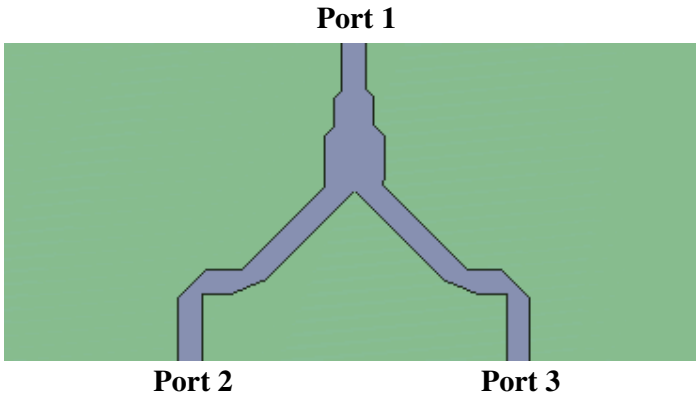

Figure 33. Improved Power Divider Model-1

Table 5. Simulation Results of Improved Power Divider Model-1 (Convergence=0.022)

	F=36.7 GHz	**F=36.85 GHz**	**F=37 GHz**
S_{11} (dB,Phase)	-40.8, 56.7	-43.1, 86.6	-41.4, 121
S_{21} (dB,Phase)	-3.47, -106	-3.47, -111	-3.47, -116

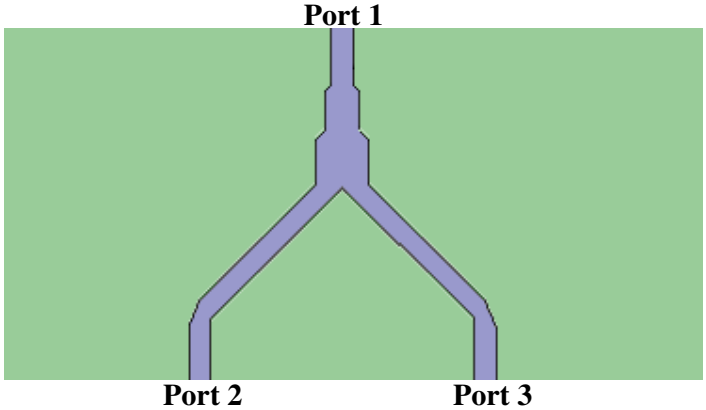

Figure 34. Improved Power Divider Model-2

Table 6. Simulation Results of Improved Power Divider Model-2 (Convergence=0.01)

	F=36.7 GHz	**F=36.85 GHz**	**F=37 GHz**
S_{11} (dB,Phase)	-26.7, -160	-27.5, -160	-28.4, -159
S_{21} (dB,Phase)	-3.28, -14.9	-3.28, -19.6	-3.28, -24.2

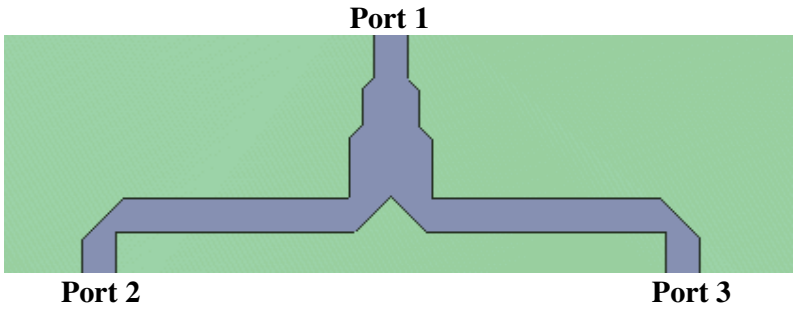

Figure 35. Improved Power Divider Model-3

Table 7. Simulation Results of Improved Power Divider Model-3 (Convergence=0.002)

	F=36.7 GHz	**F=36.85 GHz**	**F=37 GHz**
S_{11} (dB,Phase)	-30, 90.4	-29, 89.1	-28.1, 87.8
S_{21} (dB,Phase)	-3.53, 143	-3.54, 140	-3.54, 138

The distances between port 1 and 2 equal to the values of 20 mm, 16 mm and 8.5 mm approximately for improved power dividers of Model 1, Model 2 and Model 3 respectively. It is expected to have reducing transmission losses as moving from model 1 to model 3. However, Model 3 is observed to have the biggest losses. The reason for this situation is understood when the antenna parameters of power divider models are investigated. When the power of incident wave is 1 Watt, the radiated power of Model 2 equals to 0.04 Watts while the radiated power of Model 3 equals to 0.1 Watts. This might be due to the sharper discontinuities in Model 3 that leads to higher spurious radiation.

5.3. Power Divider Models Having 1 Input 16 Output Ports

The improved power divider models are also used to form complex power divider models having 1 input and 16 output ports. These models are shown on Figure 36. The power divider models of this section are simulated by using RO3003® type dielectric substrate properties as it was done on previous sections.

Three Power Divider Models are similar to each other and show good matching characteristics as given on the tables below. Power divider elements of Model 3 occupy less area; therefore the total model has lesser volume than other models.

As a result, the simulation applied to the Model 3 produces more sensitive solutions and takes a lower convergence value.

Table 8. Simulation Results of Power Divider Having 1 Input 16 Output Ports Model-1 (Convergence=0.08)

	F=36.7 GHz	**F=36.85 GHz**	**F=37 GHz**
S_{11} (dB,Phase)	-31.1, -67.2	-34.6, -83.9	-36.5, -125
S_{21} (dB,Phase)	-13.1, -18.1	-13.2, -6.5	-13.3, -30.9

Table 9. Simulation Results of Power Divider Having 1 Input 16 Output Ports Model-2 (Convergence=0.051)

	F=36.7 GHz	**F=36.85 GHz**	**F=37 GHz**
S_{11} (dB,Phase)	-31.1, -150	-35.2, 133	-33.3, 84.2
S_{21} (dB,Phase)	-13.3, -25.7	-13.4, -50	-13.5, -74.1

Table 10. Simulation Results of Power Divider Having 1 Input 16 Output Ports Model-3 (Convergence=0.03)

	F=36.7 GHz	**F=36.85 GHz**	**F=37 GHz**
S_{11} (dB,Phase)	-19.5, 113	-20.1, 95.2	-21.1, 79.5
S_{21} (dB,Phase)	-13.6, 66.3	-13.5, 51	-13.5, 35.6

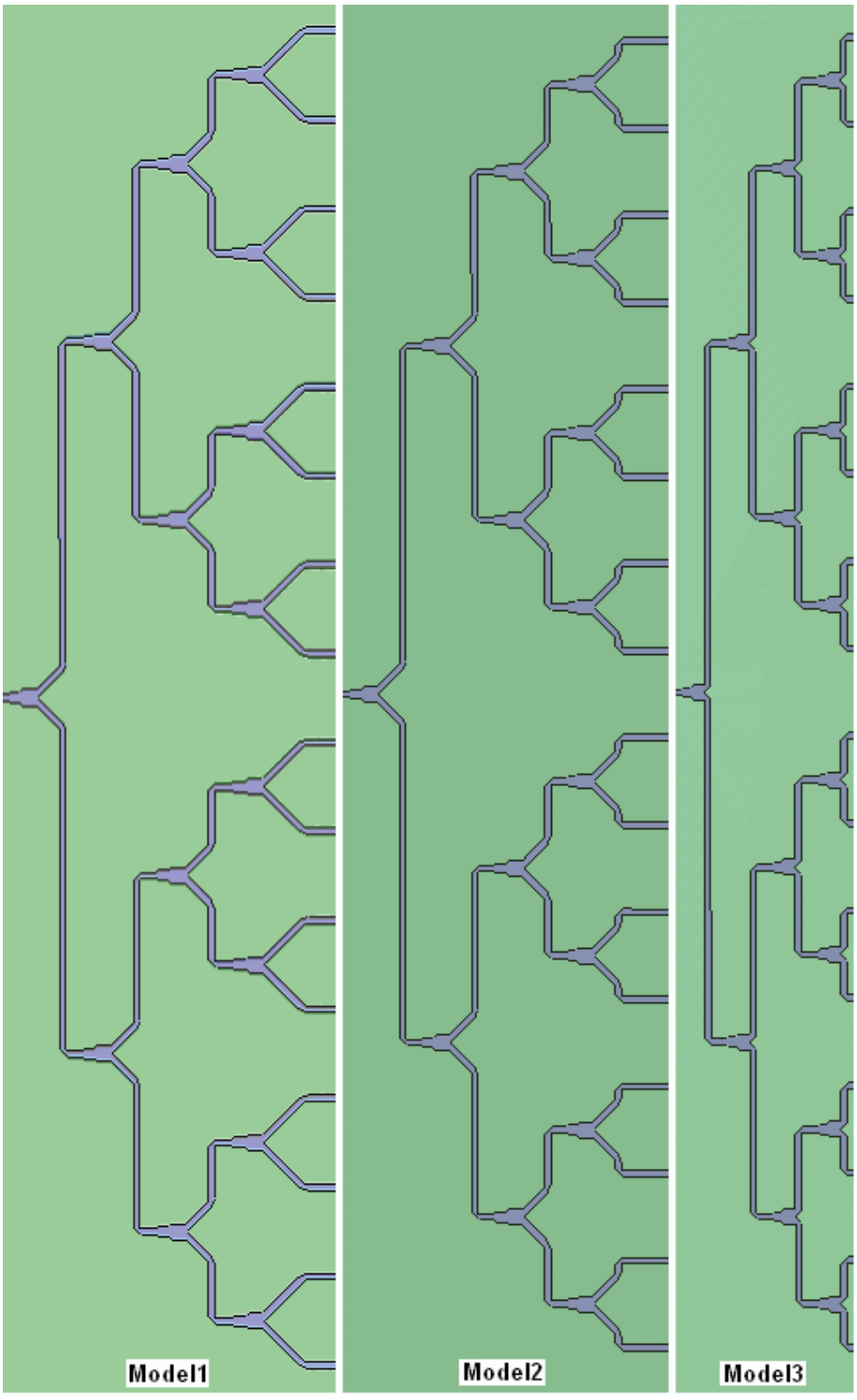

Figure 36. Power Divider Models Having 1 Input 16 Output Ports

CHAPTER 6

MICROSTRIP PATCH ARRAY DESIGN

Starting from the design of coaxial-to-microstrip launcher and power dividers and selection of the feed substrate, the studies finally comes to the point of microstrip patch array antenna design. On this chapter, the microstrip patch array antenna design is handled in five main steps and each design step is explained on different sections. Firstly, design steps for a single patch element are described. Afterwards, the parameters of an Aperture Coupled Single Patch Element are determined. Thirdly, patch elements are collected together to form an array and the design parameters of an array are introduced. Then, the feeding network alternatives are evaluated and the reasons for the selection of parallel feeding network are explained. Finally, electromagnetic simulations and parameter optimizations are described which are applied on the final design to ensure that a proper patch array antenna design is satisfied.

6.1. Patch Element Design

Microstrip patch array is a combination of patch elements. Patch array design starts from designing the single patch element. The dimensions of each patch element are independent of the patch array total element number, element spacings or the distribution of the elements on the dielectric substrate. The design of a single patch element includes 4 main steps as given below and these steps should be followed in an order.

1. Selecting a suitable antenna geometry
2. Selecting a suitable dielectric substrate
3. Choosing the element width
4. Computing the element length

6.2.1. Antenna Geometry

The rectangular and circular patches are the most common type of microstrip patch antenna geometries. In this thesis study, rectangular patch antenna is decided to be used because it is easier to fabricate. The formulations are also simpler for rectangular patch antenna.

6.2.2. Dielectric Substrate of Radiation Layer

On Section 4.2, Rogers Corporation RO3003® type is decided to be used for the dielectric substrate of the feeding layer. And, it is known from the Section 3.4 that the signal inserted from coaxial feed will be distributed to each patch element via apertures and some different kind of dielectric substrate will be used on radiation layer. This section discusses the points to account for the choice of the new dielectric substrate.

As described in Section 3.1, microstrip patch antenna should have a thicker substrate and lower permittivity, so that the radiation from patch element will be more efficient and bandwidth of the microstrip antenna is higher. It is also known that surface waves start to occur for thicker substrates. Therefore, the height of dielectric substrate is really critical parameter to determine.

Surface wave excitation takes place especially for substrates having thickness higher than $0.1\lambda_0$ [3]. The patch element is designed at the center frequency of f_r=36.85 GHz. At this frequency, the free space wavelength is calculated as λ_0=8.2 mm. Hence, the height of the dielectric substrate should not exceed 0.82 mm. In addition, the permittivity of the substrate should be as low as possible and the substrate should operate at the frequency range extending to at least 40 GHz.

Finally, the product of Rogers Corporation, RT/duroid® 5880 type dielectric substrate is decided to be used in radiation layer of the microstrip patch array antenna. The specifications of the material [32] states that RT/duroid® 5880 has a low dissipation factor (tanδ=0.0009 at 10 GHz) extending its usefulness towards K_u band (12-18 GHz) and above. An application of this substrate at frequency of 77 GHz is also reported [49]. The material has a very low permittivity value (ε_r=2.2) and different dielectric height alternatives. The dielectric height of 0.031''

(H=0.787 mm) is accepted to be suitable for the dielectric substrate choice. The thickness of the copper cladding is determined as T=0.017 mm (0.5 oz).

6.2.3. Patch Element Width

The practical width of the patch could be calculated by using the following equation where ε_r is the dielectric constant, c is the speed of light and f_r is the operating frequency [1, 5, 34].

$$W = \frac{c}{2f_r}\left(\frac{\varepsilon_r + 1}{2}\right)^{-1/2} \tag{6.1}$$

By using the center frequency value of 36.85 GHz and the RT/duroid® 5880 dielectric constant value of 2.2, the width of the patch element is calculated as W=3.2 mm. The patch element width may be chosen smaller or larger than this value. However, the efficiency is lower for smaller widths while the higher order modes excitation is higher for larger widths.

6.2.4. Patch Element Length

Patch antenna has a narrow bandwidth and it is crucial to satisfy the exact element length at the resonance frequency. Resonance frequency of a patch antenna (f_r) could be calculated by using eqn. 6.2. where m is an integer, L is the length of the patch and ε_e is the effective dielectric constant. ΔL is the line extension along the patch element length caused by the fringing fields existing along the radiating edges.

$$f_r = \frac{mc}{2(L + 2\Delta L)\sqrt{\varepsilon_e}} \qquad \text{m=1, 2, 3…} \tag{6.2}$$

The length of the radiating conductor or patch should be made approximately $\lambda/2$, so the patch starts to radiate. For the smallest patch antenna length, m should equal to one. Then, the length of the patch will be defined by eqn. 6.3 [1, 5, 33].

$$L = \frac{c}{2f_r\sqrt{\varepsilon_e}} - 2\Delta L \tag{6.3}$$

The line extension value (ΔL) should be calculated by using eqn. 6.4 [1, 5, 33] and included in eqn. 6.3. The effective dielectric constant (ε_e) and effective patch width (W_e) could be calculated by using the formulation on Appendix A. H is the height of the dielectric substrate.

$$\Delta L = 0.412H \frac{\varepsilon_e + 0.3}{\varepsilon_e - 0.258} \frac{\frac{W_e}{H} + 0.262}{\frac{W_e}{H} + 0.813} \tag{6.4}$$

By using the Matlab 7.1 software program and the codes given on Appendix B, the parameter values that are needed to determine the patch element length are calculated as given below.

W_e= 3.2374 mm, ε_e= 2.0384 (at f_r=36.85 GHz), ΔL= 0.3782 mm (at f_r=36.85 GHz)

Finally, the length of the patch element is calculated as L=2.1 mm. The resonance frequency of the patch antenna changing with the inserted signal frequency of 35GHz - 40GHz is shown on Figure 37.

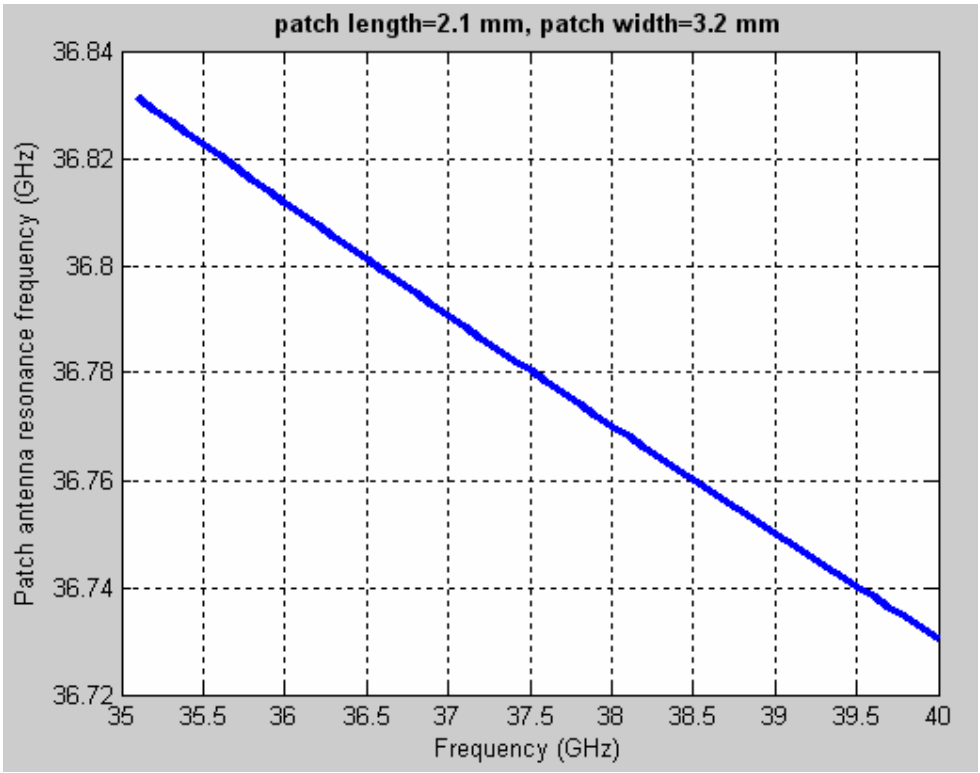

Figure 37. Patch Antenna Resonance Frequency vs. Inserted Signal Frequency

6.2. Aperture Coupled Single Patch Element

After determining the substrate properties of feeding and radiation layers and the dimensions of the patch element, the design comes to a point where these layers are connected with aperture coupling feed. The structure given on Figure 38 shows a single patch element fed by aperture coupling and an open circuit stub used to compensate the excessive reactance of the circuit. The model is simulated on HFSS™ v9.2 by using necessary dielectric substrate properties.

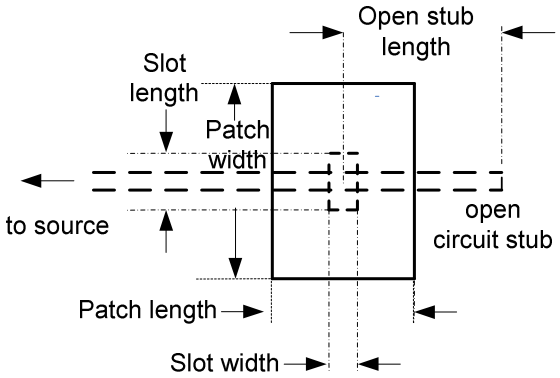

Figure 38. Aperture Coupling of a Single Patch Element

The S parameters and the antenna parameters of a single aperture fed patch antenna are obtained with the parameter values given below. The parameters except from "Open Stub Length", "Slot Length" and "Slot Width" were determined on previous sections.

- Open Stub Length = 3.12 mm
- Slot Length = 2.39 mm
- Slot Width = 0.4 mm
- Patch Length = 2.1 mm
- Patch Width = 3.2 mm
- Microstrip Line Width = 0.59 mm

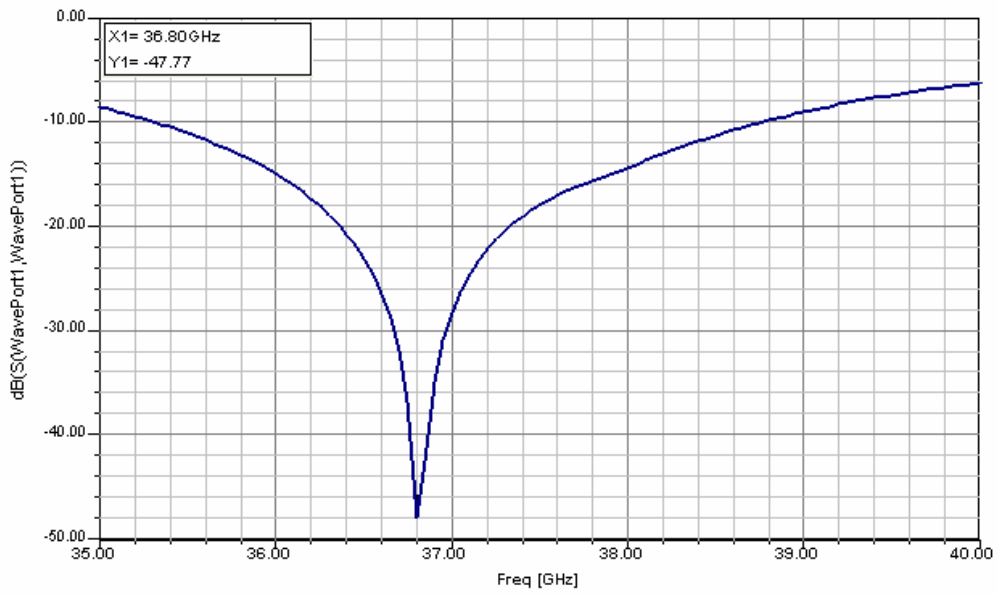

Figure 39. S_{11} vs. Frequency for Aperture Coupled Patch Antenna (Convergence=0.003)

Antenna parameters of the single aperture fed patch antenna could be summarized as below which are calculated at the frequency value of 37 GHz.

- Peak Directivity = 7.84 dB
- Peak Gain = 7.81 dB
- Peak Realized Gain = 7.80 dB
- Accepted Power = 0.998
- Radiation Efficiency = 0.994

6.3. Microstrip Patch Array Antenna Design

The spacing between adjacent antenna elements of an array should not exceed one wavelength for any frequencies within the frequency bandwidth in order to eliminate the spurious grating lobe occurrence [2]. Reducing the patch spacing below one wavelength is also useful to obtain higher gain values. However, half wavelength is the limit for small patch spacings, since lower spacings result in increase on mutual coupling effects [6]. The free space wavelength at the operating frequency band is between 8.17 mm and 8.1 mm, so the patch spacing should take value between 4.1 mm and 8.1 mm.

The overall antenna pattern of a microstrip patch array is formed with the contribution of each patch element. The antenna pattern of the array could be obtained by multiplying the single antenna pattern with a parameter called "Array Factor". Array factor varies with angle differences and it shapes the single antenna pattern to form the overall array pattern. The array factor depends on distances between patch elements, total number of the patch elements, the phase and amplitude differences of the currents between adjacent patch elements and the frequency of the field.

If we consider patch elements are equidistantly spaced (uniform array), the general formula of the array factor is derived as below [56]. The expression is given with spherical angles.

$$f(\phi,\varphi)=\sum_{m=1}^{n} a_m e^{jk_0\bar{r}_m.\bar{a}_r} \tag{6.5}$$

where a_m is the excitation coefficient, r_m is the relative position of the patch elements and n is the total number of patch elements. The coefficient a_m determines the amplitude and phase differences between patch elements and takes value relative to a reference element.

Furthermore, if we assume that patch elements are distributed in series with same distances between each other, current distribution is kept uniform in magnitude and the signal is inserted with constant phase differences between adjacent elements, the formulation of the Array Factor simplifies as below [56].

$$\left|f(\gamma)\right|=\left|\frac{\sin(n\gamma/2)}{n\sin(\gamma/2)}\right| \tag{6.6}$$

where,

n: total number of patch

$\gamma = \delta + k_0\, d \cos\theta$

where,

δ: current phase differences between adjacent patch elements

k_0: free space wave number ($k_0 = 2\pi/\lambda_0$)

d: distance between patch elements

θ: The angle between line where patch elements are placed and the line connecting the origin to the point of interest

The formulation given above could be used to plot antenna pattern for any patch array having patch elements linearly distributed and uniformly excited. By using the Matlab codes given on Appendix E, the 3 dB beamwidth values are calculated on the plane which is normal to the plane where patch elements are placed and to the line where patch elements are aligned along. To simplify, we may assume that patch elements are placed on x-z plane along the z line and the antenna pattern is calculated on z-y plane by using spherical angle θ (φ=90°). The frequency is 36.85 GHz for each case. The antenna pattern of a single patch element is created by a sinc function having 3 dB beamwidth value of 66.9°. All patch elements are assumed to be excited with equal amplitude and phase.

Table 11. 3 dB Beamwidth Values for Different Patch Spacings and Patch Numbers

3 dB BW	**n=2**	**n=4**	**n=6**	**n=8**	**n=16**	**n=32**
d=4 mm	52.5°	26°	17.2°	12.9°	6.4°	3°
d=5 mm	43.6°	20.9°	13.8°	10.3°	5°	2.4°
d=6 mm	**37.1**°	17.5°	11.5°	8.6°	4.2°	2.1°
d=7 mm	32.1°	15°	10°	**7.3**°	3.6°	1.7°
d=8 mm	28.4°	13.1°	8.6°	6.4°	3°	1.2°

While designing a patch array antenna, the array type should be determined with respect to the required antenna pattern specifications. For this thesis studies, it is decided to work on an array with 8x2 elements (16 patch elements in total). If patch spacing is determined as 6 mm (for n is equal to 2) and 7 mm (for n is equal to 8), the final product is expected to have 7.3° azimuth beamwidth and 37.1° elevation beamwidth values or vice versa. Peak directivity of this antenna is

calculated as 20.8 dB by applying these beamwidth values to the formula given below.

$$Peak\ Directivity\ (in\ dB) = 10 \times \log\left(\frac{32500}{BW_1 \times BW_2}\right) \tag{6.7}$$

6.4. Feeding Network Design

The maximum value of the gain and minimum sidelobe levels for an array antenna could be obtained when all antenna elements are fed with equal amplitude and phase values. While designing a feeding network and selecting a suitable method; this fact should be taken into account seriously.

The 3 main feeding network alternatives were given on Figure 10, 11 and 12. The distribution of the field to all of these 16 patch elements should be achieved by using one of these feeding networks. At this point, selection of one of these network alternatives is a crucial decision.

The previously discussed (Section 3.2, Figure 11) parallel feeding network has the advantage of uniform field distribution to patch elements with zero phase differences. However, this model is expected to produce high amount of losses, since it should include vast amount of power dividers. A successful power divider design is strictly mandatory for this feeding network alternative. Except from this model, there also exists another type of parallel feeding network alternative as given on Figure 40.

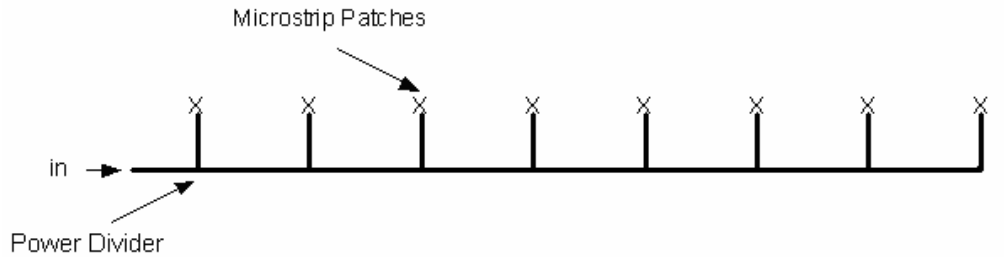

Figure 40. Parallel Feeding Network Alternative

The superiority of this feeding network comes from the fact that it includes minimum number of power dividers. The design of this model is somewhat complex if one needs to excite patch elements uniformly, since the model necessitates the usage of some special power divider models. Each power divider of the model has a different structure and different power division ratios. Because of its complexity, the model given above is kept out of interest, in case the parallel feeding network is selected. The parallel feeding network given on Section 3.3 is considered as a solution for the case of parallel feeding.

Because of its complex power divider design requirements and high losses, Parallel Series Aperture Fed Patch Array model seems to give appropriate results and some simulations are executed on the model. Patch array feeding network is modeled with two series microstrip lines connected via a single power divider. After inserting the signal into a microstrip line by a coaxial-to-microstrip launcher, the signal is divided to two series microstrip lines each of which couples 8 apertures continuously as moving towards the end of the line. Coupling the field to each patch element uniformly is a tough subject for this model. The placement of patch elements, dimensions of apertures and patches should be determined in order to do so. Series-fed aperture coupled patch array structures are inspected in literature and the configuration given on Figure 41 [2, 53-55] is encountered. This configuration is simulated on HFSS™ v.9.2 to see the applicability of the series aperture fed model. Matching characteristic is tried to be adjusted using the design parameters defined on Figure 41. The simulation results are interpreted on Section 6.4.1.

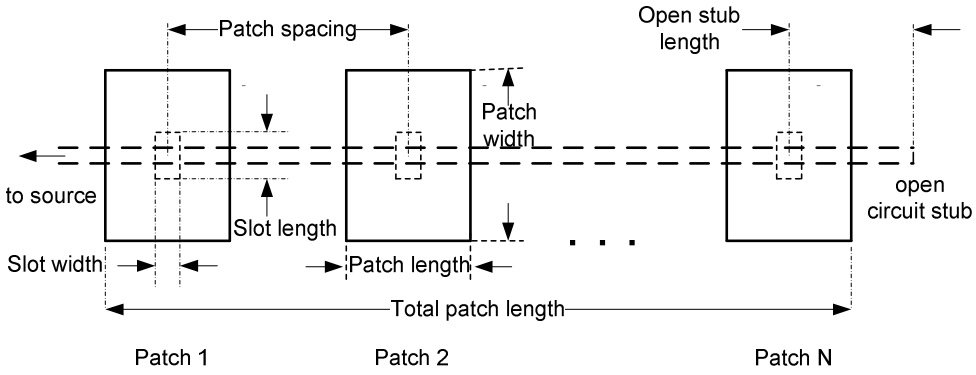

Figure 41. Parameters of Series-Fed Aperture-Coupled Patch Array Antenna

6.4.1. Series Feeding Network

The patch elements of a series aperture fed array should be aligned with patch spacing of 5.2 mm which is the guided wavelength ($\lambda_g = 0.64\lambda_0$) inside the feeding substrate (Figure 18) at center frequency of 36.85 GHz. This value is required to excite each patch with equal phases and recommended by some researchers [54, 55]. Some other researchers also advise patch spacing values of 0.7 λ_0 [53] and 0.57 λ_0 [6]. However, at the beginning, we should fix the aperture dimensions.

While developing a series aperture fed patch array antenna, the first step should be adding a new patch element just before the last patch element (rightmost patch element on Figure 41) and adjusting its parameters to obtain good matching. Aperture coupling method for this patch element differs from the aperture coupling of the last patch element because the microstrip line after the new aperture sees a matched load instead of an open circuit stub. The input impedance of the last patch element is set before to 50 Ω with the parameters given on Section 6.2 and this acts as a matched load for the preceding patch element.

Electromagnetic simulations are applied to the model having two aperture fed patch elements connected in series. It is observed that an increase on the aperture size will be responsible for high return losses. In detail, a reasonable matching with S_{11} values about -13 dB could be achieved when the aperture size is reduced with a great degree to the values 0.3 mm for slot width and 1 mm for slot length. These aperture size values are determined with respect to the sensitivities of production devices and the width of the microstrip line. The simulation results obtained by using this aperture size are shown on Table 12. For this simulation, the sizes of each patch element and aperture of the last patch are fixed to the previously determined values.

Table 12. Aperture Coupling with Two Patch Elements Connected in Series (Convergence=0.013)

	F=36.7 GHz	F=36.85 GHz	F=37 GHz
S_{11} (dB,Phase)	-12.5, 135	-13.4, 137	-14.3, 140
Peak Directivity (dB)			7.89
Peak Gain (dB)			7.84
Peak Realized Gain (dB)			7.67
Accepted Power			0.963
Radiation Efficiency			0.989

Afterwards, in order to measure the coupling level through this small aperture (slot width=0.3 mm and slot length=1 mm), another simulation model is constructed with 50 Ω output port and without the last patch element. The simulation results show that most of the signal (-0.4 dB) couples to the output port and the accepted power of the patch element is really low. Simulation results of this model are shown on Table 13.

Table 13. Aperture Coupling of Single Patch Element Having 50 Ω Output Port (Convergence=0.01)

	F=36.7 GHz	F=37 GHz
S_{11} (dB,Phase)	-14.1, 65.9	-14.2, 63.4
S_{21} (dB,Phase)	-0.4, -100	-0.4, -110
Peak Directivity (dB)		8.16
Peak Gain (dB)		5.66
Peak Realized Gain (dB)		-6.99
Accepted Power		0.054
Radiation Efficiency		0.562

The S_{11} values of both models reveal the fact that the absence of the open circuit stub for the new added aperture causes matching problems. Changing patch size, shifting the aperture and patch element perpendicular to the microstrip line are

tried to compensate the excessive reactance of the input resistance, but it was not successful enough. This excessive reactance is also tried to be reduced by reducing the aperture size. But this time, the coupling level to the patch element diminishes and almost all the signal passes over the aperture without signal coupling. All of these reasons lead to a point that an efficient Series Aperture Coupled Patch Array model is not very practical to develop.

6.4.2. Parallel Feeding Network

Beyond the design complexity and beam tilting effects, the previous section proves the poor matching property of the Series Feeding Network for aperture coupled patch arrays. Parallel Feeding Network is the other alternative for Aperture Coupled Patch Arrays. This feeding network consists of several branches each of which terminates with a single aperture fed patch element. Therefore the aperture coupling design of a single patch element is valid for all patch elements and there is no need to design another type of aperture coupling. The most important design factor for Parallel Feeding Network is to achieve efficient and low loss power division to a number of patch elements. The power divider models of Section 5.3 with 1 input and 16 output ports seems to be appropriate to distribute signal to each patch element of the array having 16 elements. However, this is not the case if the array is two dimensional like the one that will be developed and constructed for this thesis work. The previously mentioned power divider networks should be modified to distribute signal to a patch array having 8 elements on one dimension and 2 elements on other dimension. A special parallel feeding network structure is determined for this purpose where microstrip lines follow paths as drawn on Figure 42.

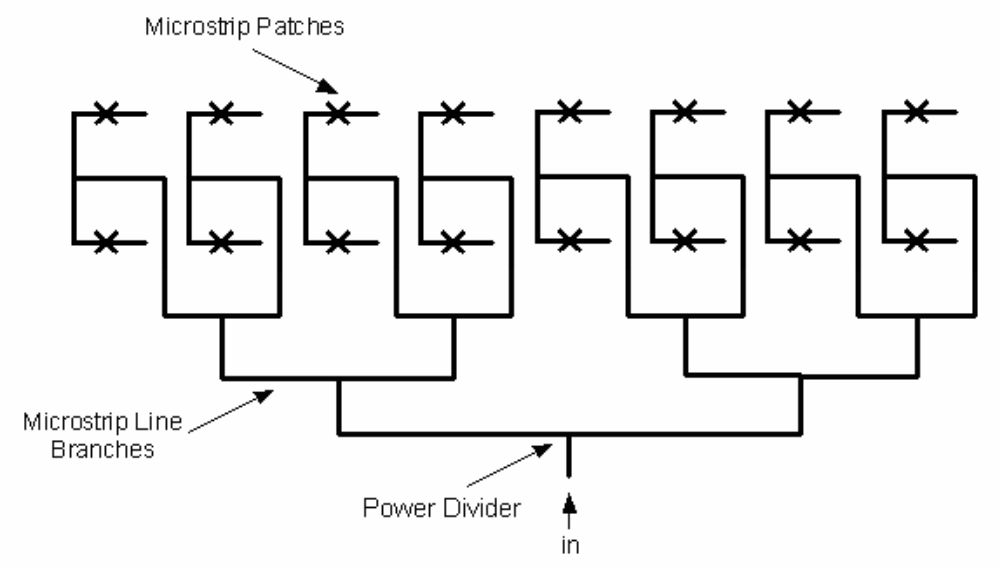

Figure 42. Parallel Feeding Network for 8x2 Patch Array

6.5. Electromagnetic Simulations

The outcomes of the previous design steps are collected in this section to form the final Microstrip Patch Array Model. The final simulation model is constructed on HFSS™ v9.2 electromagnetic simulation program to see the overall properties of the antenna system. To summarize, previously selected dielectric substrates are placed as feeding and radiation layers, ground plane is placed between these two layers, patch elements are placed on the radiation layer to form a 8x2 patch array, 1 input 16 output power divider model is placed on the feeding layer to distribute signal to each patch of the array and apertures are removed from the ground layer at necessary locations.

While doing microstrip patch array antenna simulations, the aperture for each patch element is placed at the center of rectangular patch shape. This is required to obtain maximum coupling and lower cross polarization. The patch element width and length values are fixed to the values of 3.2 mm and 2.1 mm respectively as determined at Section 6.2.3 and 6.2.4. The dielectric substrate parameters, aperture sizes, open stub lengths and microstrip line widths satisfying characteristic impedances of 50 Ω, 35.36 Ω and 25 Ω are also taken constant with the values determined before on corresponding sections. The length of the 35.36 Ω microstrip

line is used as the optimization parameter to minimize the return loss and determine the center frequency of the design.

Two main simulation models are constructed starting from 1x2 or 2x2 patch array model, continuing with the 4x2 patch array and finally ending with the 8x2 patch array model. This iterative method is followed to see whether the matching properties stay constant as array grows or some mutual effects deteriorate the matching characteristic. Simulation models are shown on the following figures and the results are collected on the tables for each model. The models are similar to each other and should be named appropriately to reduce confusion. So, the first model is named as Y-model while the second model is named as T-model.

The main object of these simulations is to obtain a parallel aperture coupled 8x2 microstrip patch array model having good matching properties. Once this is satisfied, the patch spacings could be aligned to necessary values. As a result, the patch spacings of the Y-model are kept 8 mm.

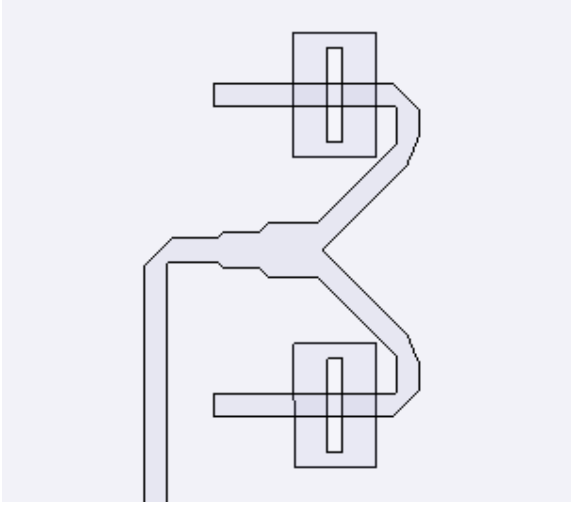

Figure 43. 1x2 Microstrip Patch Array Y-Model

Table 14. Simulation Results of 1x2 Microstrip Patch Array Y-Model (Convergence=0.015)

	F=36.7 GHz	**F=36.85 GHz**	**F=37 GHz**
S_{11} (dB,Phase)	-18.2, -58.6	-20.3, -66.2	-23.1, -70.2
Peak Directivity (dB)			10.57
Peak Gain (dB)			10.46
Peak Realized Gain (dB)			10.44
Accepted Power			0.995
Radiation Efficiency			0.974
3 dB BW Theta (Phi=90°)			90°
3 dB BW Phi (Theta=90°)			27°

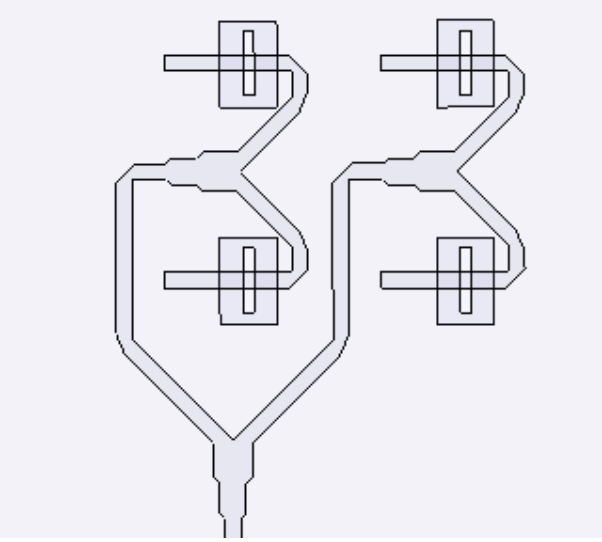

Figure 44. 2x2 Microstrip Patch Array Y-Model

Table 15. Simulation Results of 2x2 Microstrip Patch Array Y-Model (Convergence=0.018)

	F=36.7 GHz	**F=36.85 GHz**	**F=37 GHz**
S_{11} (dB,Phase)	-18.2, -46.7	-21.5, -87.3	-22, -148
Peak Directivity (dB)			11.79
Peak Gain (dB)			11.63
Peak Realized Gain (dB)			11.60
Accepted Power			0.994
Radiation Efficiency			0.964
3 dB BW Theta (Phi=90°)			29°
3 dB BW Phi (Theta=90°)			28°

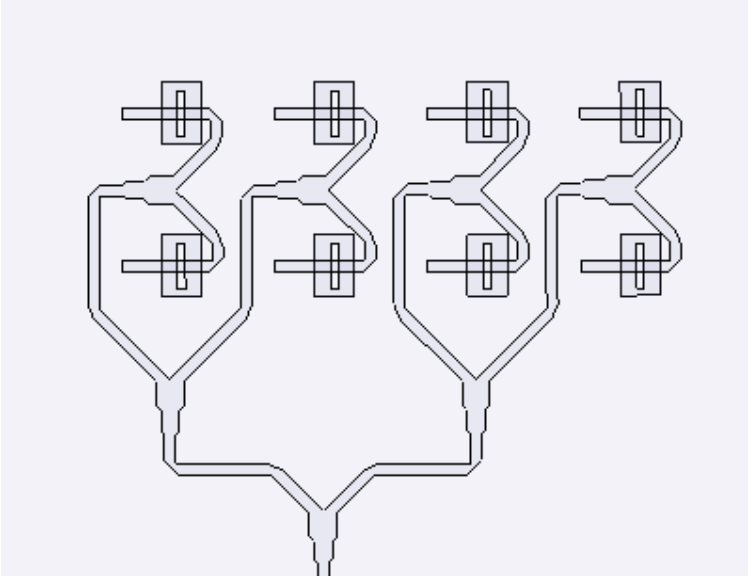

Figure 45. 4x2 Microstrip Patch Array Y-Model

Table 16. Simulation Results of 4x2 Microstrip Patch Array (Convergence=0.013)

	F=36.7 GHz	**F=36.85 GHz**	**F=37 GHz**
S_{11} (dB,Phase)	-13.2, -36.7	-14.9, -71.5	-16.1, -116
Peak Directivity (dB)			14.69
Peak Gain (dB)			14.44
Peak Realized Gain (dB)			14.33
Accepted Power			0.976
Radiation Efficiency			0.944
3 dB BW Theta (Phi=90°)			13.5°
3 dB BW Phi (Theta=90°)			29°

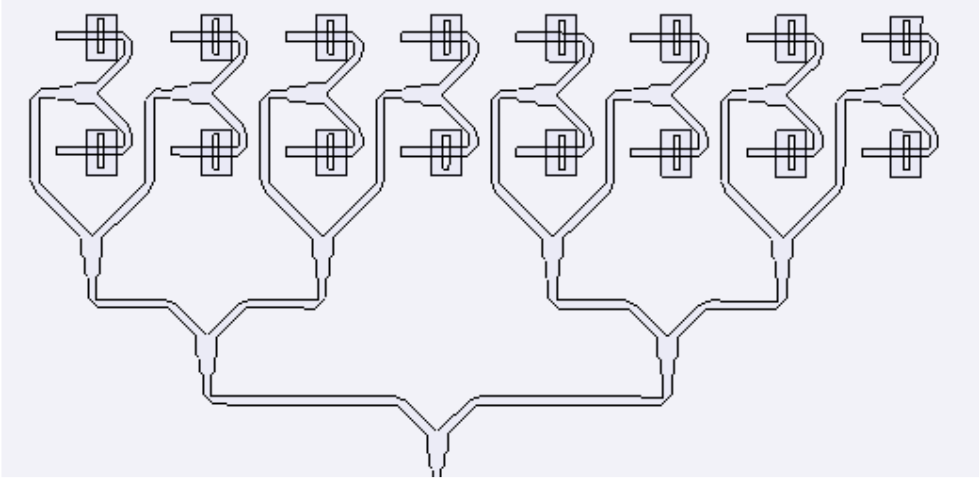

Figure 46. 8x2 Microstrip Patch Array Y-Model

Table 17. Simulation Results of 8x2 Microstrip Patch Array Y-Model (Convergence=0.102)

	F=36.7 GHz	**F=36.85 GHz**	**F=37 GHz**
S_{11} (dB,Phase)	-8.52, -143	-8.26, 167	-7.67, 119
Peak Directivity (dB)			17.53
Peak Gain (dB)			16.97
Peak Realized Gain (dB)			16.15
Broadside Directivity (dB)			13.75
Broadside Gain (dB)			13.19
Broadside Real. Gain (dB)			12.37
Accepted Power			0.829
Radiation Efficiency			0.88
3 dB BW Theta (Phi=90°)			7°
3 dB BW Phi (Theta=90°)			29.5°

When the simulation results are interpreted, Y-model is concluded to become instable as patch array grows. The return loss value increases substantially and reaches to the value of -8 dB as more patch elements are connected with power dividers. Aperture coupled patch elements and power dividers show frequency dependent characteristics and this may result in mismatches when they brought together to form a patch array.

As a consequence, this simulation model is aborted and a new kind of simulation model (T-model) is started to be dealt with. For T-model, patch spacings are selected to be equal to the design values of Section 6.3 which are 6 mm and 7 mm for the array of 8 and 2 patch elements respectively.

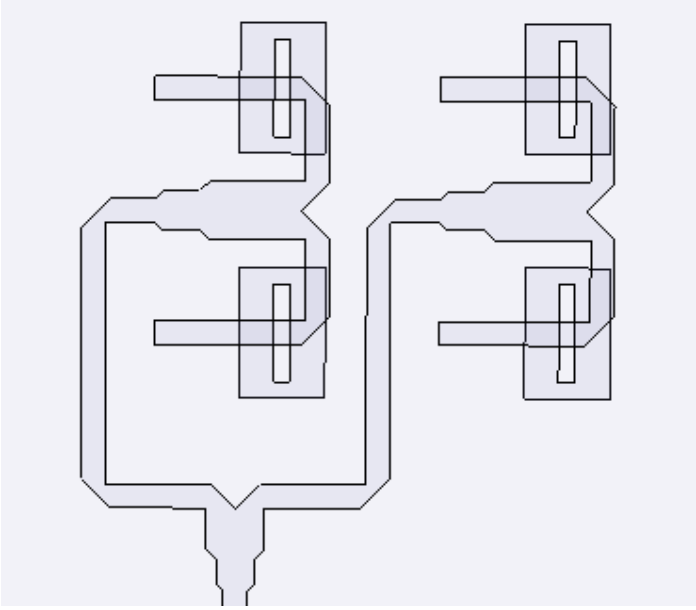

Figure 47. 2x2 Microstrip Patch Array T-Model

Table 18. Simulation Results of 2x2 Microstrip Patch Array T-Model (Convergence=0.006)

	F=36.7 GHz	**F=36.85 GHz**	**F=37 GHz**
S_{11} (dB,Phase)	-22.6, -123	-26, -161	-27, 145
Peak Directivity (dB)			12.42
Peak Gain (dB)			12.31
Peak Realized Gain (dB)			12.3
Accepted Power			0.998
Radiation Efficiency			0.975
3 dB BW Theta (Phi=90°)			30°
3 dB BW Phi (Theta=90°)			35°

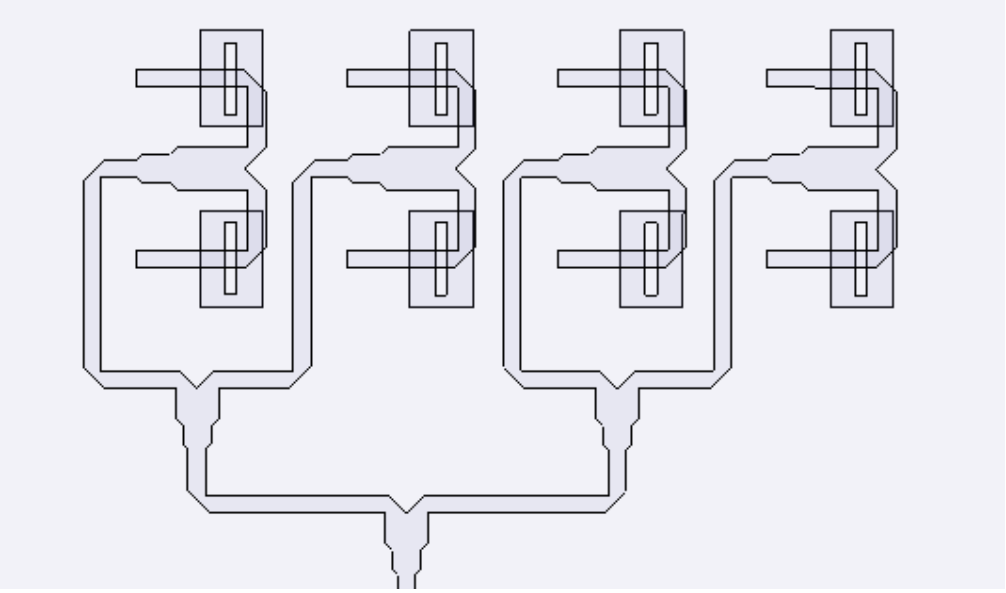

Figure 48. 4x2 Microstrip Patch Array T-Model

Table 19. Simulation Results of 4x2 Microstrip Patch Array T-Model (Convergence=0.018)

	F=36.7 GHz	**F=36.85 GHz**	**F=37 GHz**
S_{11} (dB,Phase)	-18.7, -135	-20.5, -171	-21.7, 147
Peak Directivity (dB)			15.49
Peak Gain (dB)			15.32
Peak Realized Gain (dB)			15.29
Accepted Power			0.993
Radiation Efficiency			0.961
3 dB BW Theta (Phi=90°)			16°
3 dB BW Phi (Theta=90°)			35°

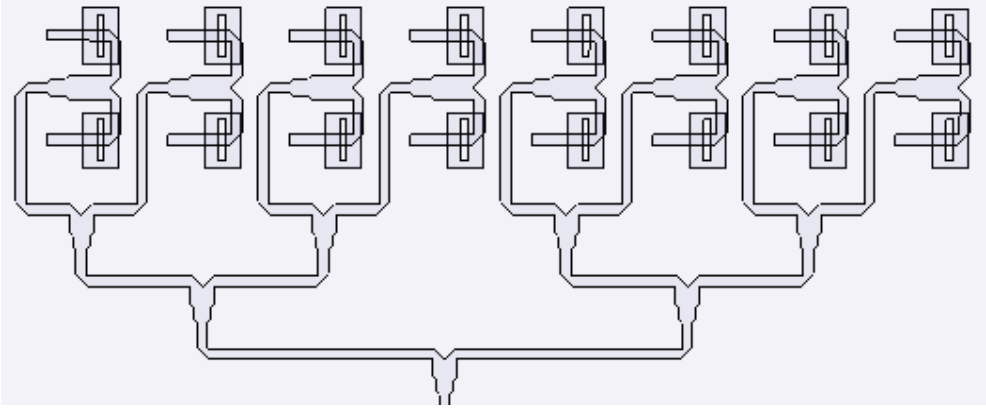

Figure 49. 8x2 Microstrip Patch Array T-Model

Table 20. Simulation Results of 8x2 Microstrip Patch Array T-Model (Convergence=0.012)

	F=36.7 GHz	**F=36.85 GHz**	**F=37 GHz**
S_{11} (dB,Phase)	-13.2, -76	-14.8, -116	-16.3, -164
Peak Directivity (dB)			18.29
Peak Gain (dB)			17.98
Peak Realized Gain (dB)			17.88
Accepted Power			0.977
Radiation Efficiency			0.933
3 dB BW Theta (Phi=90°)			7.5°
3 dB BW Phi (Theta=90°)			33°

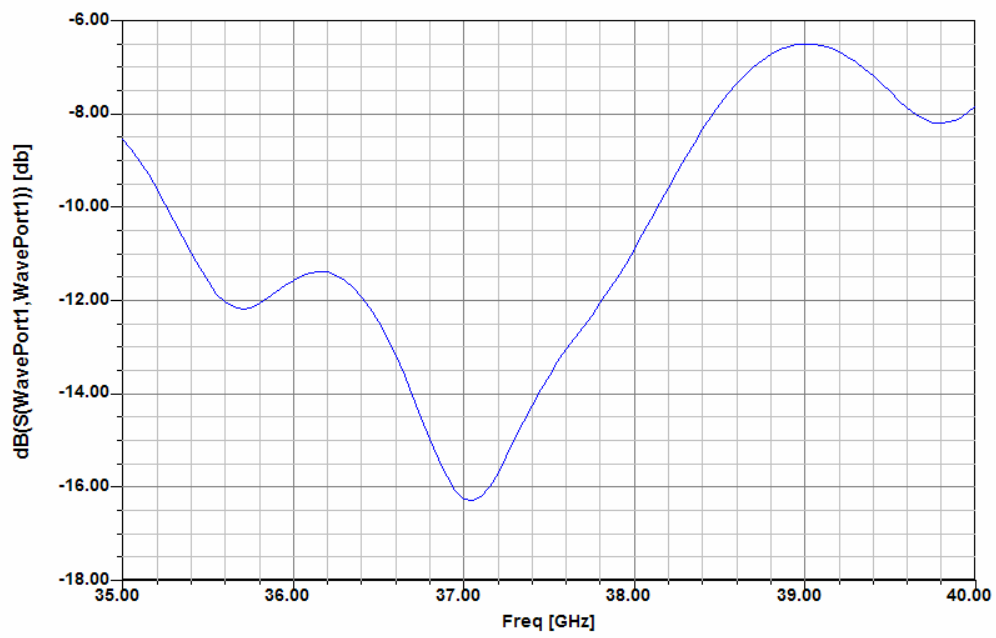

Figure 50. S_{11} vs. Frequency for 8x2 Microstrip Patch Array T-Model

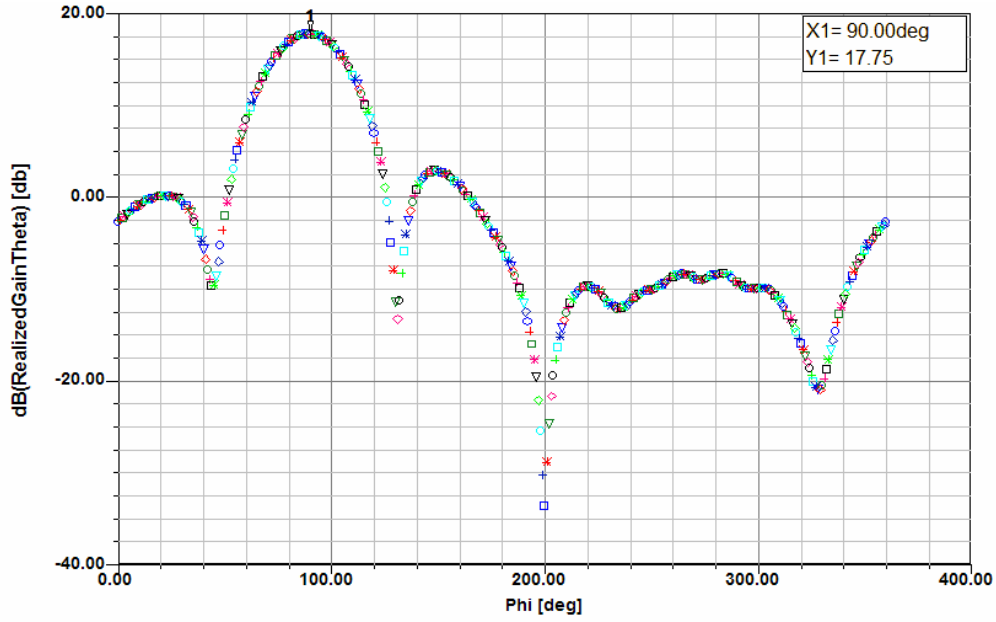

Figure 51. Elevation Pattern of the 8x2 Microstrip Patch Array T-Model

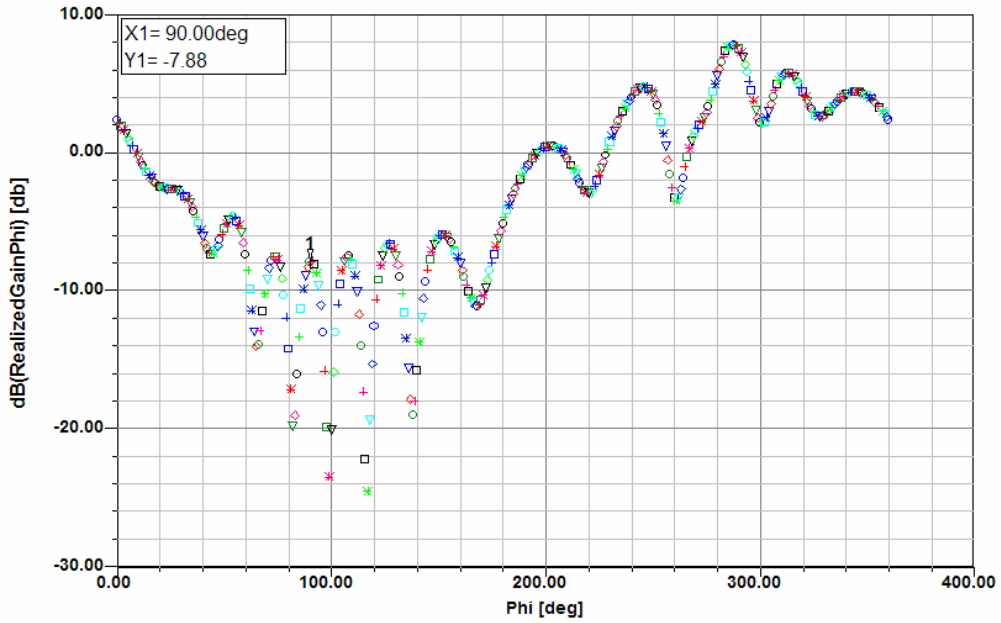

Figure 52. Elevation Cross Polarization Pattern of the 8x2 Microstrip Patch Array T-Model

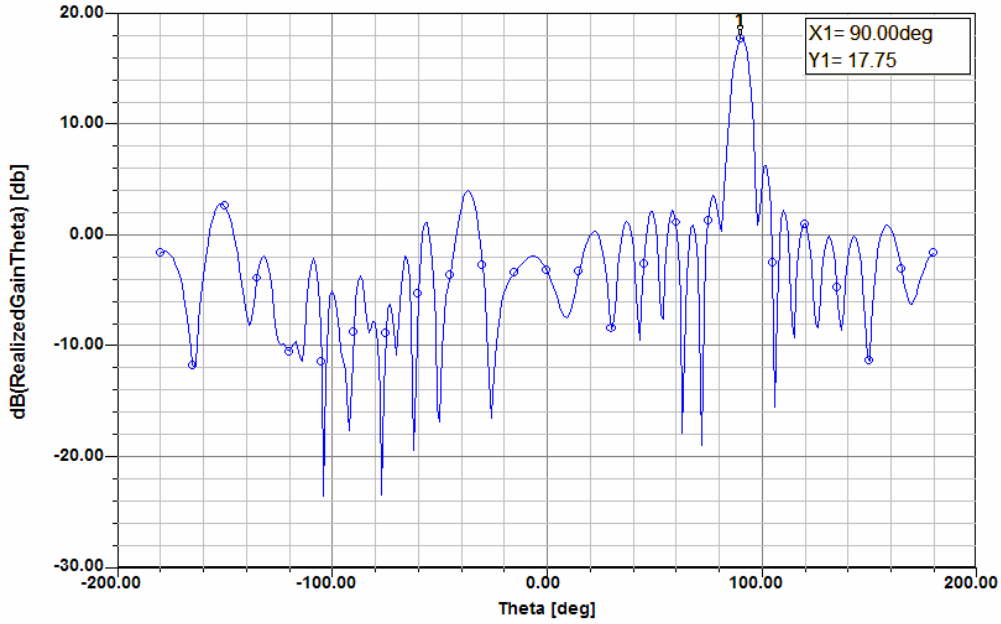

Figure 53. Azimuth Pattern of the 8x2 Microstrip Patch Array T-Model

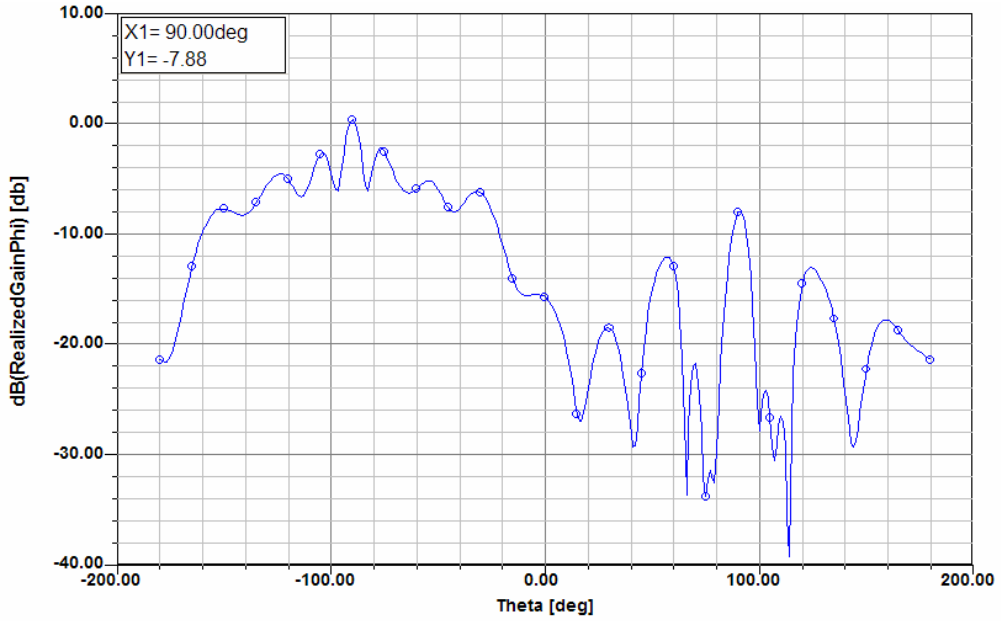

Figure 54. Azimuth Cross Polarization Pattern of the 8x2 Microstrip Patch Array T-Model

Different from the Y-Model, T-model shows similar matching characteristics for small and large patch arrays around the center frequency. The simulation model, antenna parameters and S_{11} values of 8x2 element microstrip patch array are shown on Figure 49, Figure 50 and Table 20. The antenna and the cross polarization patterns in azimuth and elevation planes at the center frequency of 36.85 GHz are also shown on Figure 51, 52, 53 and 54. The simulation results show that this model has good matching values and expected antenna patterns. The main beam is in broadside direction where φ and θ are equal to 90°. The cross polarization level in broadside direction is about 25 dB lower than the peak gain value. The peak gain of the antenna is obtained as 18 dB.

The simulation results reveal that antenna beamwidth values are 7.5° in azimuth and 33° in elevation which were calculated as 7.3° and 37.1° respectively on Section 6.3. The theoretically calculated and simulated results comply with each other for azimuth plane but not in elevation plane. This is because of the high number of patch elements in azimuth plane and low number of patch elements in elevation plane. The 8 patch elements in azimuth plane make the calculated beamwidth values be more similar to the simulated results. On the contrary, the

only 2 patch elements in elevation plane leads the theoretical calculations to be more dependent on the single antenna pattern and introduce less accurate array beamwidth values. Electromagnetic simulation program solves such models more accurately and without assumptions as it is done before such as coupling the field to each patch element with equal amplitudes and phases. So, the results of HFSS™ v9.2 are more likely to be relied on.

The distribution of the patch elements on the radiation layer is not symmetrical with respect to the substrate boundaries. In addition, the ground plane of the antenna is taken as finite for the simulation model. Hence, the sidelobes of the azimuth and elevation patterns are not symmetrical as it could be seen from Figure 51 and 53.

The simulation model of 8x2 microstrip patch array antenna (T-model) is decided to be produced as a prototype and measured experimentally. The top and the bottom layers of each substrate and the mechanical box of the prototype antenna could be observed in detail on Appendix F. The exact coincidence of substrate layers will be satisfied by using some alignment holes placed on dielectric substrates (big holes surrounding the substrates). The alignment holes are used for minimizing the failure when two dielectric substrates are brought together as top and bottom layers. If these alignment holes crate perfect circles when two dielectric substrates come together, the apertures on feeding layer and the patch elements of radiation layer are also expected to align correctly and maximum coupling is achieved. The experimentally measured antenna parameters and S_{11} parameter of the microstrip patch array antenna will be given on Chapter 7.

CHAPTER 7

VERIFICATION OF THE THEORETICAL DESIGN MODEL

The entire design process of a microstrip patch array antenna is explained on this report. A patch array antenna with 8x2 elements was fully designed on previous chapters by following some design steps. On this chapter, the theoretical outcomes of this antenna design are tried to be verified by producing a prototype antenna and taking some measurements on the product. The prototype antenna is made of 4 items and the complete patch array antenna is built by integrating these items. Therefore, the obtained measurements are valid for the total process including theoretical design, production of the items and integration of the antenna items. The necessary parameters of the final product are measured and the results are used to verify the full design and production process. The measurements are interpreted with respect to their theoretically calculated values.

7.1. Aperture Fed Patch Array Antenna Production

The aperture fed patch array antenna consists of 4 items. Two of these items are different type of dielectric substrate materials, the other one is a mechanical fixture the last item is the connector. These items should be integrated carefully to obtain an efficient product. The connector structure was introduced on Chapter 4 and detailed drawings of other items are given on Appendix F.

The most important step of the integration is attaching substrate materials and the mechanical fixture. While attaching the dielectric substrate materials, one should pay attention to the point that the ground plane of the feeding layer is also the ground plane of the radiation layer and there should not be any hollow place between these substrates. In addition, the alignment holes of the substrates should match perfectly in order to have the centers of the apertures and the patch elements

coincide. These alignment holes should also be brought face to face to the inner screwing holes of the mechanical fixture. The locations of these screwing holes are selected to satisfy a small compensation gap between the feeding layer and the connector hole. The screwing holes also place the patch elements on the center of the bottom window where the antenna radiates from. After all these points are satisfied, dielectric substrate materials and the mechanical fixture should be attached to each other by screwing through these holes. The screwing holes support the 3 sides of the substrates. The other side is supported by the inner conductor of the connector. However, the strength of the inner conductor is not high enough and this side should also be glued to the bottom wall of the mechanical fixture. The upper and lower sides of the produced antenna are shown on Figure 55 and 56.

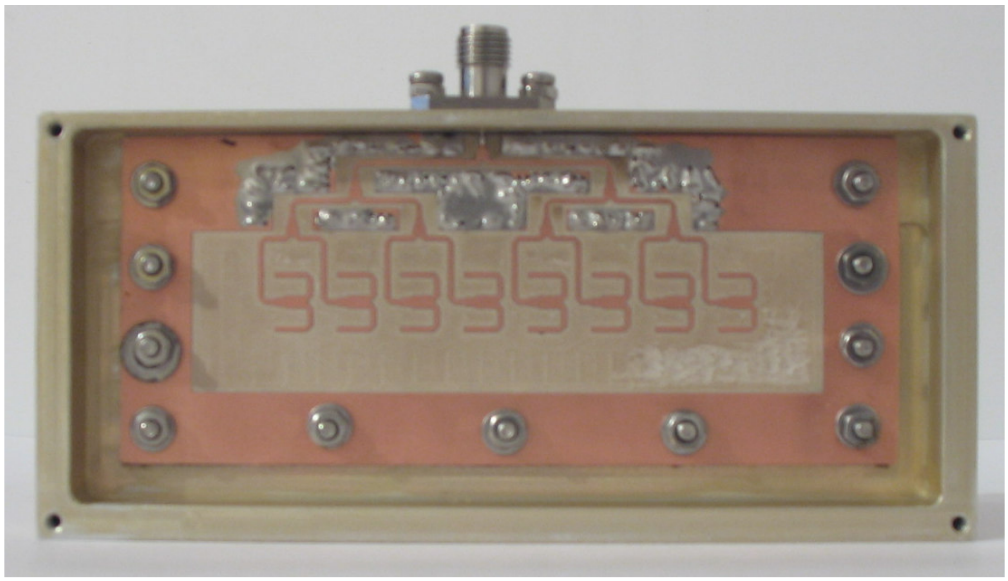

Figure 55. Feeding Side of the Produced Antenna

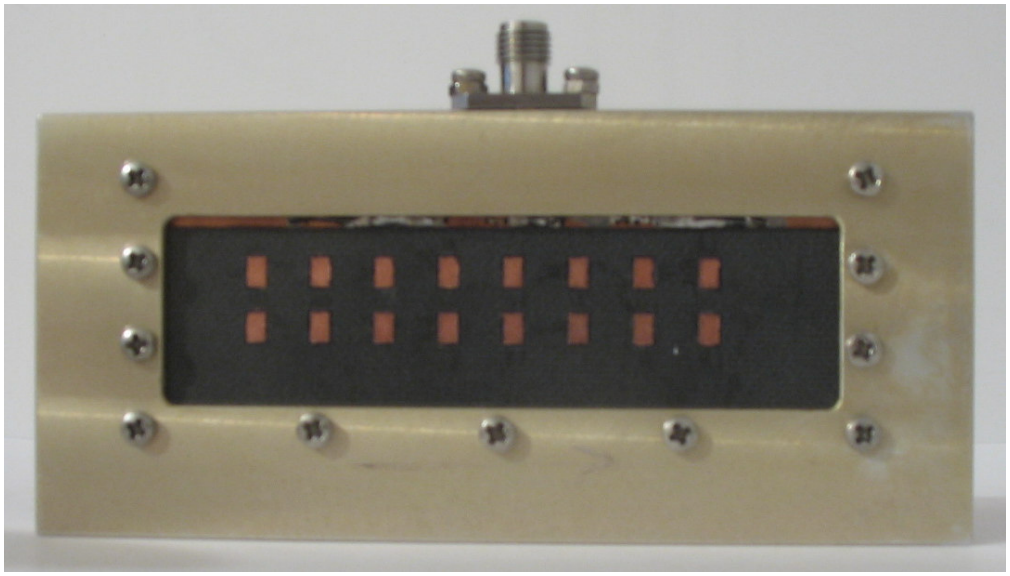

Figure 56. Radiation Side of the Produced Antenna

7.2. Measurements of the Antenna Parameters and S_{11} values

Antenna parameters and S_{11} values are measured at the laboratory by using special measurement devices such as network analyzer, spectrum analyzer, oscilloscope and computer. Antenna pattern measurements are obtained by using the set-up shown on Figure 57 which is constructed in a special room. The walls of this room are covered by absorbers to reduce reflections. As seen on the figure, the prototype antenna is fixed to the far side and the radiator antenna is placed at the closer side of the room. Two sides of the prototype antenna are covered by absorbers to eliminate distortions on the antenna pattern caused by metallic walls. Due to high degree of signal losses at frequencies up to 40 GHz, 2 different amplifiers are used at different ends of this set-up; one is connected to the radiator antenna while the other one is connected to the prototype antenna. The increased power level makes it possible to see the sidelobes of the antenna patterns. The graphs of these measurements are shown on Figure 58, 59, 60 and 61.

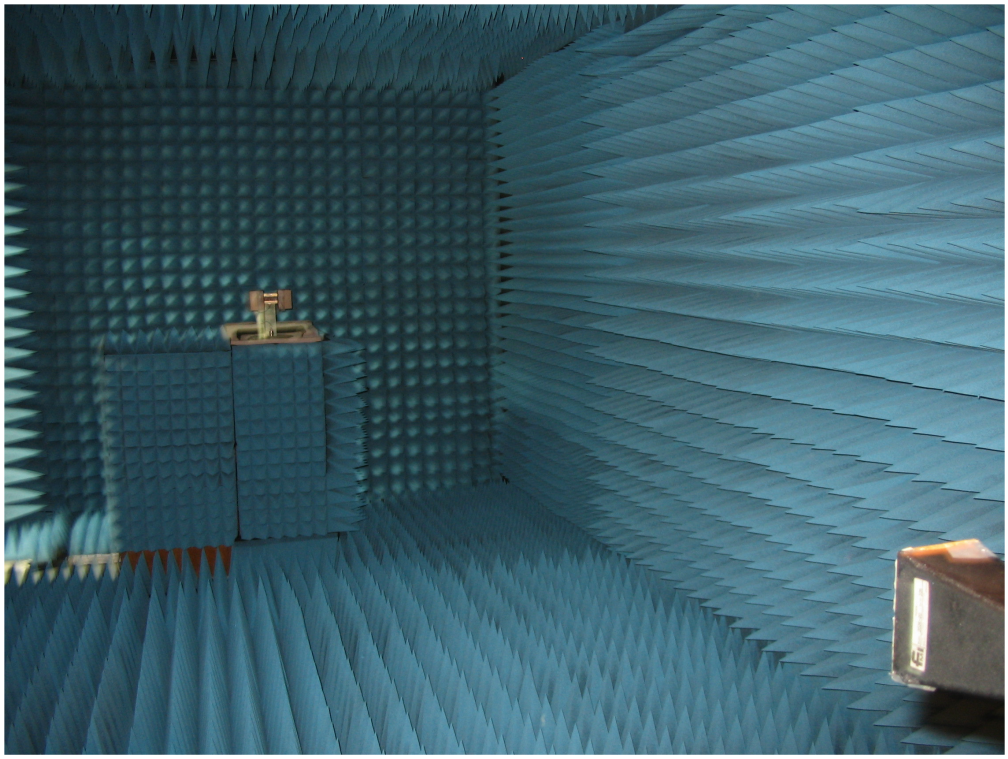

Figure 57. Microstrip Patch Array Antenna Pattern Measurement Set-Up

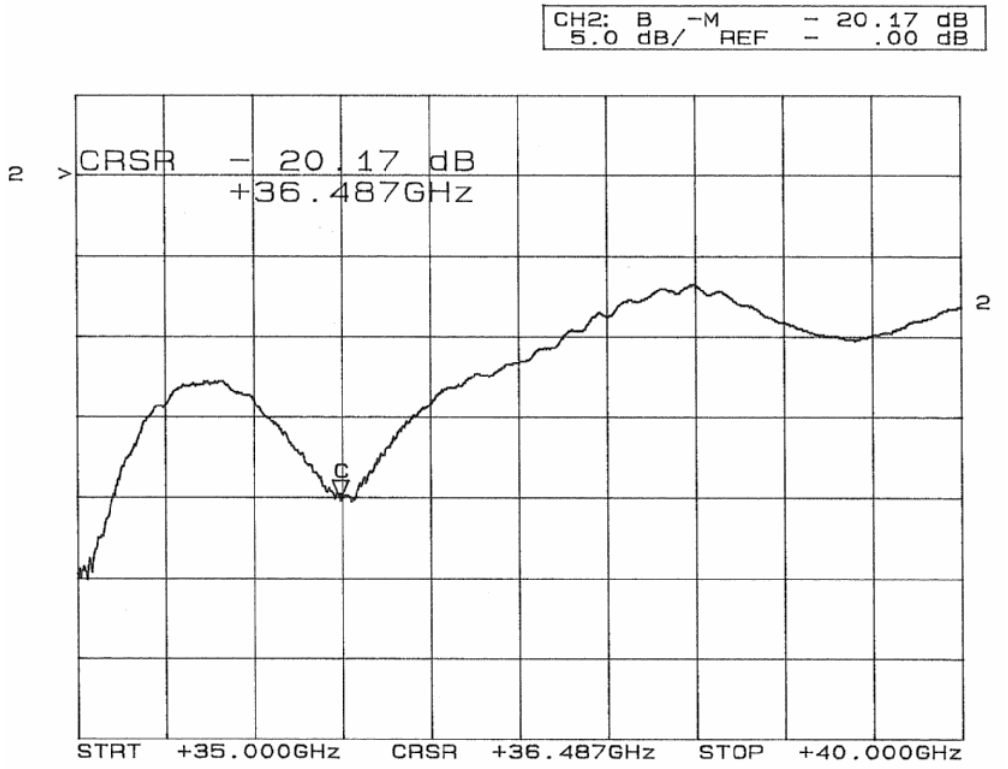

Figure 58. S_{11} vs. Frequency for Microstrip Patch Array Antenna without Box Cover

Figure 59. S_{11} vs. Frequency for Microstrip Patch Array Antenna with Box Cover

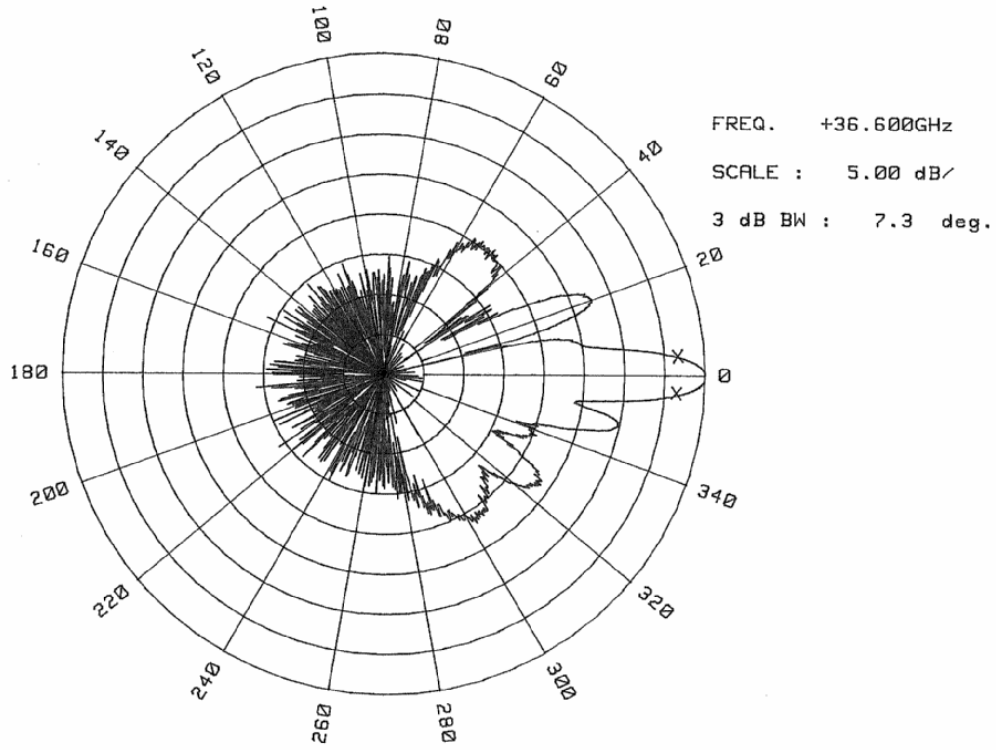

Figure 60. Azimuth Pattern of the Microstrip Patch Array Antenna

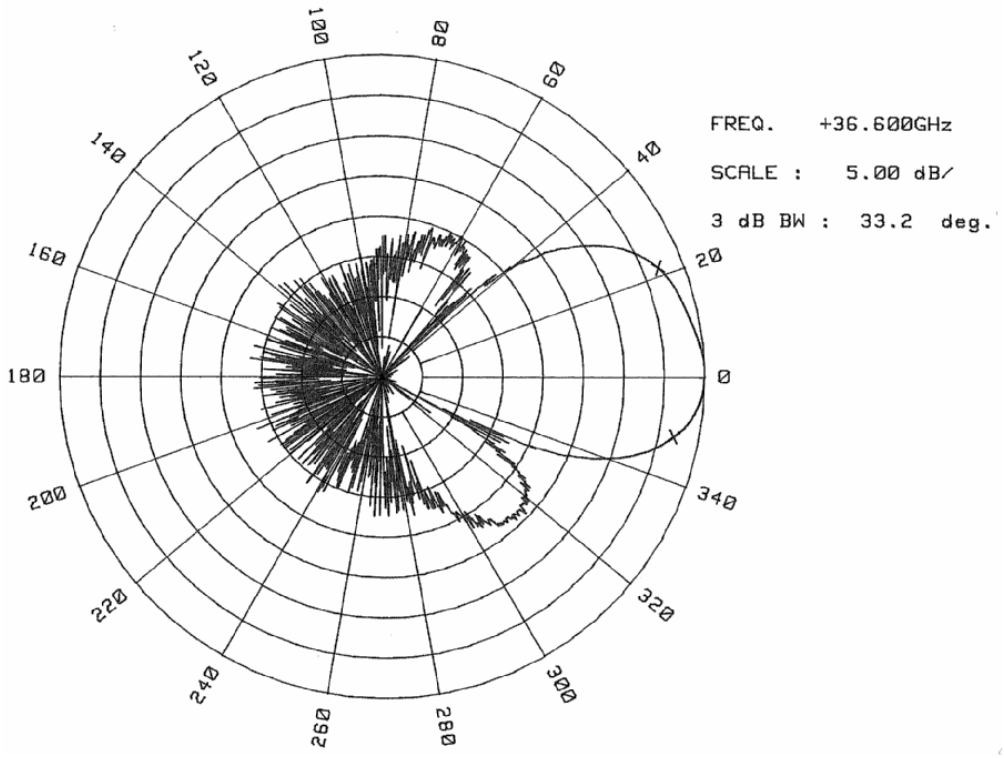

Figure 61. Elevation Pattern of the Microstrip Patch Array Antenna

By applying the beamwidth values given on Figure 60 and 61 on eqn. 6.7, the peak directivity of the antenna is calculated as 21.3 dB.

7.3. Comparison between Theoretical and Measured Results

The design steps of the microstrip patch array antenna include 3 different phases of parameter evaluation. At first, the parameters are calculated by using some formulations derived theoretically. Afterwards, the overall antenna system is modeled on HFSS™ v9.2 and the parameter values are obtained as simulation results. Finally, the simulated model is fabricated as a prototype and physical measurements are applied to the antenna. All of these results are collected on Table 21.

The design of the patch array antenna starts from determining the center frequency of 36.85 GHz and the frequency bandwidth value of 300 MHz or higher. These values are written on Table 21 as formulation results. The antenna is designed to have maximum frequency bandwidth and this bandwidth value could only be

obtained by using simulation and measurement results. The frequency values satisfying S_{11} values lower than -15 dB are taken to be operating frequencies. The difference between the maximum and minimum values of these frequencies is calculated as the frequency bandwidth and written on the following table. In order to diminish the backside radiation, the produced antenna will be used with a closed metallic box cover. As a result, the S parameter values of Figure 59 are used to fill the required fields of Table 21.

Table 21. Parameter Values Obtained by Formulation, Simulation and Measurement

	Formulation Results	**Simulation Results**	**Measurement Results**
Center Frequency	36.85 GHz	37.05 GHz	36.65 GHz
Frequency Bandwidth	>300 MHz	500 MHz	850 MHz
3 dB Azimuth Beamwidth	7.3°	7.5°	7.3°
3 dB Elevation Beamwidth	37.1°	33°	33°
Azimuth First Sidelobe	-13 dB	-11.5 / -14 dB	-10 / -12.5 dB
Elevation First Sidelobe	-11.5 dB	-15 / -17.5 dB	-16 / -20 dB
Peak Directivity	20.8 dB	18.3 dB	21.3 dB

The fabricated patch array antenna and the simulation model of the patch array antenna differ from each other with respect to some points as listed below.

- Simulation model does not include metallic fixture where dielectric substrate materials and the connector is placed.
- Simulation model does not include connector model.
- Simulation model does not include copper plates around microstrip lines and the vias connecting these plates with the ground plane.

Due to the differences listed above, simulation and physical measurement results are expected to have some discrepancies. However, the parameters given on Table 21 take very similar values.

The center frequency of the patch array simulation is 200 MHz higher and the center frequency of the antenna product is 200 MHz lower than the required center frequency value of 36.85 GHz. This frequency shift value is only about 0.5 % of the required center frequency and it is accepted to be very small at this frequency range.

The antenna parameters also show very similar properties including the asymmetrical distribution of first sidelobe levels. As it was mentioned in Section 6.5, the 3 dB beamwidth values of formulation results are approximate values, since they are calculated by assuming the same sinc pattern (3 dB BW= 67°) for elevation and azimuth plane of a single patch element. More accurate beamwidth values could be evaluated by using the correct elevation and azimuth antenna patterns of the single patch element. The similarity of the beamwidth values for simulation and measurement results also verifies this situation.

To sum up, the peak directivity values of formulation and measurement results are calculated by a simple formula given on eqn. 6.7. However, this formula gives approximate values and the accurate values could be obtained by integrating the antenna pattern as it is done on HFSS simulation program. Therefore, the directivity value of the simulation results should be relied on.

CHAPTER 8

CONCLUSION

On this report, coaxial-to-microstrip launcher and microstrip patch array models are investigated at frequencies up to 40 GHz. These design models, especially around this frequency range, are accepted as not fully investigated research areas. Because of its complexity, inclination to failure and sensitivity drawbacks, most of the time these design models are not interested by researchers. In brief, there are not many studies on literature at this frequency range and the studies given on this report is considered to be helpful for anyone looking for experience.

A full design procedure is introduced on this report by taking a special type of microstrip patch array antenna as an example. This antenna type includes a coaxial-to-microstrip launcher, a parallel feeding network, aperture coupling and a patch array with 8x2 elements. Coaxial-to-microstrip launchers are described by giving investigation results on connector models. The available connector types are fully modeled by electromagnetic simulation programs and matching characteristics of these connectors are obtained. Feeding methods of patch antennas, power divider models and array antenna structures are also presented on related sections of this report by explaining their roles on microstrip patch array antenna design.

The studies given on this report is ended by producing a typical microstrip patch array antenna which is designed to have some required properties. The matching properties and antenna parameters of the prototype antenna are found to be consistent with predetermined theoretical values. This consequence points that patch array antenna model is successful and highly satisfactory. The success of prototype antenna production verifies many design steps introduced on this report such as coaxial-to-microstrip launcher design, usefulness of the coplanar

waveguide structure, dielectric substrate selections, power divider designs, determination of aperture and patch element dimensions and patch array design.

The information given on this report intends to be helpful on future developments. For example, parallel aperture fed microstrip patch array model having larger than 8x2 patch elements could be designed by spending not much extra time. Besides, it should be noted that design steps of this report are not the only way of designing a microstrip patch array antenna. This thesis studies include some assumptions and selections such as types of dielectric substrate materials and connector. One may also develop another efficient microstrip patch array antenna model by giving different decisions and using another type of materials. The efforts given on this thesis study is only about choosing a path and seeing if it works.

REFERENCES

[1] C. A. Balanis, *Antenna Theory Analysis and Design Second Edition,* John Wiley & Sons, United States of America, 1997.

[2] J. F. Zurcher and F. E. Gardiol, *Broadband Patch Antennas*, Artech House, United States of America, 1995.

[3] G. Kumar and K. P. Ray, *Broadband Microstrip Antennas*, Artech House, United States of America, 2003.

[4] Y. T. Lo and S. W. Lee, *Antenna Handbook Theory Applications and Design*, Van Nostrand Reinhold Company, United States of America, 1988.

[5] I. J. Bahland and P. Bhartia, *Microstrip Antennas*, Artech House, Dedham, MA, 1980.

[6] W. L. Stutzman and G. A. Thiele, *Antenna Theory and Design*, John Wiley & Sons, United States of America, 1981.

[7] J. R. James and P. S. Hall, *Handbook of Microstrip Antennas*, Vols. 1 and 2, Peter Peregrinus, London, UK, 1989.

[8] GRIFFIN, J. M., and FORREST, J. R.: 'Broadband circular disc microstrip antenna', *Electron. Letts.*, 18 Mar. 1982, pp. 266-269.

[9] FONG, K. S., PUES, H. F., and WITHERS, M. J.: 'Wideband multilayer coaxial-fed microstrip antenna element' *ibid*. 23 May 1985, pp. 497-499.

[10] HALL, P.S.: 'Probe compensation in thick microstrip patches' *ibid*. 21 May 1987, pp. 606-607.

[11] H.F. Lee and W. Chen, *Advances in Microstrip and Printed Antennas,* New York: John Wiley & Sons, 1997.

[12] M. Pozar and S. D. Targonski, "Improved Coupling for Aperture-Coupled Microstrip Antennas," *Electronic Letters*, Vol. 27, No. 13, 1991, pp. 1129-1131.

[13] R. A.Sainati, *CAD of Microstrip Antennas for Wireless Applications*, Norwood, MA: Artech House, INC, 1996.

[14] V. Rathi, G. Kumar, and K. P. Ray, "Improved Coupling for Aperture-Coupled Microstrip Antennas," *IEEE Trans. Antennas Propagat.*, Vol. AP-44, No. 8, 1996, pp.1196-1198.

[15] D. M. Pozar, "A Microstrip Antenna Aperture Coupled to a Microstrip Line," *Electronic Letters*, Vol. 22, pp. 49-50, January 1985.

[16] G. Gronau and I. Wolff, "Aperture-Coupling of a Rectangular Microstrip Resonator," *Electronic Letters*, Vol. 22, pp. 554-556, May 1986.

[17] J. C. MacKinchan, et al., "A Wide Bandwidth Microstrip Sub-Array for Array Antenna Application Using Aperture Coupling," IEEE AP-S Int. Symp. Digest' 1989' pp.878-881.

[18] J. S. Roy, et al., "Some Experimental Investigations on Electromagnetically Coupled Microstrip Antennas on Two Layer Substrate," *Microwave Optical Tech. Letters*, Vol. 4, No. 9, 1991, pp.238-238.

[19] P. B. Katehi and N. G. Alexopoulos, "On the Modeling of Electromagnetically Coupled Microstrip Antennas- The Printed Strip Dipoles," *IEEE Trans. Antennas Propagat.*, Vol. AP-32, No. 11, pp.1179-1186, November 1984.

[20] H. G. Oltman and D. A. Huebner, "Electromagnetically Coupled Microstrip Dipoles," *IEEE Trans. Antennas Propagat.*, Vol. AP-29, No. 1, pp.151-157, January 1981.

[21] D. M. Pozar and B. Kaufmann, "Increasing the Bandwidth of a Microstrip Antenna by Proximity Coupling," *Electronic Letters*, Vol. 23, No. 8, 1987, pp. 368-369.

[22] D. M. Pozar, "Microstrip Antennas," *Proc. IEEE*, Vol. 80, No.1, pp. 79-81, January 1992.

[23] D. M. Pozar, "Microstrip Antenna Aperture-Coupled to a Microstrip Line," *Electronic Letters,* Vol. 21, No. 2, 19985, pp. 49-50.

[24] A Henderson, A. E. England, and J. R. James, "New low-loss millimeter wave hybrid microstrip antenna array," *Eleventh European Microwave Conference,* Amsterdam, The Netherlands, September 1981.

[25] R. E. Munson, "Conformal Microstrip Antennas and Microstrip Phased Arrays," *IEEE Trans. Antennas & Propagation,* Vol. AP-22, pp. 74-78, Jan 1974.

[26] D. H. Schaubert, "Microstrip Antennas," *Electromagnetics,* Vol. 12, pp. 381-401, July-December 1992.

[27] D. R. Jackson and N. G. Alexopoulos, "Simple Approximate Formulas for Input Resistance, Bandwidth, and Efficiency of a Resonant Rectangular Patch," *IEEE Trans. Antennas & Propagation*, Vol. 3, pp. 407-410, March 1974.

[28] M. Petersson, "Microstrip Solutions for Innovative Microwave Feed Systems," Linköping University, October 2001.

[29] K. C. Gupta, R. Garg, I. Bahl and P Bhartia, *Microstrip Lines and Slotlines*, Artech House, INC, 1996.

[30] E. H. England, "A Coaxial to Microstrip Transition," *IEEE Trans. Microwave Theory & Techniques*, pp. 47-48, January 1976.

[31] J. Chenkin, "dc to 40 GHz Coaxial-to-Microstrip Transition for 100-µm-Thick GaAs Substrates," *IEEE Trans. Microwave Theory & Techniques*, Vol. 37, No. 7, pp. 1147-1150, July 1989.

[32] Rogers Corporation, "RT/duroid® 5870 /5880 High Frequency Laminates," http://www.rogerscorporation.com/mwu/pdf/5000data.pdf, August 2004, Last Accessed at July 2006.

[33] M. Leung, "Microstrip Antenna Design Using Mstrip40" http://www.e-technik.fh-kiel.de/~splitt/html/Mstrip40LabManual.pdf, November 2002, Last Accessed at June 2006.

[34] Schroeder, K.G., "Miniature Slotted-Cylinder Antennas," *Microwaves*, Vol. 3, Dec. 1964, pp. 28-37.

[35] R. E. Collin, *Foundations for Microwave Engineering*, McGraw-Hill International Editions, 2nd Edition, United States of America, 1992.

[36] M. A. R. Gunston and J. R. Weale, Variation of Microstrip Impedance with Strip Thickness, *Electron. Lett.*, vol. 5, p.697, 1969.

[37] H. A. Wheeler, Transmission Line Properties of a Strip on a Dielectric Sheet on a Plane, *IEEE Trans*., vol. MTT-25, pp. 631-647, August, 1977.

[38] E. O. Hammerstad, Accurate Models for Microstrip Computer-aided Design, *IEEE MTTT-S Int. Microwave Symp. Dig.*, pp. 407-409, 1980

[39] E. O. Hammerstad, Equations for Microstrip Circuit Design, Proc. Europeam Micro. Conf., Hamburg, W. Germany, pp. 268-272, September, 1975.

[40] S. Y. Poh, W. C. Chew, and J. A. Kong, Approximate Formulas for Line Capacitance and Characteristic Impedance of Microstrip Line, *IEEE Trans*., vol. MTT-29, pp. 135-142, February, 1981.

[41] M. V. Schneider, Microstrip Lines for Microwave Integrated Circuits, Bell System Tech. J., vol. 48, pp.1422-1444, 1969.

[42] E. O. Hammerstad, *loc. cit* (1975 paper).

[43] M. Kobayshi, A Dispersion Formula Satisfying Recent Requirements in Microstrip CAD, *IEEE Trans*., vol. MTT-36, pp. 1246-1250, August, 1988.

[44] Rogers Corporation, "RO3000® Series High Frequency Circuit Materials," http://www.rogerscorporation.com/mwu/pdf/3000data.pdf, August 2004, Last Accessed at August 2006.

[45] SRI Connector Gage Company, "SMA Female PCB Mount 21-146-1000-01" http://www.sriconnectorgage.com/pages/products/PDF/21-146-1000-01%20-%20Sheet1.pdf, January 2006, Last Accessed at July 2006.

[46] Huber Suhner AG, *Coaxial Connectors General Catalogue*, Edition 2003, p.178, 452.

[47] MAJEWSKI, M.L., ROSE, R.W. and SCOTT, J.S.: 'Modeling and characterization of microstrip to coaxial transitions', *IEEE Trans.*, 1981, MTT-29, pp. 799-805.

[48] PUES, H.F. and VAN DE CAPELLE, A.R.: 'Computer aided experimental characterization of microstrip to coaxial transition', Proc. 14th European Microwave Conference, 1984, pp. 137-141.

[49] Labtech Limited, "Microwave Materials", www.labtechltd.com/pdf_datasheets/microwavefh8.pdf, August 2006, Last Accessed at July 2006.

[50] SRI Connector Gage Company, "SMA Design Specifications" http://www.sriconnectorgage.com/pages/products/sma/smaa.asp, August 2006, Last Accessed at June 2006.

[51] Anritsu, "K Connector® Sliding Contacts for Microstrip Part Number: K110-1/K110-3", http://www.us.anritsu.com/downloads/files/10200-00032.pdf#search=%22K110%20sliding%20contacts%20installation%22, September 2005, Last Accessed at August 2006.

[52] Anritsu, "W1-103F Connector Microstrip to W1 Female Flange Mount Connector", http://www.us.anritsu.com/downloads/files/10305-00010.pdf, July 2005, Last Accessed at July 2006.

[53] C. Wu, J. Wang, R. Fralich and J. Litva, "Analysis of a Series-Fed Aperture Coupled Patch Array Antenna," *Microwave and Optical Tech. Lett.,* vol. 4, no. 3, pp. 110-113, Feb 1991.

[54] C. Wu, J. Wang, R. Fralich and J. Litva, “Study on a Series-Fed Aperture Coupled Microstrip Patch Array,” *IEEE Trans*., vol. 82-4, pp.1762-1765, 1990.

[55] D. J. Lathrop and D. H. Schaubert, “Design of Series-Fed, Aperture Coupled Microstrip Arrays,” *IEEE Trans*., vol. 66-7, pp.1110-1113, 1991.

[56] M. T. Birand, *Notes for an Introductory Course on Antennas and Propagation*, Department of Electrical and Electronics Engineering, Middle East Technical University.

APPENDIX A

For any given dielectric substrate, one can fabricate a microstrip transmission line by removing the required parts of upper copper and forming a line over the dielectric substrate with a particular width (W). The most important characteristic of such a transmission line is its characteristic impedance and it could be evaluated by using the microstrip line parameters (Figure 62) on relevant formulations [35]. In order to match the microstrip transmission line with other circuit elements, the characteristic impedance is mostly aligned to 50 Ω. This alignment could only be done by adjusting the microstrip line width value (W) during the fabrication process.

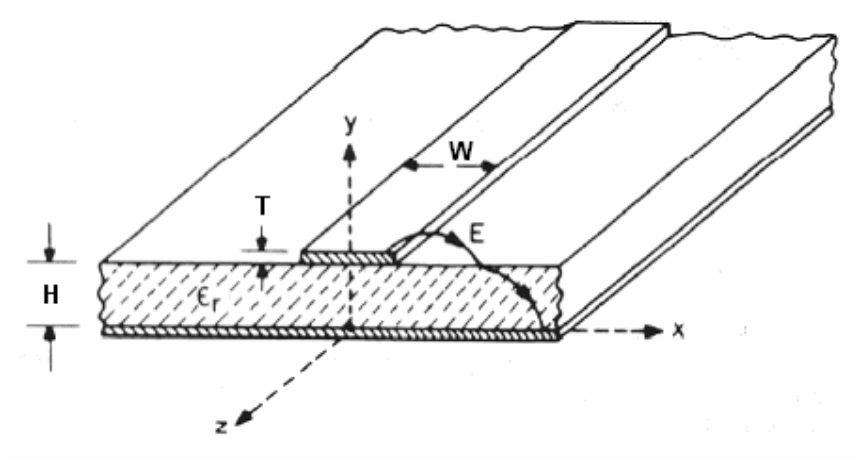

Figure 62. Microstrip Line Parameters [29]

Due to the fringing fields along the edges of the microstrip line, the width of the microstrip line is extended. The extended width is defined as effective width (W_e) and it is calculated by using the following formulas [36].

$$We = W + 0.398\,T\left(1+\ln\left(\frac{4\pi W}{T}\right)\right), \qquad \frac{W}{H} \le \frac{1}{2\pi} \tag{A.1}$$

$$We = W + 0.398\,T\left(1+\ln\left(\frac{2H}{T}\right)\right), \qquad \frac{W}{H} > \frac{1}{2\pi}$$

The formulation for the capacitance per meter of the microstrip line is shown in eqn. A.2 [37-40].

$$C_a = \frac{2\pi\varepsilon_r}{\ln\left(\frac{8H}{W_e}+\frac{W_e}{4H}\right)}, \qquad \frac{W_e}{H} \le 1 \tag{A.2}$$

$$C_a = \varepsilon_r\left[\frac{W_e}{H}+1.393+0.667\ln\left(\frac{W_e}{H}+1.444\right)\right], \qquad \frac{W_e}{H} > 1$$

Between the frequencies 2 GHz and 4 GHz, effective dielectric constant at low frequency ($\varepsilon_{e,lf}$) is calculated as [41-42];

$$\varepsilon_{e,lf} = \frac{\varepsilon_r+1}{2}+\frac{\varepsilon_r-1}{2}\left(1+\frac{12H}{W_e}\right)^{-1/2} + F(\varepsilon_r,H) - 0.217(\varepsilon_r-1)\frac{T}{\sqrt{W_e H}} \tag{A.3}$$

where,

$$F(\varepsilon_r,H) = 0.02(\varepsilon_r-1)\left(1-\frac{W_e}{H}\right)^2, \qquad \frac{W_e}{H} \le 1$$

$$F(\varepsilon_r,H) = 0, \qquad \frac{W_e}{H} > 1$$

For the frequencies higher than 4 GHz, the eqn. A.3 is not valid anymore. The effective dielectric constant for higher frequencies $\varepsilon_{e,hf}$ could be defined by the following formula [43].

$$\varepsilon_{e,hf} = \frac{\varepsilon_r - \varepsilon_{e,lf}}{1+\left(\frac{f}{f_a}\right)^m} \tag{A.4}$$

where,

$$f_a = \frac{f_b}{0.75 + \left(0.75 - 0.332\varepsilon_r^{-1.73}\right)\frac{W_e}{H}}$$

$$f_b = \frac{47746}{H\sqrt{\varepsilon_r - \varepsilon_{e,lf}}} \tan^{-1}\left(\varepsilon_r \sqrt{\frac{\varepsilon_{e,lf} - 1}{\varepsilon_r - \varepsilon_{e,lf}}}\right)$$

$$m = m_0 m_c \leq 2.32$$

$$m_0 = 1 + \frac{1}{1 + \sqrt{\frac{W_e}{H}}} + 0.32\left(1 + \sqrt{\frac{W_e}{H}}\right)^{-3}$$

$$m_c = 1 + \frac{1.4}{1 + \frac{W_e}{H}}\left(0.15 + 0.235e^{-0.45\frac{f}{f_a}}\right)^{-3}, \qquad \frac{W_e}{H} \leq 0.7$$

$$m_c = 1, \qquad \frac{W_e}{H} > 0.7$$

The characteristic impedance of the microstrip line could be evaluated by putting previously calculated parameter values into the formula given below. Depending on the frequency, $\varepsilon_{e,\,lf}$ or $\varepsilon_{e,\,hf}$ should be used as the effective dielectric constant parameter (ε_e).

$$Z_c = \sqrt{\frac{\in_0 \mu_0}{\varepsilon_e}} \frac{1}{C_a} \tag{A.5}$$

$$\lambda_{guided} = \frac{\lambda_0}{\sqrt{\varepsilon_e}} \tag{A.6}$$

APPENDIX B

```
width=0.583; %microstrip line width
length=2.1; %patch length
subs_h=0.254; %substrate height
copp_h=0.035; %copper height
e=3 ; %dielektric constant

e0=(10^(-9))/(36*pi);
m0=4*pi*(10^(-7));

for i=1:50,
    freq(i)=35+0.1*i;
end
size_freq=size(freq);
size_f=size_freq(2);

%for microstrip line calculations switch off the following 2 lines
%width=3*10^2/(sqrt((e+1)/2)*2*36.75);
%width=(round(width*10))/10; %patch width

%effective microstrip line or patch width
if (width/subs_h)<=1/(2*pi),
    width_eff= width+0.398*copp_h*(1+log(4*pi*width/copp_h));
else
    width_eff= width+0.398*copp_h*(1+log(2*subs_h/copp_h));
end

%low frequency solution
temp=((e+1)/2)+((e-1)/2)/sqrt(1+12*subs_h/width_eff)-0.217*(e-
1)*copp_h/sqrt(width_eff*subs_h);
if (width_eff/subs_h)<1,
    f=0.02*(e-1)*(1-width_eff/subs_h)*(1-width_eff/subs_h);
else
    f=0;
end
e_eff=temp+f;

%calculating the capacitance value
if (width_eff/subs_h)<=1,
    c=2*pi*e0/log(8*subs_h/width_eff+width_eff/(4*subs_h));
else
  c=e0*(width_eff/subs_h+1.393+0.667*log(width_eff/subs_h+1.444));
end

%high frequency solution
f_b=47.746*atan(e*sqrt((e_eff-1)/(e-e_eff)))/(subs_h*sqrt(e-
e_eff));
f_a=f_b/(0.75+(0.75-0.332*e^(-1.73))*width/subs_h);
m_0=1+1/(1+sqrt(width/subs_h))+0.32*(1+sqrt(width/subs_h))^(-3);
if (width/subs_h)<=0.7,
 m_c=1+1.4*(0.15-0.235*exp(1).^(-0.45*freq/f_a))/(1+width/subs_h);
```

```
else
    m_c=ones(1,size_f);
end
m=m_0*m_c;
for i=1:size_f,
    if m(i)>2.32,
        m(i)=2.32;
    end
end
e_eff_hf=e-(e-e_eff)./(1+(freq/f_a).^m);

%characteristic impedance and wavelength calculation
for i=1:size_f,
    if freq(i)>4,
       z0(i)=sqrt(e0*m0/e_eff_hf(i))/c;
       lambda(i)=3*(10^2)/(freq(i)*sqrt(e_eff_hf(i)));
       hf(i)=1;
    else
       z0(i)=sqrt(e0*m0/e_eff)/c;
       lambda(i)=3*(10^2)/(freq(i)*sqrt(e_eff));
       hf(i)=0;
    end
end

%resonance frequency calculation
delta_length=0.412*subs_h*((e_eff_hf+0.3)./(e_eff_hf-
0.258))*(((width_eff/subs_h)+0.262)/((width_eff/subs_h)+0.813));
res_freq=3*10^2./(2*(length+2*delta_length).*sqrt(e_eff_hf));

figure(1)
h=plot(freq,res_freq);
xlabel('Frequency (GHz)');
ylabel('Patch antenna resonance frequency (GHz)')
set(h,'color',[0 0 1]);
set(h,'linewidth',3);
h=title('patch length=2.1 mm, patch width=3.2 mm');
set(h,'fontweight','bold')
grid on

figure(2)
h=plot(freq,z0);
xlabel('Frequency (GHz)');
ylabel('Characteristic Impedance (ohm)')
set(h,'color',[0 0 1]);
set(h,'linewidth',3);
h=title('microstrip line width=0.583 mm');
set(h,'fontweight','bold')
grid on

figure(3)
h=plot(freq,lambda);
xlabel('Frequency (GHz)');
ylabel('Guided wavelength (mm)')
set(h,'color',[0 0 1]);
set(h,'linewidth',3);
h=title('microstrip line width=0.583 mm');
set(h,'fontweight','bold')
grid on
```

APPENDIX C

Characteristic Impedance of a Cylindrical Transmission Line:

$$Z_0 = \frac{59.95}{\sqrt{\varepsilon_r}} \ln\left(\frac{b}{a}\right) \tag{C.1}$$

where ε_r is the characteristic impedance of the material between two conductors, 'b' is the inner radius of the outer conductor and 'a' is the radius of the inner conductor (Figure 63).

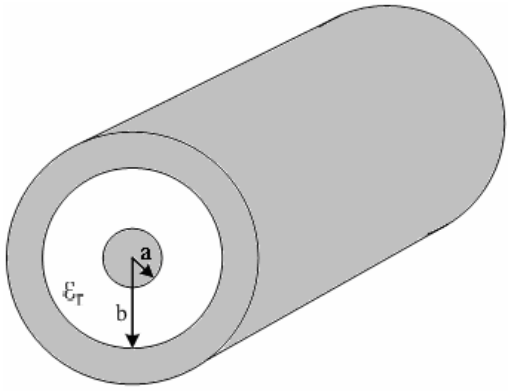

Figure 63. Parameters of Cylindrical Transmission Line

APPENDIX D

Case 1: Compensation gap length= 0 mm, Air gap radius= 0.4 mm:

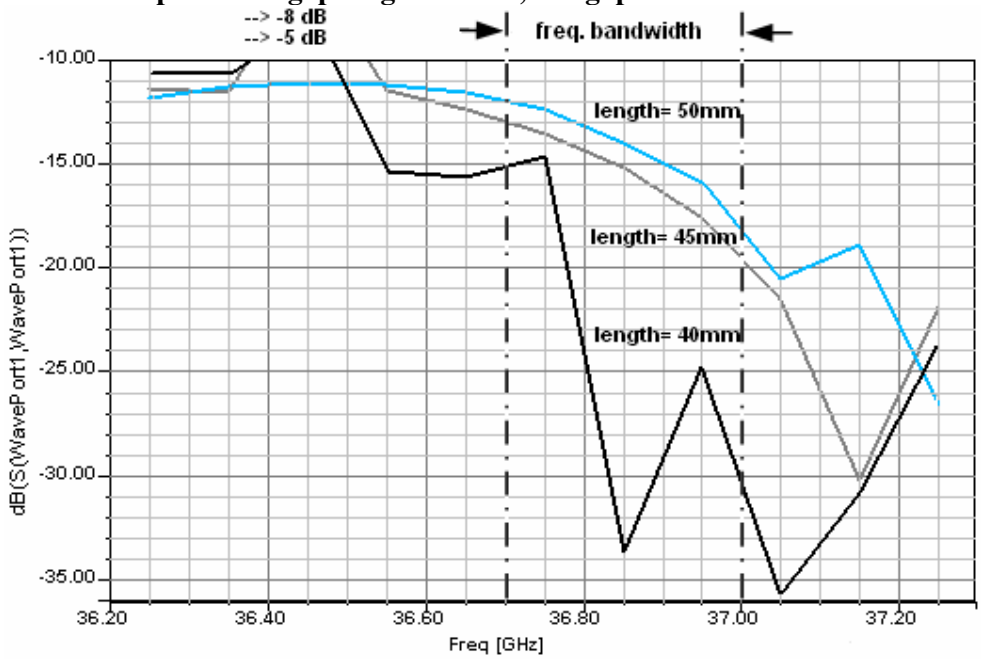

Figure 64. S_{11} vs. Frequency for Case 1

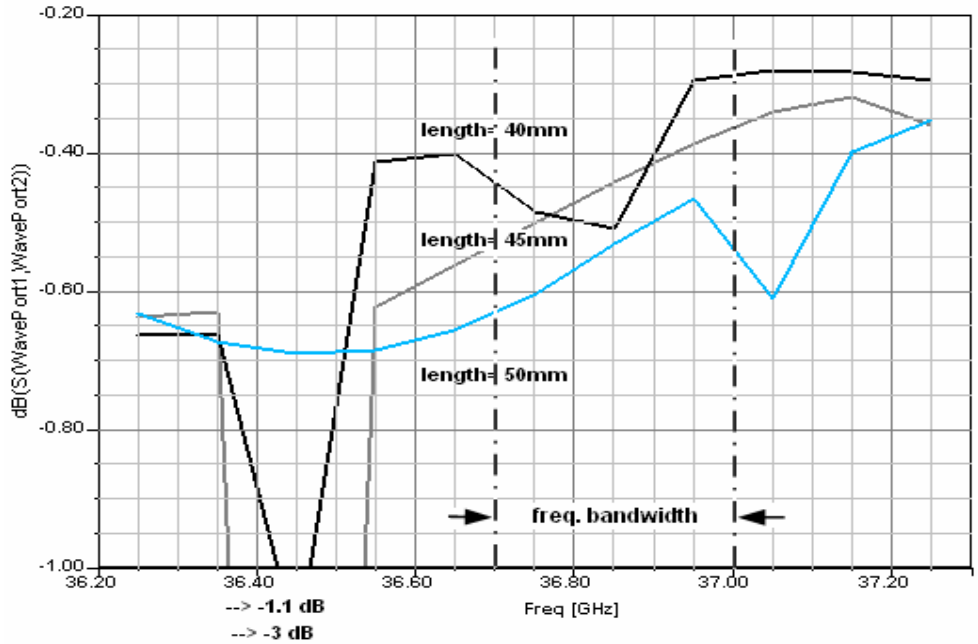

Figure 65. S_{21} vs. Frequency for Case 1

Case 2: Compensation gap length = 0.1 mm, Air gap radius= 0.4 mm

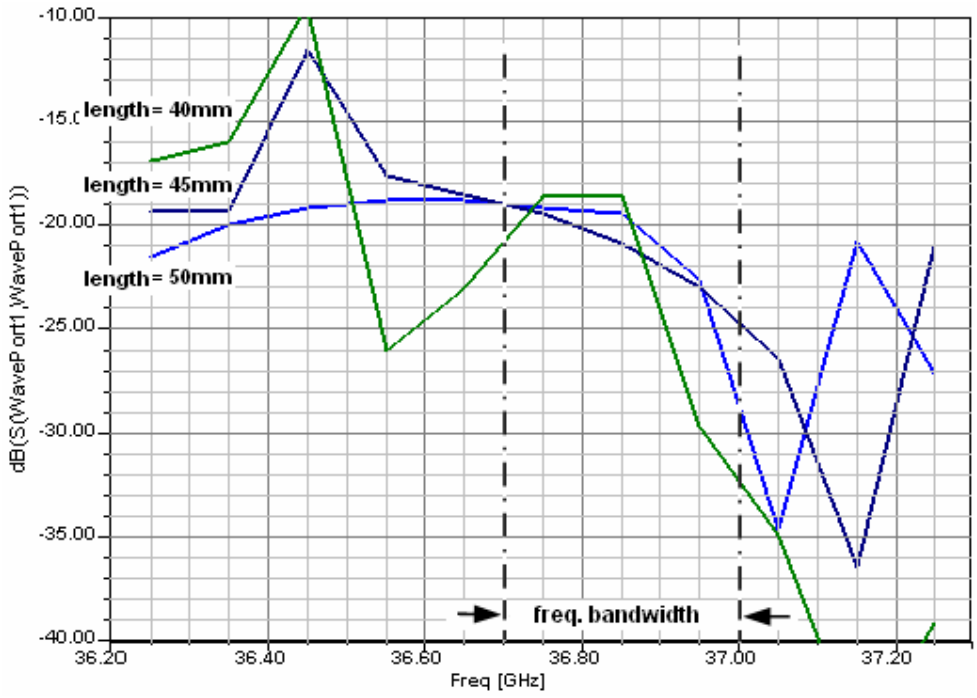

Figure 66. S_{11} vs. Frequency for Case 2

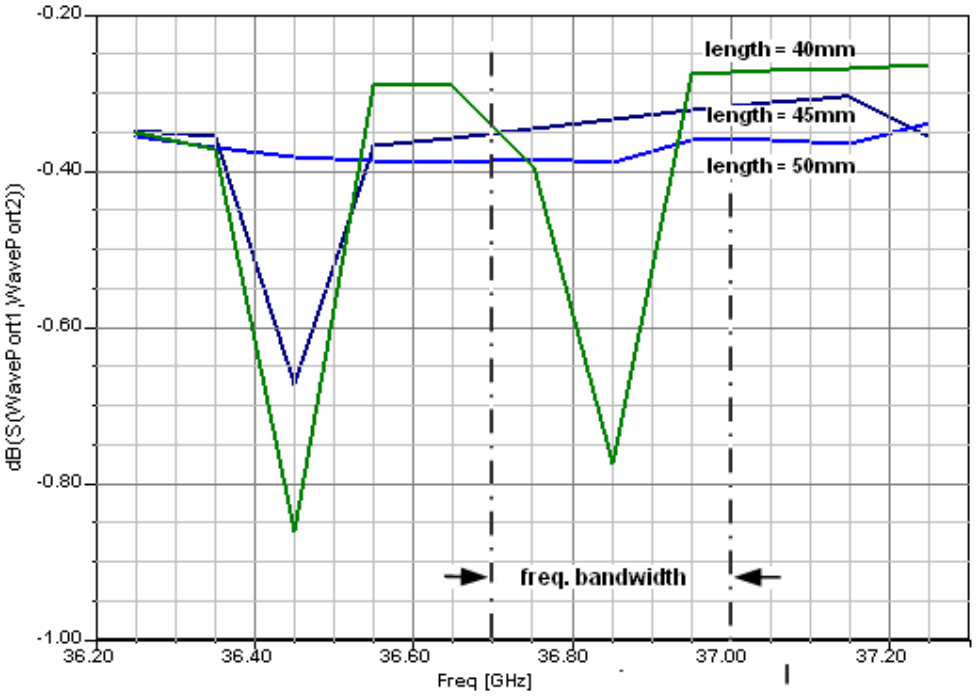

Figure 67. S_{21} vs. Frequency for Case 2

Case 3: Compensation gap length = 0.2 mm, Air gap radius= 0.4 mm

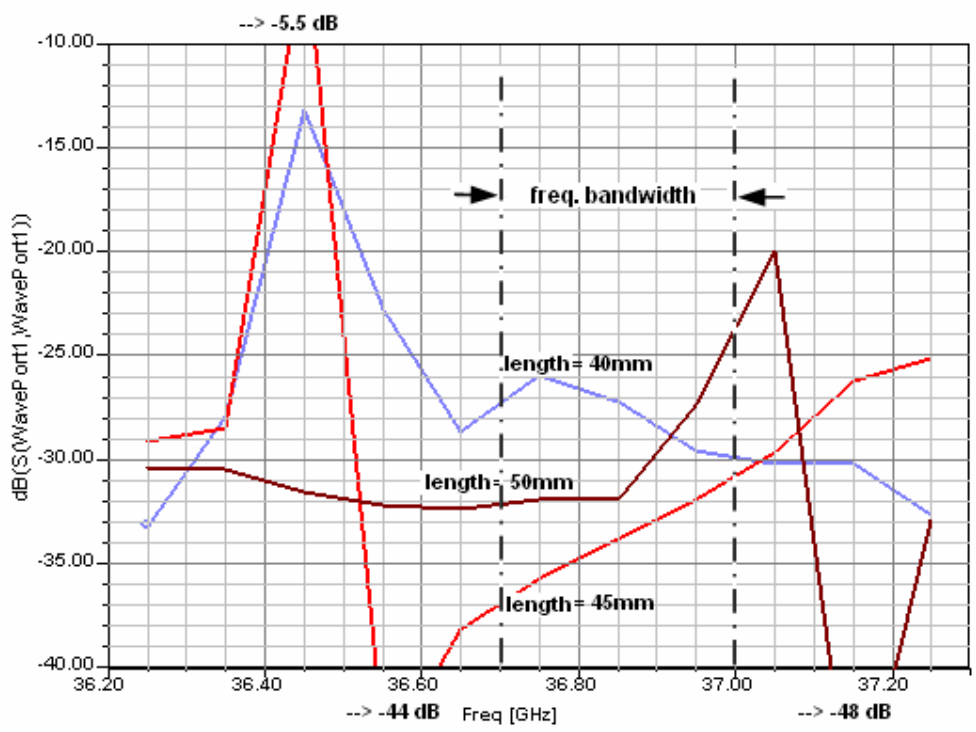

Figure 68. S_{11} vs. Frequency for Case 3

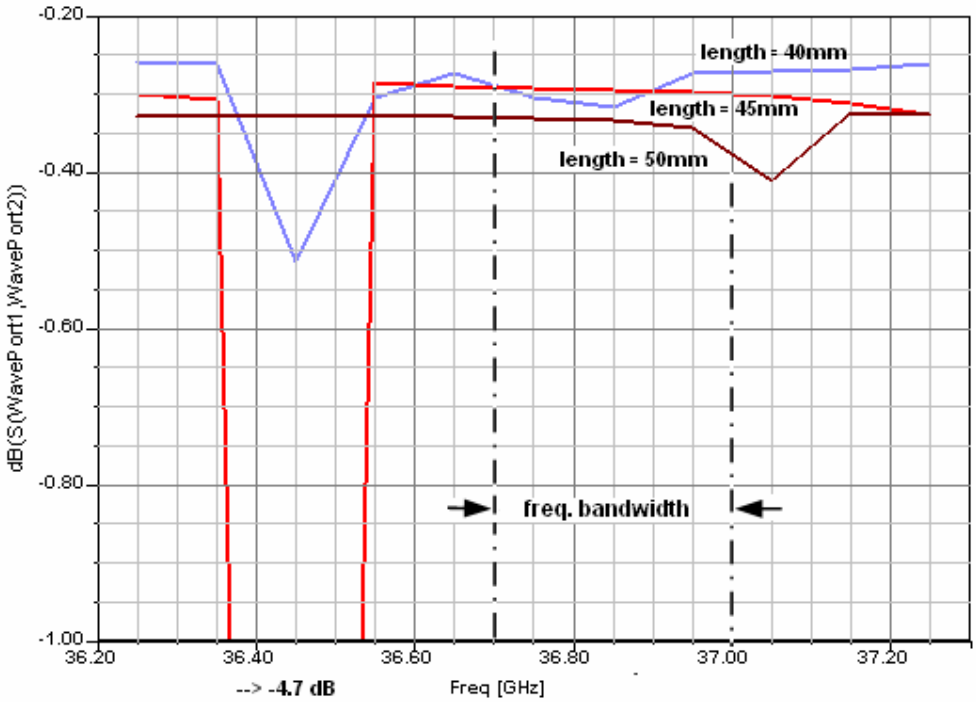

Figure 69. S_{21} vs. Frequency for Case 3

Case 4: Substrate length= 40 mm, Air gap radius= 0.4 mm

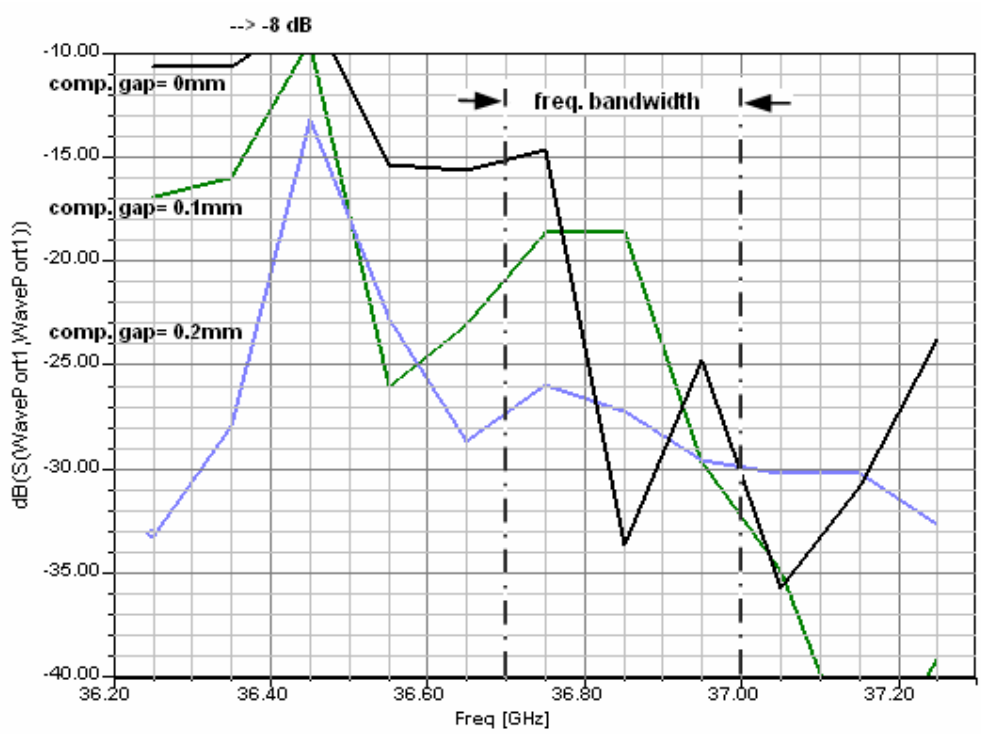

Figure 70. S_{11} vs. Frequency for Case 4

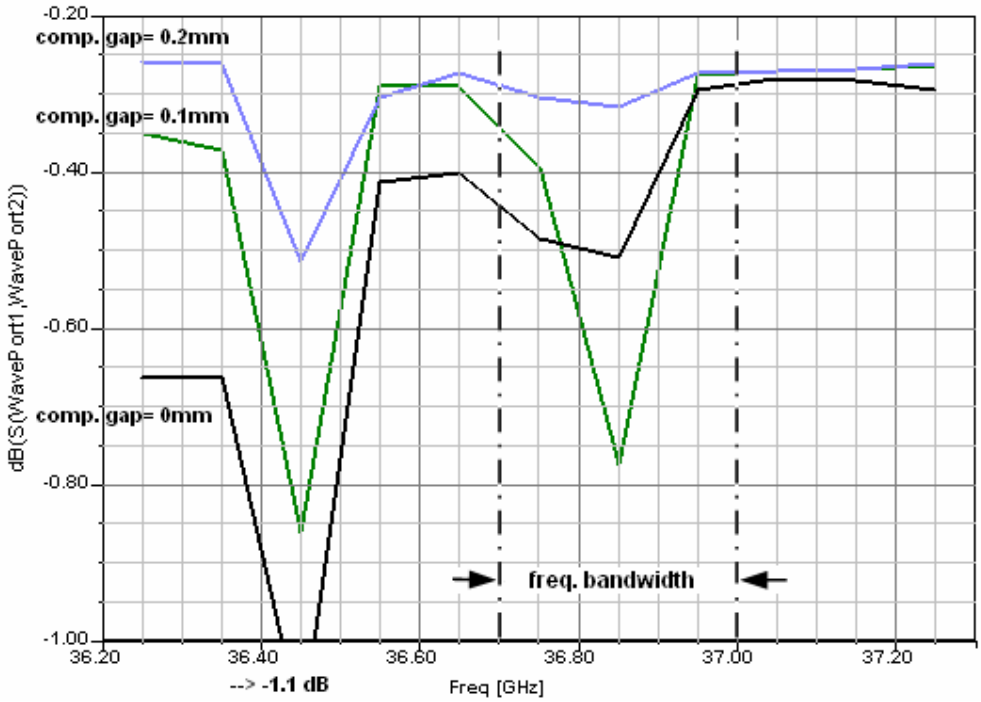

Figure 71. S_{21} vs. Frequency for Case 4

Case 5: Substrate length= 45 mm, Air gap radius= 0.4 mm

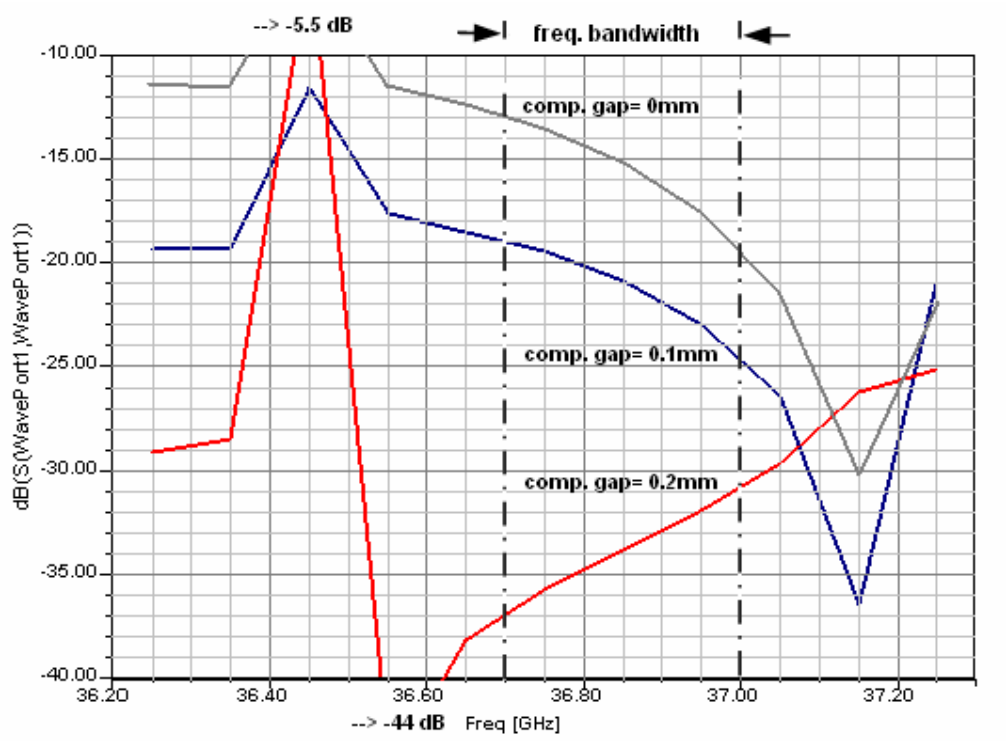

Figure 72. S_{11} vs. Frequency for Case 5

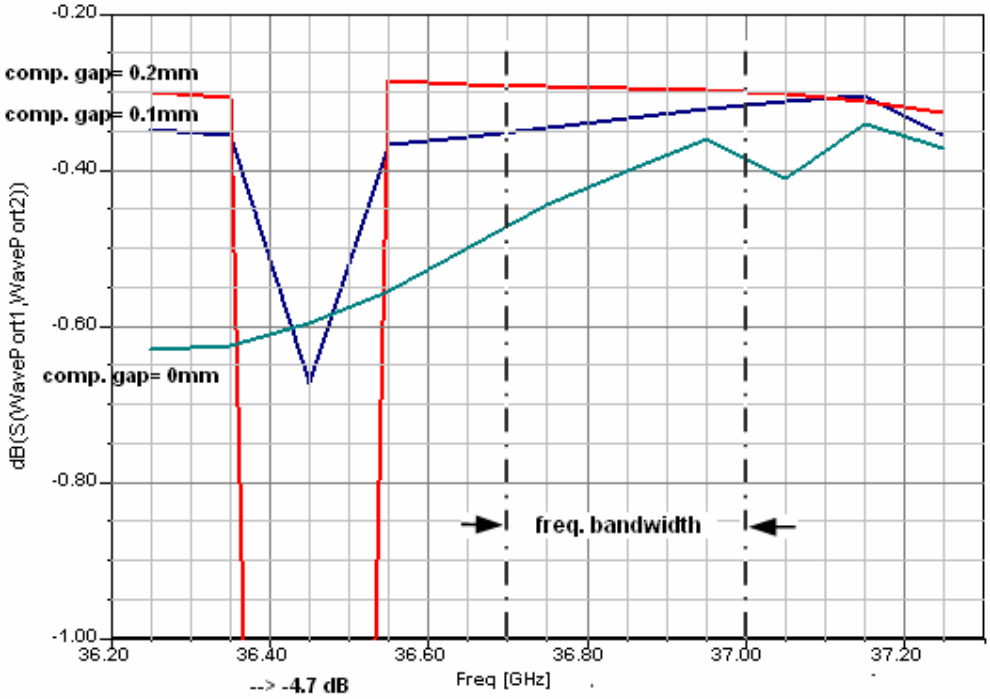

Figure 73. S_{21} vs. Frequency for Case 5

Case 6: Substrate length= 50 mm, Air gap radius= 0.4 mm

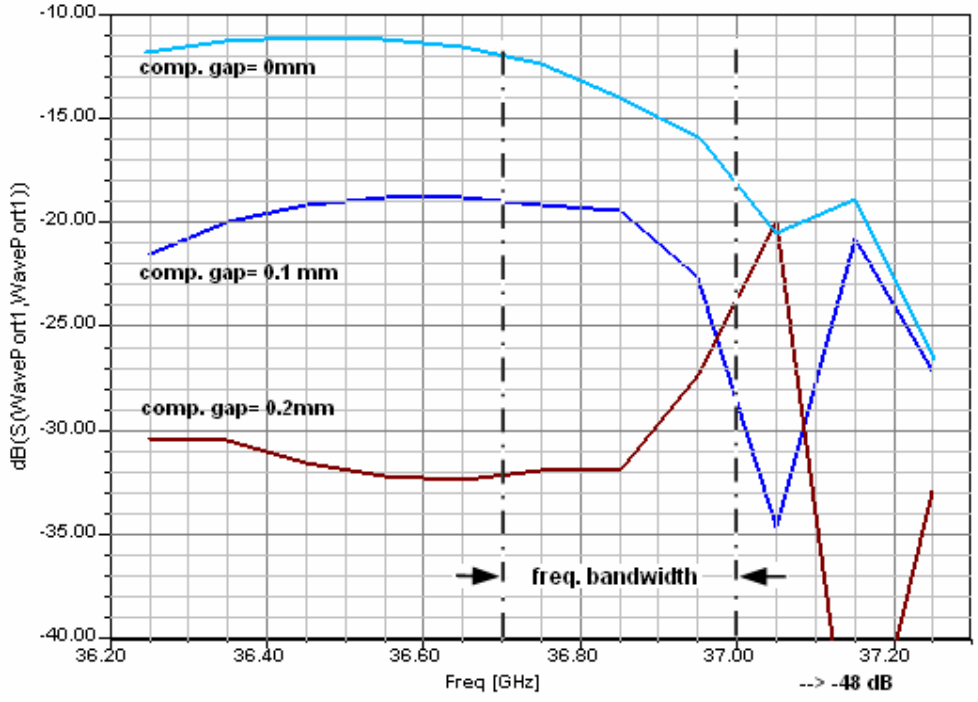

Figure 74. S_{11} vs. Frequency for Case 6

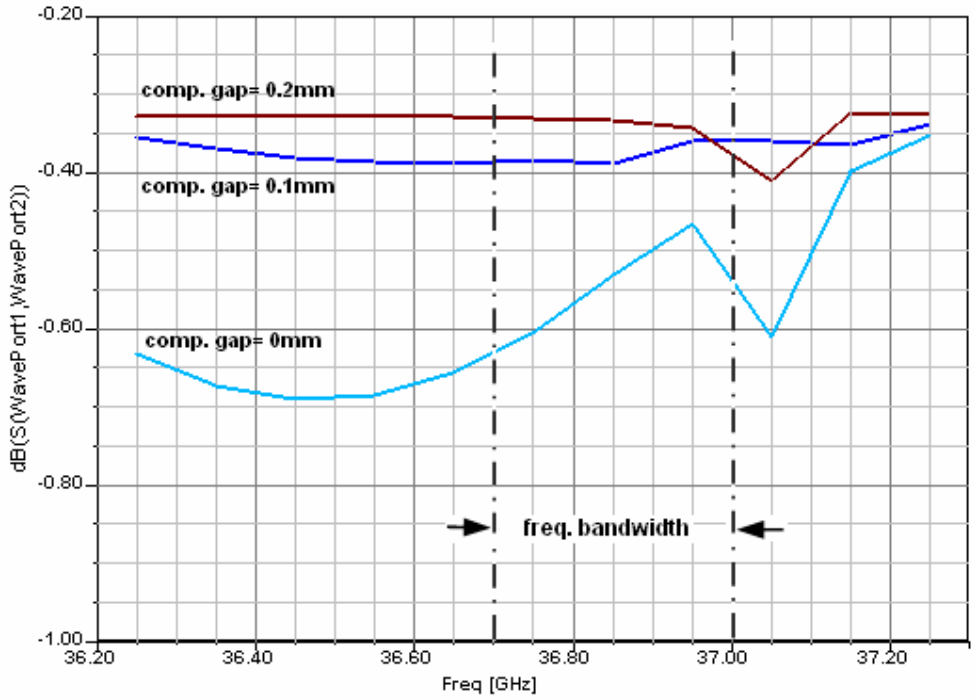

Figure 75. S_{21} vs. Frequency for Case 6

Case 7: Substrate length= 40 mm, Compensation gap length= 0.1 mm

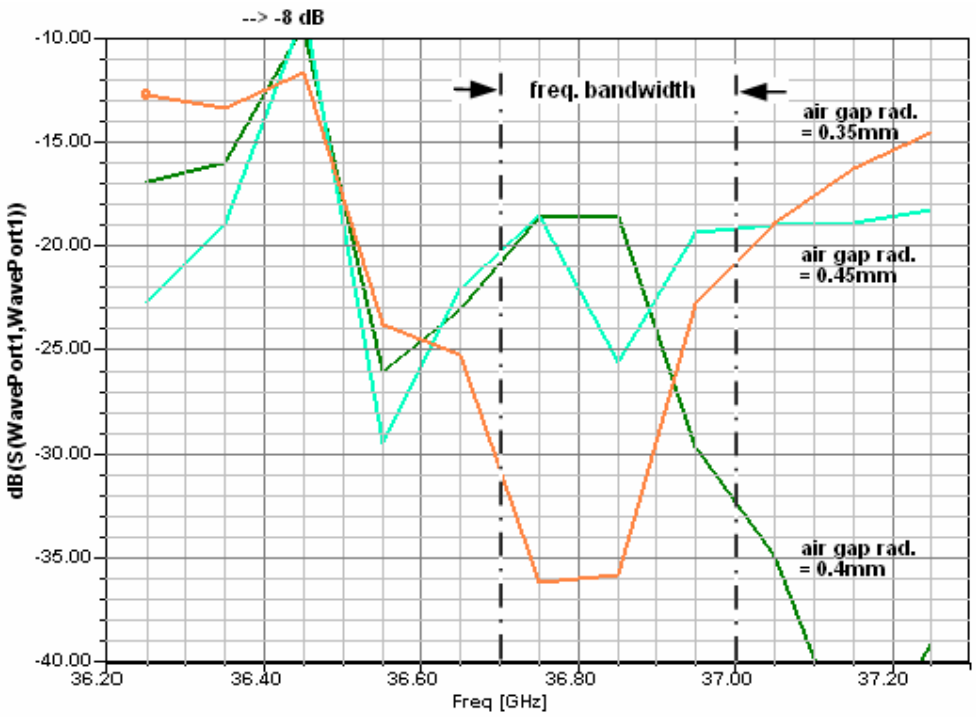

Figure 76. S_{11} vs. Frequency for Case 7

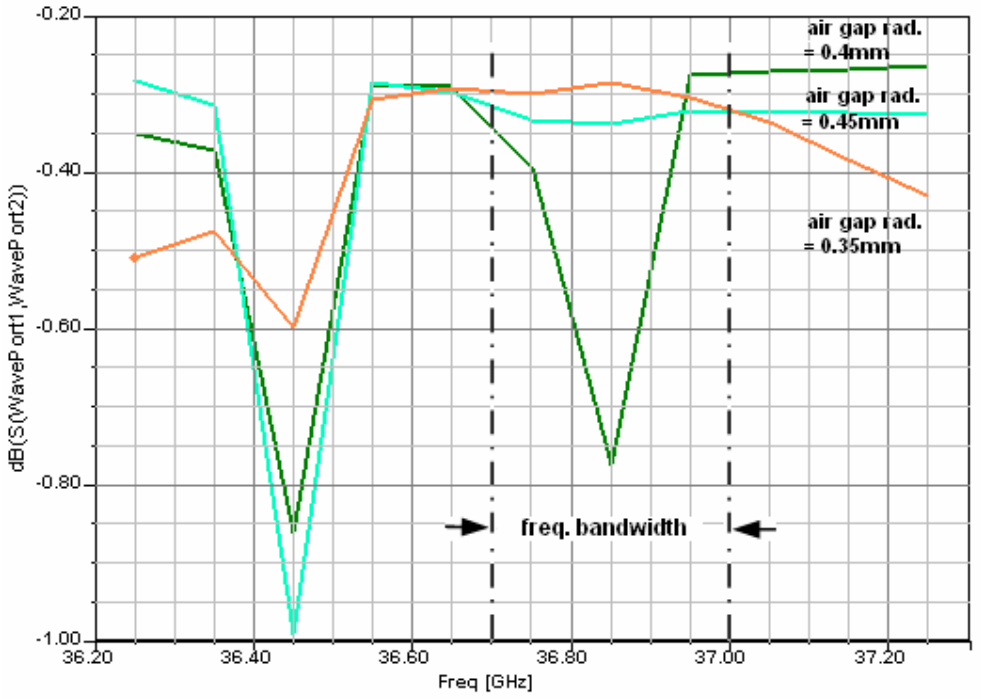

Figure 77. S_{21} vs. Frequency for Case 7

Case 8: Substrate length= 50 mm, Compensation gap length= 0.1 mm

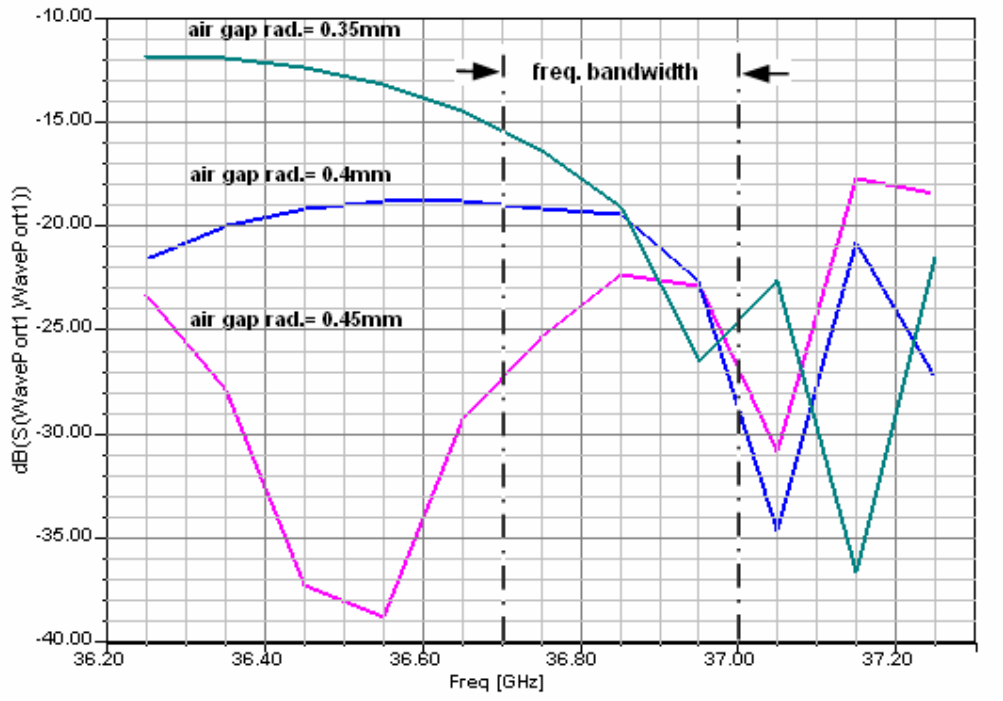

Figure 78. S_{11} vs. Frequency for Case 8

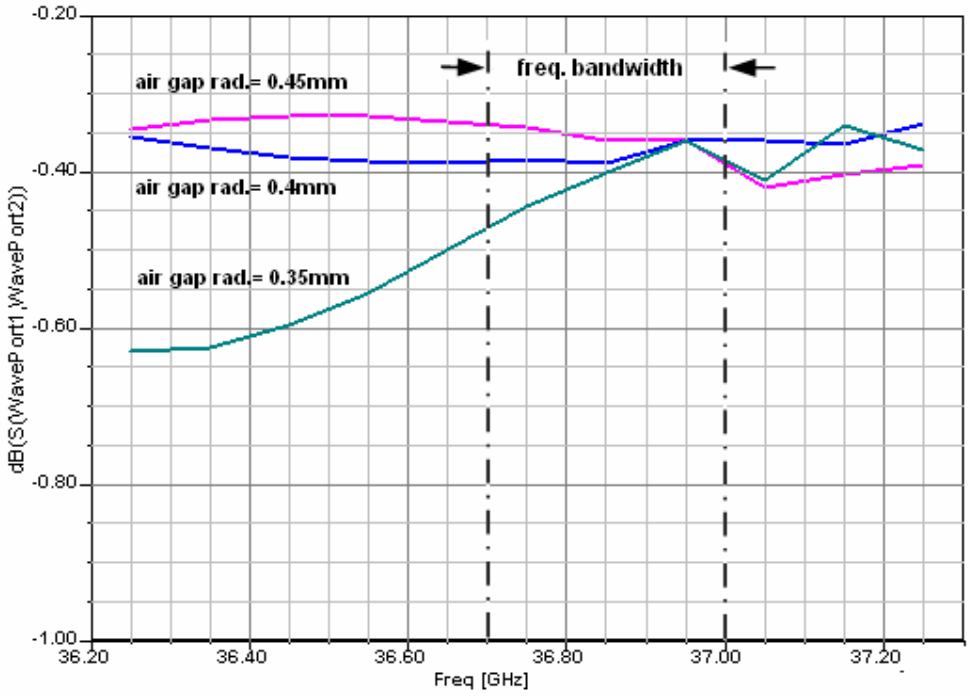

Figure 79. S_{21} vs. Frequency for Case 8

APPENDIX E

```
% antenna frequency
freq=36.85;
% array element number
n=8;
% phase difference between adjecent elements in degree
phase=0;
%distance between patch elements in millimeter
d=7;

lambda0=3e2/freq;
theta=linspace(0,180,181);

for i=1:181,
    temp=0.5*(phase*pi/180+2*pi*d*cos(pi*theta(i)/180)/lambda0);
    arr_fac(i)=abs(sin(n*temp)/(n*sin(temp)));
end

t = linspace(-0.8,0.8,181);
sinc_pat = sinc(t);

arr_pat=sinc_pat.*arr_fac;

figure(1)
h=plot(theta,arr_fac)
xlabel('Theta (degree)');
ylabel('Field Value (volt)')
set(h,'color',[0 0 1]);
set(h,'linewidth',1);
h=title('Array Factor');
set(h,'fontweight','bold')

figure(2)
h=plot(theta,20*log10(sinc_pat));
xlabel('Theta (degree)');
ylabel('Field Value (volt)')
set(h,'color',[0 0 1]);
set(h,'linewidth',1);
h=title('Single Patch Antenna Pattern');
set(h,'fontweight','bold')

figure(3)
h=plot(theta,20*log10(arr_pat));
xlabel('Theta (degree)');
ylabel('Field Value (volt)')
set(h,'color',[0 0 1]);
set(h,'linewidth',1);
h=title('Patch Array Antenna Pattern');
set(h,'fontweight','bold')
```

APPENDIX F

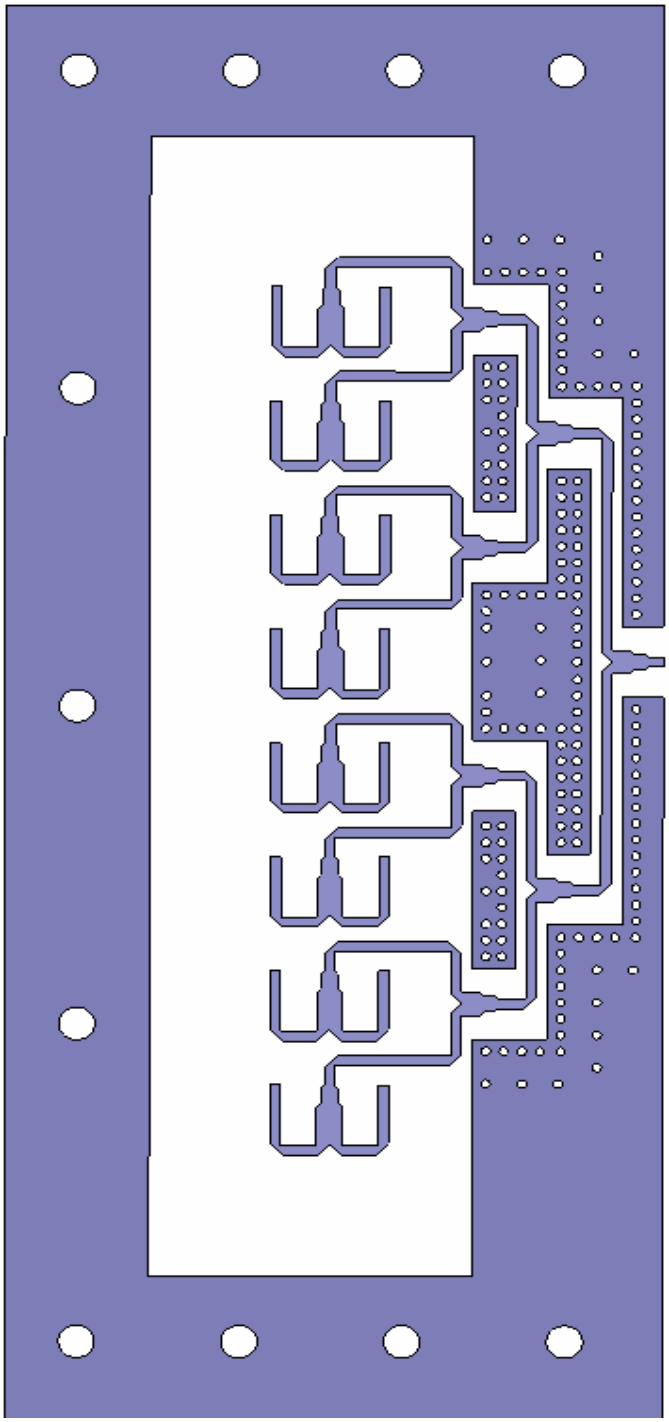

Figure 80. Top Layer of the Fabricated 8x2 Parallel Feeding Network

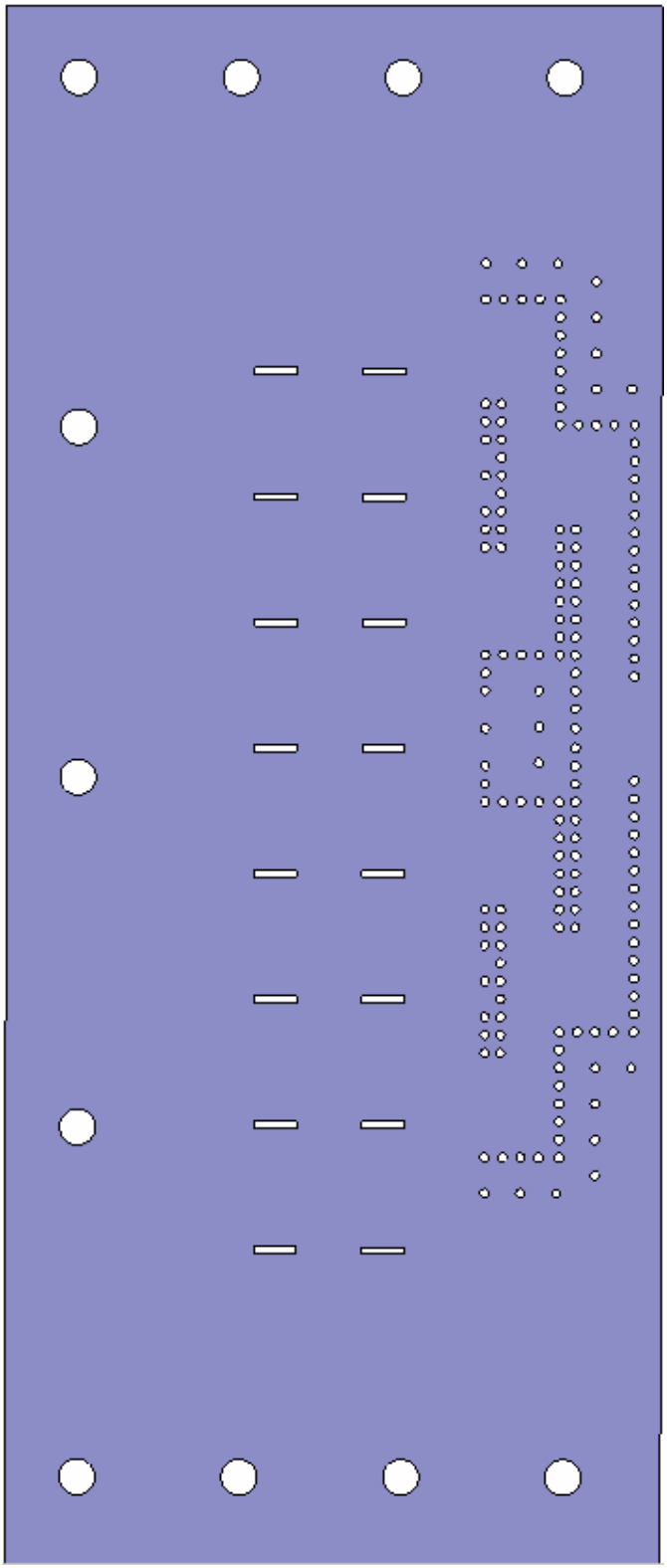

Figure 81. Bottom Layer of the Fabricated 8x2 Parallel Feeding Network

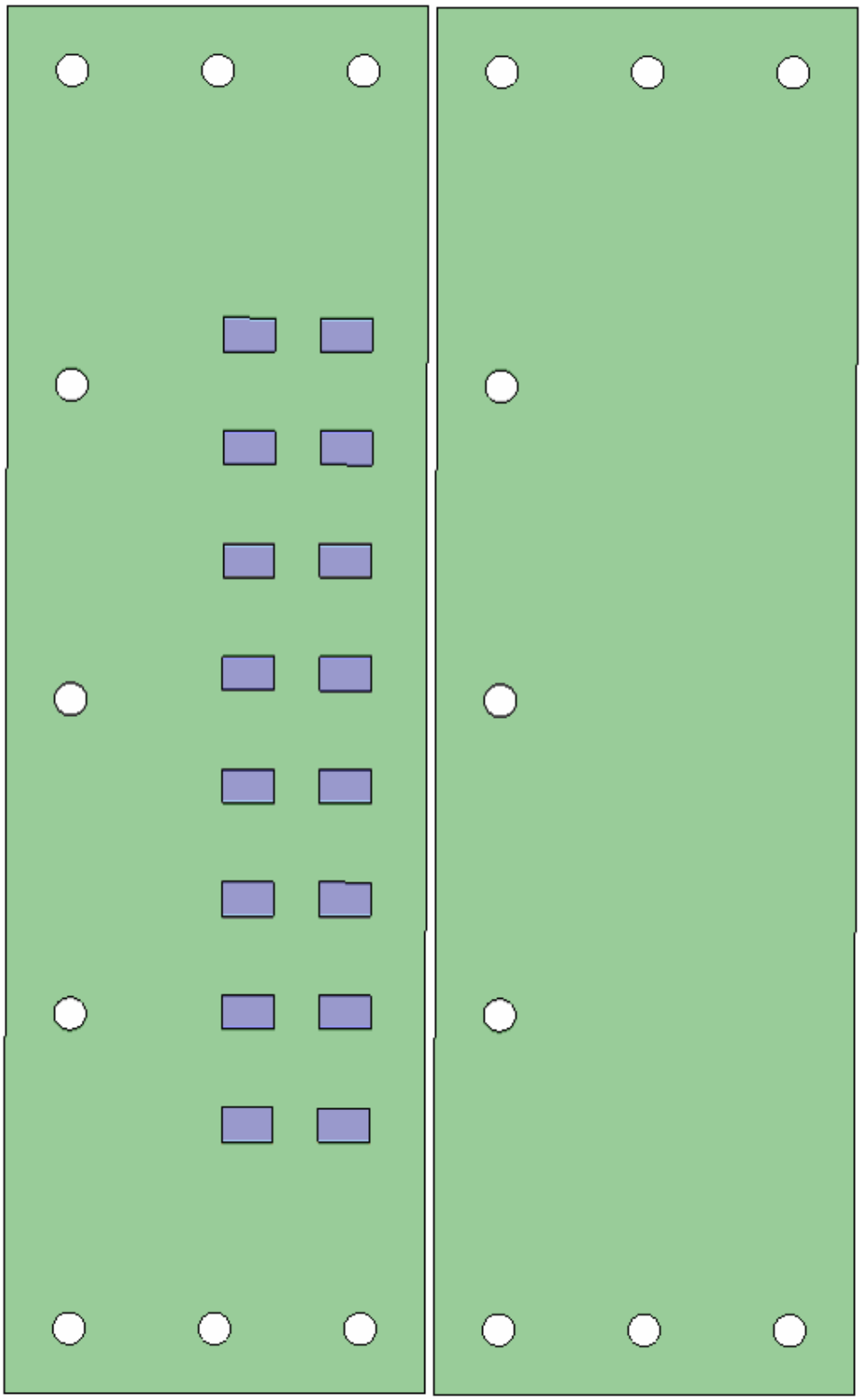

Figure 82. Top and Bottom Layer of the Fabricated 8x2 Patch Array

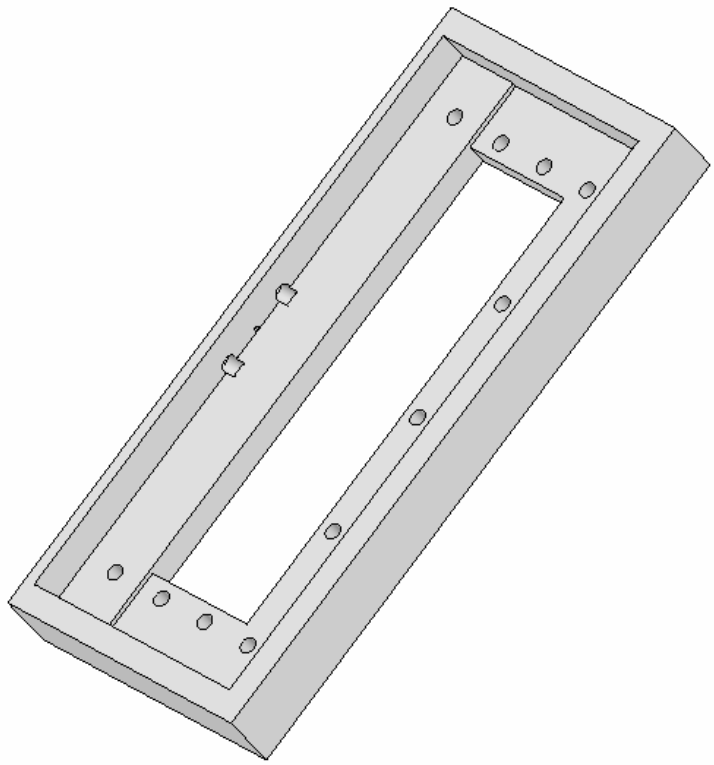

Figure 83. Mechanical Fixture of the Fabricated 8x2 Patch Array Antenna